1980

A Quantitative Evaluation of Landsat for Monitoring Suspended Sediments in a Fluvial Channel.

Soon Tae Kim
Louisiana State University and Agricultural & Mechanical College

KIM, SOON TAE

A QUANTITATIVE EVALUATION OF LANDSAT FOR MONITORING SUSPENDED SEDIMENTS IN A FLUVIAL CHANNEL

The Louisiana State University and Agricultural and Mechanical Col. PH.D. 1980

A QUANTITATIVE EVALUATION OF LANDSAT FOR MONITORING SUSPENDED SEDIMENTS IN A FLUVIAL CHANNEL

A Dissertation

Submitted to the Graduate Faculty of the
Louisiana State University and
Agricultural and Mechanical College
in partial fulfillment of the
requirements for the degree of
Doctor of Philosophy

in

The Department of Geography and Anthropology

by
Soon Tae Kim
B.A., Seoul National University, 1971
M.S., Louisiana State University, 1974
M.Ap.Stat., Louisiana State University, 1977
May, 1980

ACKNOWLEDGMENTS

This study could not have been completed without the assistance and cooperation of NASA/Earth Resources Laboratory.

Words are not enough to express my gratitude for the help and friendship of Dr. Anthony J. Lewis, my advisor. I am also especially indebted to Dr. R. A. Muller for his moral support. My gratitude also goes out to the remaining members of my dissertation committee: Drs. R. H. Cartmill, D. W. Smith, S. Khorram, P. E. Schilling, M. B. Newton, Jr., C. Harlo.

Special thanks are due to Young Joon Choi who provided assistance at critical times.

I am also indebted to many people for their assistance. Unfortunately, time does not allow me to mention them all here.

I wish my parents were still alive to see my dissertation today.

TABLE OF CONTENTS

Page

APPENDICES

LIST OF TABLES

LIST OF FIGURES

ABSTRACT

Since the launch of Landsat-1 in July, 1972, the orbital remote sensing system has made significant contribution to earth science research. Landsat's repetitive "earth observations" are of great value for monitoring changes in earth surface conditions through time. Investigation of suspended sediment concentrations in natural water bodies is one of the major areas of Landsat applications.

An attempt has been made to evaluate the utility of Landsat Multispectral Scanner (MSS) digital data for monitoring suspended sediment concentrations in a natural river channel using Tarbert Landing, Mississippi on the lower Mississippi River as the test site. Specific purposes of the study were: 1) to investigate vertical distribution of suspended sediment concentrations at the cross section of the river channel; 2) to develop a method of eliminating environmental effects from the MSS digital data obtained during successive Landsat overpasses; 3) to evaluate the statistical properties of MSS digital data as related to suspended sediment concentrations in the surface layers of a natural river; and 4) to evaluate the feasibility of estimating suspended sediment concentrations in entire depth of the river channel via Landsat MSS digital data.

The hydrological data utilized in this study were collected by the U.S. Corps of Engineers, New Orleans District, at Tarbert Landing during 1974-75 and included discharge, velocity, suspended sediment concentrations, and water sampling depth. Analyses of the data for

the vertical distribution of suspended sediments employed both the diffusion model and the linear model.

Analyses of the hydrological data indicated that the diffusion model does not adequately describe the relationship between suspended sediment concentrations in surface and subsurface layers of the river. Poor performance of the diffusion model is attributable to the over-simplifying assumptions applied to the model, notably the two-dimensional flow. The full rank linear model was better than the diffusion model in accurately estimating sediment concentrations, particularly the silt-clay fraction. However, the linear model suffered from a large sample variance.

Computer Compatible Tapes (CCT's) from three cloud-free Landsat overpasses (July 11, 1974; December 2, 1974; April 15, 1975) were obtained and processed at the NASA's Earth Resources Laboratory in Slidell, Louisiana. MSS 4-channel radiance data from the CCT's were analysed using the Corps of Engineers' suspended sediment data as the surface truth and the linear model.

Analyses of the MSS radiance data and the surface truth showed that the actual suspended sediment concentrations in the surface layers of a natural river can be estimated with better than 80% accuracy when using all four MSS channels in the linear model. Results from the analyses also indicated that most of the information on suspended sediments is contained in the MSS channels 4 and 5. The negative relationship found between channel 5 and suspended sediments was not as anticipated, however, a complete explanation of this phenomenon was not available.

The transformation method developed in this study to eliminate the environmental effects should prove to be very useful. The basic principles involved in the transformation should be readily applicable to any other type of investigations that deal with monitoring surface physical phenomena through successive Landsat overpasses.

CHAPTER I

INTRODUCTION

Background

A basic premise of remote sensing is that the spectral signatures from the target are primarily determined by physical and physiological characteristics of the target. An immediate implication of this postulate is that the spectral signatures, emitted and reflected, from the earth surface may be utilized to detect any target of interest under certain conditions. In many cases, however, the actual interaction between the electromagnetic spectrum and the targets is not yet fully understood. Furthermore, several factors influence the spectral signatures being received by the sensor in the actual remote sensing mission: atmospheric conditions, sun angle, sensor system limitations, and so on. As a result, considerable efforts have been made for over a decade, through various types of modelling and experimentation, to elaborate the theory of remote sensing and, subsequently, to make its applications more useful to scientific endeavor as well as to the public interest in general.

Since the first orbital photography became available in 1961 by the unmanned MA-4 Mercury spacecraft, growing interest heightened in the use of orbital photography for natural resource evaluation. This interest eventually led the U.S. Geological Survey (USGS) and NASA to

the development and flight of the first Earth Resources Technology Satellite, now known as Landsat, on July 23, 1972 (Fischer, et al., 1975). To date, the Landsat program has drawn much attention from scientists in the many disciplines of social and natural sciences, particularly in earth science disciplines such as geology, geography, hydrology, and oceanography. Many earth science investigators agree that Landsat provides them with a research tool of great value.

Perhaps, the most significant function of Landsat as a research tool is that it collects information over an area of considerable spatial extent (approximately 185 x 185 kilometers per image) at multi-temporal stages. It is then clearly indicated that within the limitation of Landsat ground resolution some physical changes taking place in the area through time may be identified and monitored. Ever since the launch of Landsat numerous attempts have been made to identify or estimate target properties of interest by utilizing Landsat data and to monitor particular physical changes (or processes in general) through successive Landsat overpasses. In doing so, it is mandatory to acquire at each time of the satellite overpass surface truth[1] (or so-called training samples) based on a measurement plan.

Yet, a rather critical question may arise: Suppose that, as a particular example, an attempt is made to monitor the surface concentration of suspended sediments in part of a fluvial channel via Landsat (which may be somewhat indicative of the entire sediment flow in that segment of the channel). Let us further suppose that a few surface truth sample locations are selected in the segment of the

---

[1]The term surface truth generally refers to information about the target at ground level.

channel. What should be realized is that Landsat is no longer useful as a data collection tool. In this instance the field crew collects nearly all the information at each time of the Landsat overpass and does so more accurately. A basic solution to this problem (so far as the Landsat application is concerned) is to find ways to eliminate the surface truth collection at every time of the satellite overpass, so that Landsat performs as the single source of data. If such an eventuality were realized, it can be seen that the scope of the solution would extend not only to the instance illustrated, but extends to almost all cases of monitoring physical processes by means of successive satellite overpasses. In other words, once the monitoring algorithm is trained by the collection of surface truth data and an acceptable accuracy is attained, the entire monitoring system via the orbital platform could operate without the surface truth team. Indeed, the development of such a monitoring system would be considered a major step in the development of orbital remote sensing, particularly from the standpoint of practical and operational remote sensing applications.

To achieve this goal requires, however, correction of the Landsat radiance data for the environmental effects such as different sun angles and atmospheric conditions, at the time of an overpass. In fact, many Landsat investigations have utilized the method of so-called band ratioing, first introduced by Vincent (1972), to create random variables representing the spectral signatures received by the Landsat Multispectral Scanner (MSS). In doing so several MSS band (channel) ratios were formed and the relationships between the ratios and the target properties, say, sediment concentrations, were evaluated. It

appears that by using the MSS band ratios many investigators (e.g., Ashley and Rea, 1975; Anderson, et al., 1977; Weismiller, et al., 1977) intended to solve the problem of different sun angles in successive overpasses of the satellite. Yet, it should be clearly understood that variations in the band ratios result from a combined effect of different environmental settings and the target properties (i.e., changes in sediment concentrations). If the ratios are considered to be random variables representing the MSS spectral signatures, then there is little logic on which use of the MSS band ratios can be justified for the purpose of evaluating the relationship between target properties and the MSS spectral signatures.

Monitoring suspended sediments in natural water bodies from remote platforms has perhaps been one of the most active fields of investigation of the use of remote sensing in the study of water resources. With the launch of Landsat-1, numerous studies on suspended sediments with non-orbital imagery in the 1960s were subsequently extended to Landsat. Apparently, the main objectives of these investigations to date have been to evaluate the use of Landsat data, in either image or digital form, for monitoring suspended sediment concentrations in surface water. While image data alone may be sufficient for some suspended sediment studies (Klemas, Borchardt, and Treasure, 1973), much attention has been paid to digital data recorded on Computer Compatible Tapes (CCT's). This is because the digital data constitute quantative radiance data from the surface targets collected by the Landsat Multispectral Scanner (MSS).

Many Landsat investigators have attempted to define the relationship between the MSS digital data and suspended sediment

concentrations in various types of water bodies (Williamson and Grabau, 1973; Klemas, et al., 1974; Johnson, 1975; Johnson, Cressy, and Dallam, 1975; Brooks, 1975; Yarger and McCauley, 1975; Trexler and Barker, 1975). Most of these studies, however, were limited by insufficient data (either Landsat or surface truth) and, in some cases, inadequate analytical methods. The concensus of these studies was that only three MSS bands, 4, 5, and 6, could be utilized for the study of suspended sediments with Landsat. Some disagreements were also reported; Johnson (1975) claimed that band 5 alone could be successfully used and no substantial improvement was found with the use of all four bands, while Johnson, Cressy, and Dallam (1975) did not find any significant relationship between band 5 and suspended sediments.

Fluvial sediments have been of considerable interest to hydrologists, hydraulic engineers, sedimentologists, geomorphologists, and many others. Comprehensive outlines of numerous studies on suspended sediments in natural river channels are given by Einstein (1964) and Bogárdi (1972). To date, a complete theoretical solution for the problem of suspended sediment transport does not seem feasible, and the distance between the theory and the "real world" is well illustrated by several investigations (Nordin, 1963; Nordin and Dempster, 1963; Colby, 1964).

It should be clear that any attempt to explain the theoretical formulation of the hydraulic laws of suspended sediment flow is beyond the scope of this study. Rather, a major interest in this study lies in the feasibility of making inference on the concentrations of suspended sediments in a natural river channel from Landsat MSS radiance data. Indeed, this question has long remained unanswered and has been

generally considered "theoretically impossible," because no known remote sensor utilizing electromagnetic spectrum is capable of penetrating through the surface layer of natural water bodies heavily loaded with sediment. If the vertical distributions of suspended sediment concentrations have an identifiable relationship to the surface concentrations and a reliable relationship is found between suspended sediments in the surface layer of the river and the Landsat MSS radiance data, then estimation of suspended sediment concentrations for the entire depth is feasible from Landsat MSS radiance data.

Purpose

The purpose of this study is to evaluate the utility of Landsat MSS digital data for monitoring suspended sediment concentrations in the natural river channel, using the lower Mississippi River at Tarbert Landing, Mississippi as the test site (Figure 1). Specific purposes of the study are:

1) to investigate characteristics of suspended sediment flow, in particular, vertical distribution of suspended sediment concentrations at the cross section of the lower Mississippi River at Tarbert Landing.
2) to develop a method of eliminating environmental effects from the MSS digital data obtained through successive Landsat overpasses.
3) to evaluate the statistical properties of MSS digital data as related to suspended sediment concentrations in the surface layers of a natural river.

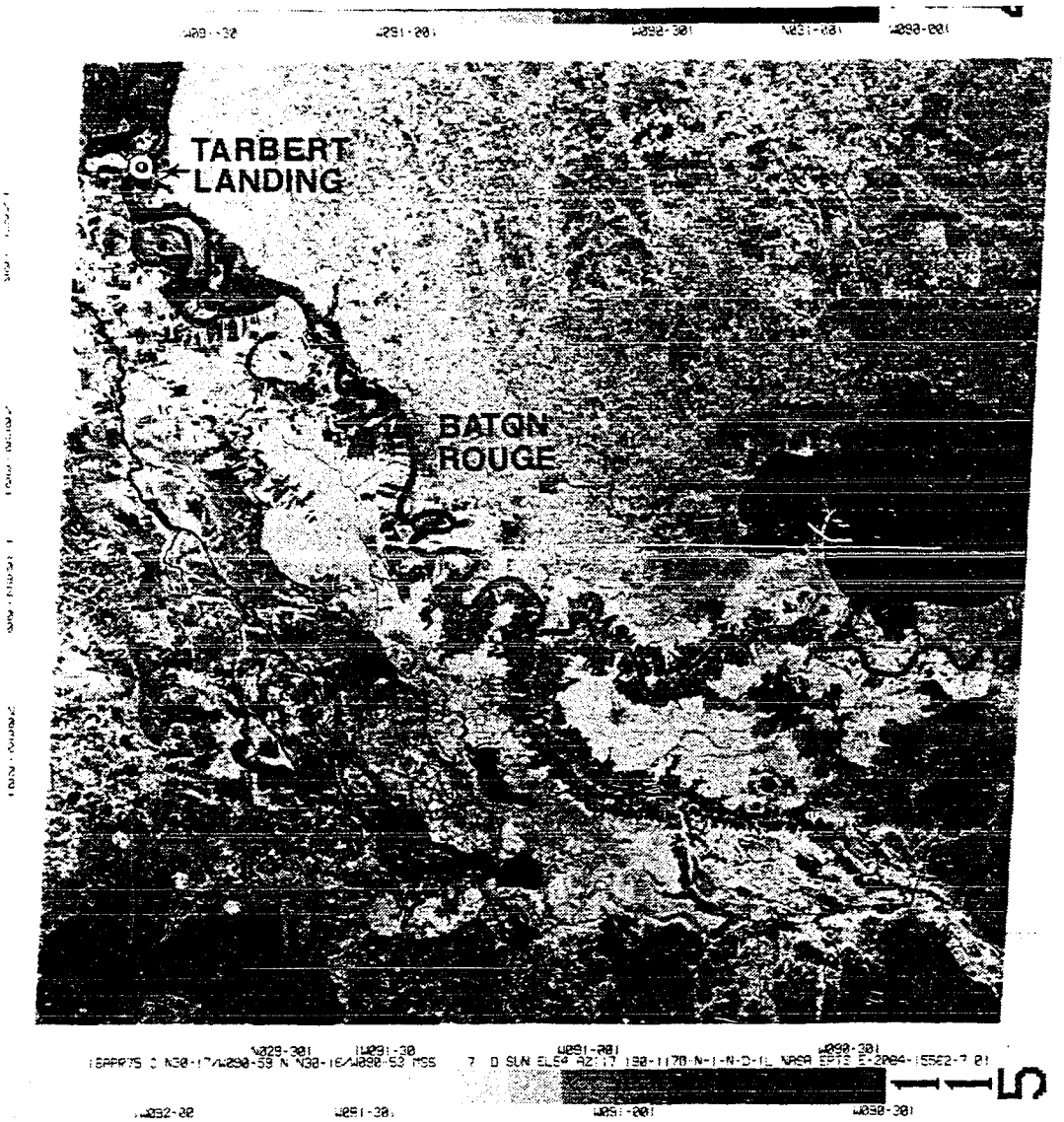

Fig. 1.--Landsat scene showing geographic location of study area (white circle).

4) to evaluate the feasibility and/or reliability of estimating suspended sediment concentrations in the entire depth of the river channel via Landsat MSS digital data.

CHAPTER II

ESTIMATION OF SUSPENDED SEDIMENT CONCENTRATIONS IN SUBSURFACE LAYERS

As mentioned previously, estimation of suspended sediment concentration in the subsurface layers of river water is one of the primary goals of this study. This chapter investigates the feasibility of obtaining reasonably accurate estimates of suspended sediment concentration by employing two contrasting approaches: 1) a theoretical approach which utilizes a deterministic model, and 2) an empirical approach using a statistical model. Later in the study, the two approaches will be evaluated in terms of their success in estimating the suspended sediment concentration and the problems involved in each of the two approaches will be discussed.

Methods

Data Collection

The U.S. Corps of Engineers, New Orleans District, periodically collects water samples of the Mississippi River at Tarbert Landing, Mississippi, and compiles a record of hydrological data.[1] The water samples are taken at five different depths in each of eight locations across the river channel (Figure 2), by using a point-integrating

[1] A sample of hydrological data compiled for a given sampling date is shown in Appendix 1.

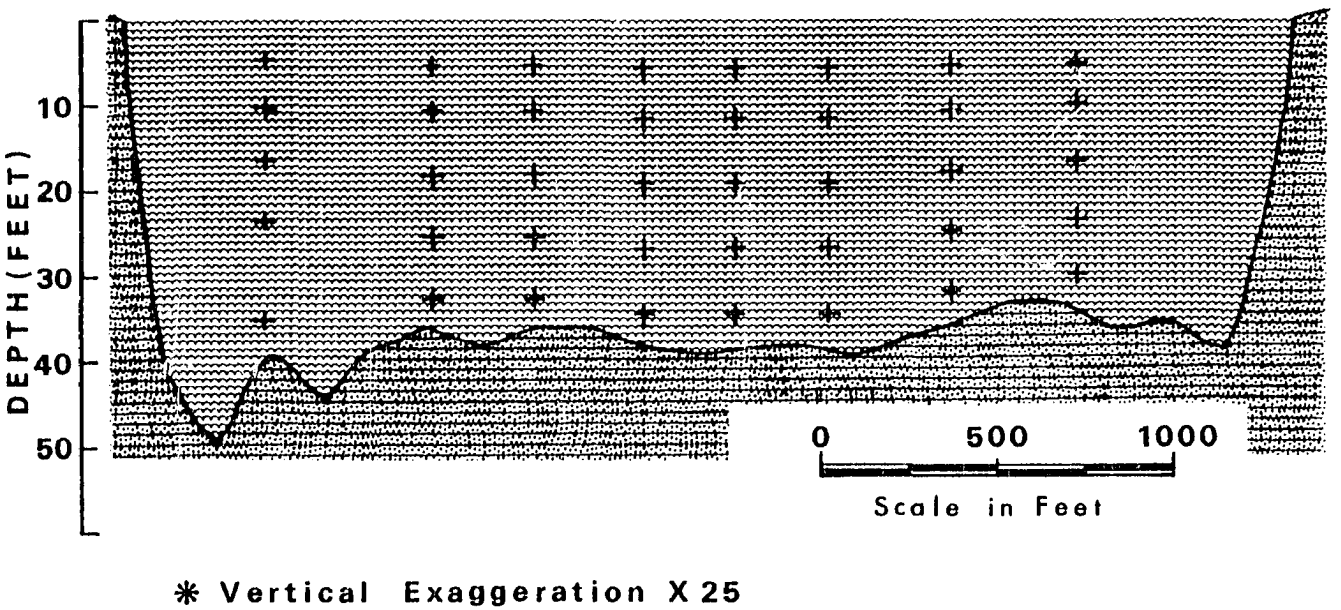

(source: U.S. Army Corps of Engineers, New Orleans District)

Fig. 2.--A typical cross section of the river channel at Tarbert Landing. The cross marks represent the water sampling points.

suspended sediment cable-and-reel sampler (US P-61 type). Typically, therefore, a total of 40 water samples are collected on a given sampling date along the entire cross section of the river channel. The water samples collected are labelled and sent to the water quality laboratory at the U.S. Geological Survey (USGS), Water Resources Division, in Baton Rouge, Louisiana for the suspended sediment analysis.

In the laboratory, the water samples are stored and allowed to settle in a dark room for approximately three weeks. After the settling period, the clear water is removed from the water sample bottle and the remaining solid particles are separated into two grain size categories (sand and silt-clay fractions) by using the U.S. standard sieve #230 (0.0625 mm in sieve openings).[1] The sand retained on the #230 sieve is washed into a pre-tared 100 cc beaker. The fine particles that pass through the #230 sieve are divided into two portions by a mechanical splitter; one half is washed into a 100 cc beaker and the other half into a 2,000 cc beaker. The larger beaker is used to collect cumulative fines from the 40 samples. Thus, the sediment in each water sample is partitioned into two 100 cc beakers, one for the sands and the other for one half of the fine particles, and also contributes to the sum of the fines collected in the 2,000 cc beaker.

---

[1]Sand fraction refers to the sediment particles coarser than 0.0625 mm and silt-clay fraction to those finer than 0.0625 mm. These grain size categories are currently utilized by the U.S. Corps of Engineers, New Orleans District, in compiling hydrological data.

The 2,000 cc beaker collects one half of the fine particles from each water sample. The fines accumulated from the entire 40 samples are utilized for the analysis of grain size distribution of the silt-clay fraction.

The two 100 cc beakers from each water sample are placed in an 175° C oven for about 18 hours. After the beakers have been completely dried, each beaker is weighed to 0.0001 grams to obtain the gross weight of the solid particles and the beaker. The net weight of the solid particles is then obtained by subtracting the tare weight from the gross weight for each grain size category. In addition, the (dried) sands are sieved to obtain the grain size distribution using the U.S. standard sieves #18 (1 mm), #35 (0.5 mm), #60 (0.25 mm), #120 (0.125 mm), and #230 (0.0625 mm). The cumulative weight on each sieve is measured to 0.0001 grams.[1]

Finally, the suspended sediment concentration in parts per million (p.p.m.) is computed as follows:

$$\text{Total concentration} = \frac{\text{SANDW} + 2 \times \text{HFINE}}{\text{total volume of sample}} \times 1{,}000{,}000$$

$$\text{Sand concentration} = \frac{\text{US230}}{\text{total volume of sample}} \times 1{,}000{,}000$$

Silt-clay concentration =

Total concentration - Sand concentration

where SANDW denotes net weight of the sand retained on the #230 wet sieve, HFINE net weight of one half of the fine particles, and US230 cumulative weight of the (dried) sands retained on the #230 dry sieve.

---

[1] A sample of laboratory data is shown in Appendix 2.

Further details on the laboratory procedures and the computational methods for the suspended sediment analysis are given by the USGS Water Resources Division (1973) and Chirieleison (1974).

The hydrological data utilized in this study are for the period of 1974-75 and include measurements of the hydrologic variables such as discharge, velocity, suspended sediment concentrations, and water sampling depth (Appendix 1).

Theoretical Approach: Diffusion Model

The diffusion model is not the only deterministic model that currently exists in the field; however, in view of the model's accuracy and mathematical complexities involved it seems to be most widely accepted and utilized in the engineering and geological sciences (e.g., Blatt, Middleton, and Murray, 1972). A detailed treatment of the diffusion model as well as a review of other theoretical models is given by Graf (1971). Similar accounts are also found in Einstein (1950), Scheidegger (1970), Bogárdi (1972), and Yalin (1977).

According to Graf (1971) and others, suspension of solid particles in a (convective) turbulent flow field can be generally described with the diffusion equation

$$\frac{\partial C}{\partial t} = - u_i \frac{\partial C}{\partial x_i} + \frac{\partial}{\partial x_i} \left(\varepsilon_i \frac{\partial C}{\partial x_i} \right) \qquad (1)$$

where C is the suspended sediment concentration, u_i the field velocity, x_i the axes of a Euclidean space, and ε_i the diffusion

coefficient that combines the coefficients of molecular and turbulent diffusion. In a three-dimensional flow field, therefore, (1) becomes

$$\frac{\partial C}{\partial t} = - u_1 \frac{\partial C}{\partial x_1} - u_2 \frac{\partial C}{\partial x_2} - u_3 \frac{\partial C}{\partial x_3} + \frac{\partial}{\partial x_1}\left(\varepsilon_1 \frac{\partial C}{\partial x_1}\right)$$

$$+ \frac{\partial}{\partial x_2}\left(\varepsilon_2 \frac{\partial C}{\partial x_2}\right) + \frac{\partial}{\partial x_3}\left(\varepsilon_3 \frac{\partial C}{\partial x_3}\right) \qquad (2)$$

Under the assumptions, however, that 1) $\partial C/\partial t = 0$; 2) $\partial C/\partial x_1 = \partial C/\partial x_3 = 0$; 3) mechanisms of mass and momentum transfers are identical; and 4) diffusivity of sediment particles in a turbulent flow is the same as that of fluid particles ($\varepsilon_s = \varepsilon_2$), the general diffusion equation (2) reduces to

$$0 = - u_2 \frac{\partial C}{\partial x_2} + \frac{\partial}{\partial x_2}\left(\varepsilon_s \frac{\partial C}{\partial x_2}\right) \qquad (3)$$

where ε_s is the diffusivity of sediment particles in x_2 direction. Note that with an additional assumption of

$$\frac{\partial u_2}{\partial x_2} = 0 \qquad (4)$$

(3) can be rewritten as

$$0 = \frac{\partial}{\partial x_2}\left(- u_2 C + \varepsilon_s \frac{\partial C}{\partial x_2}\right) = \upsilon_s C + \varepsilon_s \frac{\partial C}{\partial x_2} \qquad (5)$$

where υ_s, the settling velocity of the sediment particle, replaces the negative u_2 values.

The diffusion equation (5) is, as it is meant to be, "unrealistic"; that is, it only represents the (vertical) distribution of suspended sediments under uniform turbulence condition. In an effort to make it more realistic (under non-uniform turbulence conditions), consider the following relationships in a two-dimensional channel:

$$\frac{\tau_y}{\tau_0} = \frac{D - y}{D} \tag{6}$$

$$\frac{du}{dy} = \frac{u_*}{ky} \tag{7}$$

$$\tau_y = \rho \varepsilon \frac{du}{dy} \tag{8}$$

where u (field velocity in x_1 direction) and y (flow depth) replace u_1 and x_2, respectively, and τ_y the shear stress at the depth y, τ_0 the shear stress at the bottom, D the total flow depth, u_* the shear velocity, k the Karman's constant, ρ the fluid density, and ε the diffusivity of the fluid. From (6), (7), and (8), and invoking the assumption $\varepsilon_s = \varepsilon$,

$$\varepsilon_s = k u_* (D - y) \frac{y}{D} \tag{9}$$

Substituting (9) for ε_s in (5) and subsequent integration of dC/C yields[1]

$$\frac{C}{C_a} = \left(\frac{D - y}{y} \quad \frac{a}{D - a}\right)^z \tag{10}$$

where C_a is the "reference concentration at a distance a [from the bottom]" (Graf, 1971, p. 173), and $z = \upsilon_s/ku_*$. Note that the sediment concentration C of a given grain size[2] at any distance y from the bottom can be determined if C_a and z are known.

In order to evaluate the accuracy of (10), the equation can be rewritten as

$$\log \frac{C}{C_a} = z \log \left(\frac{D - y}{y} \quad \frac{a}{D - a}\right)$$

or could be generalized as

$$Y = z \; X \tag{11}$$

which is a form of linear regression equation without an intercept term. Since fitting of the data is required to determine the accuracy of (10), a modification of (11) is made such that

---

[1] According to Graf (1971), the solution (10) was first introduced by Rouse (1937).

[2] Because of the relationship $z = \upsilon_s/ku_*$, (10) is clearly influenced by the settling velocity υ_s, which is in turn determined by the grain size of solid particles.

$$Y = \beta_1 X + \xi \tag{12}$$

where it is assumed[1] that $\xi \sim (0, \sigma^{2*})$ and β_1 replaces z in (11). Also, a further modification of (11) is attempted such that

$$Y = \beta_0 + \beta_1 X + \xi \tag{13}$$

where β_0 is an intercept term.[2] Results from (12) and (13), in terms of their prediction (or estimation) accuracies, will be compared in a later section.

As described previously, the (vertical) sediment distribution equation (10), or (11), is derived for a particular grain size based on a two-dimensional flow. Therefore, analyses of the 1975 hydrological data using (12) are conducted according to the grain size categories (i.e., sand and silt-clay fractions separately) and the verticals (individual locations across the channel). In the data analyses using (12), the depth nearest to the water surface (Figure 2) is taken as the reference depth "a" given in (10).[3] In addition, the sediment data from the entire eight verticals are analysed without considering individual verticals. Also, a new variable flow

---

[1]The error term ξ is further assumed to have an approximate normal distribution.

[2]Note that the term β_0 in (13) does not appear in (10). Strictly speaking, therefore, (13) is not an equation of sediment distribution directly derived from the diffusion model.

[3]As may be indicated in Figure 2, the reference depth in the 1975 data varies from 1 to 3 meters below the water surface. Therefore, the total depth (D) in (10) is not equal to the reference depth (a).

"stage" is introduced so that the year is divided into two stage periods,[1] high stage (January through July 15) and low stage (July 15 through December), so that the data can be analysed according to the stages. For the purpose of comparison, (13) is also utilized in the analysis.

Empirical Approach: Linear Model

In the (univariate, full rank) linear model, the basic assumption is made that there is a linear relationship[2] of the form

$$Y = \beta_0 + \beta_1 X_1 + \beta_2 X_2 + \ldots + \beta_k X_k + e \qquad (14)$$

between the dependent variable Y and the independent variables X_j, $j = 1, 2, \ldots, k$. By defining

$$Y = \begin{bmatrix} y_1 \\ y_2 \\ \cdot \\ \cdot \\ \cdot \\ y_n \end{bmatrix}, \quad X = \begin{bmatrix} 1 & x_{11} & x_{12} & \cdots & x_{1k} \\ 1 & x_{21} & x_{22} & \cdots & x_{2k} \\ \cdot & \cdot & \cdot & \cdots & \cdot \\ \cdot & \cdot & \cdot & \cdots & \cdot \\ \cdot & \cdot & \cdot & \cdots & \cdot \\ 1 & x_{n1} & x_{n2} & \cdots & x_{nk} \end{bmatrix}, \quad B = \begin{bmatrix} \beta_0 \\ \beta_1 \\ \cdot \\ \cdot \\ \cdot \\ \beta_k \end{bmatrix}, \text{ and } E = \begin{bmatrix} e_1 \\ e_2 \\ \cdot \\ \cdot \\ \cdot \\ e_n \end{bmatrix}$$

---

[1] Division of the two stage periods is merely arbitrary. In Figure 3, the high stage corresponds to the period of average water discharge greater than 500,000 c.f.s.

[2] Choice of a statistical model, i.e., either linear or non-linear model may be subject to argument. Selection of the linear model over non-linear model is explained in the following discussion section. More detailed treatment of the theory of full rank linear model can be found in any advanced statistics textbook. See, for example, Searle (1971).

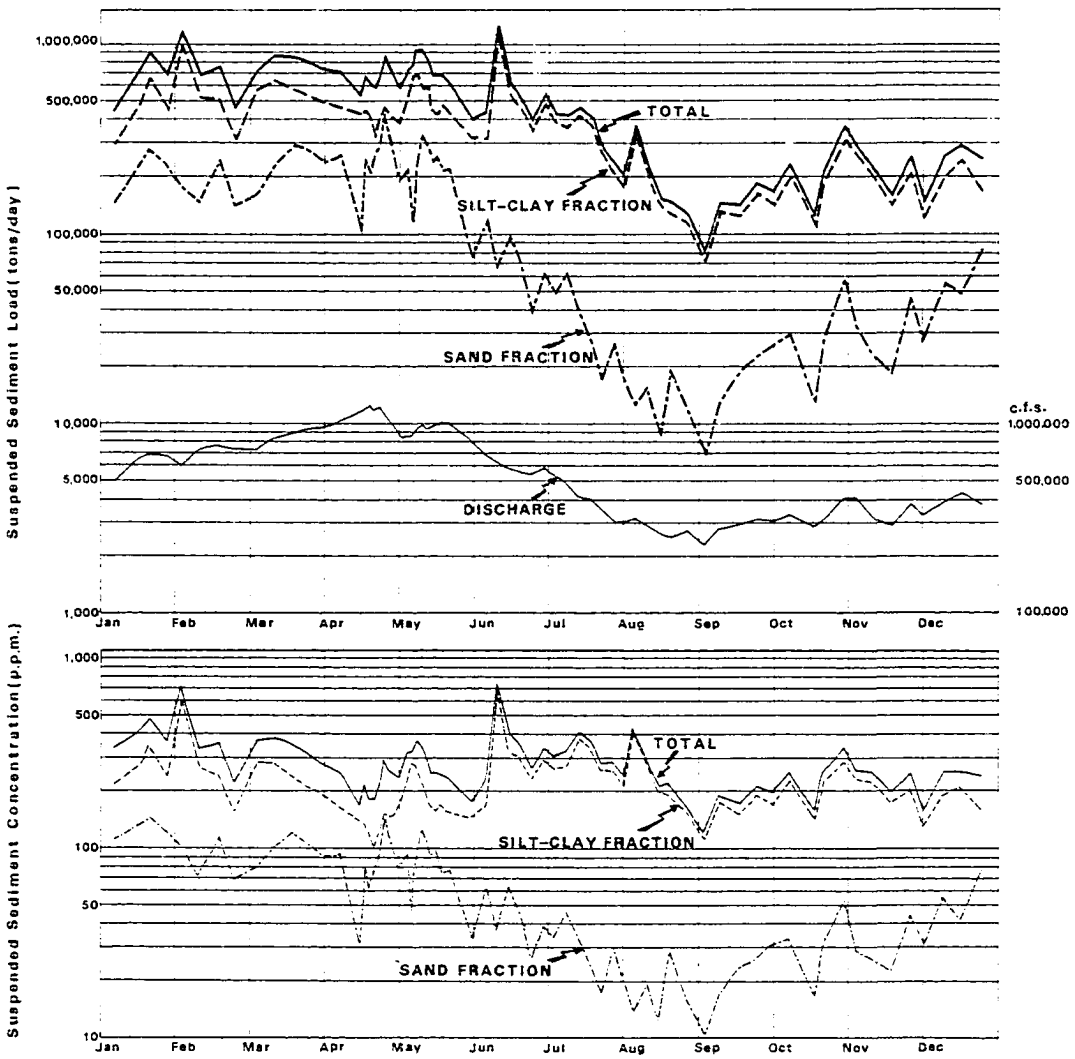

(source: U.S. Army Corps of Engineers, New Orleans District)

Fig. 3.--Discharge and suspended sediment of the Mississippi River at Tarbert Landing, Mississippi, in 1975.

the observations are represented as

$$\begin{bmatrix} y_1 \\ y_2 \\ . \\ . \\ . \\ y_n \end{bmatrix} = \begin{bmatrix} 1 & x_{11} & x_{12} & . & . & . & x_{1k} \\ 1 & x_{21} & x_{22} & . & . & . & x_{2k} \\ . & . & . & . & . & . & . \\ . & . & . & . & . & . & . \\ . & . & . & . & . & . & . \\ 1 & x_{n_1} & x_{n_2} & . & . & . & x_{nk} \end{bmatrix} \begin{bmatrix} \beta_0 \\ \beta_1 \\ . \\ . \\ . \\ \beta_k \end{bmatrix} + \begin{bmatrix} e_1 \\ e_2 \\ . \\ . \\ . \\ e_n \end{bmatrix} \tag{15}$$

or

$$\underset{(nx1)}{Y} = \underset{\{nx(k+1)\}}{X} \underset{\{(k+1)x1\}}{B} + \underset{(nx1)}{E} \tag{16}$$

where

$$E(Y) = X\,B \qquad \text{and} \qquad var(Y) = \sigma^2 I \tag{17}$$

For the purpose of making statistical tests possible, it is further assumed that

$$E \sim N(0,\ \sigma^2 I) \qquad \text{thus} \qquad Y \sim N(X\,B,\ \sigma^2 I) \tag{18}$$

The elements β_j of B are then estimated by[1]

$$\hat{B} = (X'X)^{-1} X'Y \tag{19}$$

---

[1]The unique solution for $\hat{B}$ in (19) corresponds to the least square estimator, with the constraint in (17), to the maximum likelihood estimator, with (18), and to the best linear unbiased estimator (b.l.u.e.) (Searle, 1971).

where

$$\hat{B} \sim N (B, \ (X'X)^{-1} \sigma^2) \tag{20}$$

It is immediately implied from (20) that

$$\widehat{var}(\hat{B}) = (X'X)^{-1} \hat{\sigma}^2 \tag{21}$$

where

$$\hat{\sigma}^2 = \frac{1}{n-k-1} \ Y' \{ I - X (X'X)^{-1} X' \} Y \tag{22}$$

The so-called fitted values (or predicted values) of y_i are obtained by

$$\hat{Y} = X \hat{B} \tag{23}$$

where

$$E(\hat{Y}) = X B \qquad var(\hat{Y}) = X (X'X)^{-1} X' \sigma^2 \tag{24}$$

Accordingly,

$$\widehat{var}(\hat{Y}) = X (X'X)^{-1} X' \hat{\sigma}^2 \tag{25}$$

The null hypothesis of primary interest is such that

$$H_0: \quad B^* = \begin{bmatrix} \beta_1 \\ \beta_2 \\ . \\ . \\ . \\ \beta_k \end{bmatrix} = 0 \tag{26}$$

which is equivalent to

$$H_0: \underset{k\times(k+1)}{\begin{bmatrix} 0 & 1 & 0 & 0 & \cdots & 0 \\ 0 & 0 & 1 & 0 & \cdots & 0 \\ 0 & 0 & 0 & 1 & \cdots & 0 \\ . & . & . & . & \cdots & . \\ . & . & . & . & \cdots & . \\ . & . & . & . & \cdots & . \\ 0 & 0 & 0 & 0 & \cdots & 1 \end{bmatrix}} \underset{(k+1)\times 1}{\begin{bmatrix} \beta_0 \\ \beta_1 \\ \beta_2 \\ . \\ . \\ . \\ \beta_k \end{bmatrix}} = \underset{k\times 1}{\begin{bmatrix} 0 \\ 0 \\ 0 \\ . \\ . \\ . \\ 0 \end{bmatrix}}$$

$$K' \qquad B \qquad = \qquad M \tag{27}$$

Using the matrix notation in (27), the consequences of the Cochran-Fischer theorem and the definition of the non-central F-distribution, the test statistic

$$F_c = \frac{\left(\frac{Q_H}{\sigma^2}\right)\Big/ k}{\left(\frac{Q_E}{\sigma^2}\right)\Big/ n-k-1} \sim F' \{ k, n-k-1, \lambda_H = \frac{1}{2\sigma^2} (K'B - M)' [K' (X'X)^{-1} K]^{-1} (K'B - M) \} \tag{28}$$

is formed, where

$$Q_H = (K'\hat{B} - M)' \; [K' (X'X)^{-1} K]^{-1} \; (K'\hat{B} - M) \qquad (29)$$

and

$$Q_E = Y' \{ I - X (X'X)^{-1} X' \} Y \qquad (30)$$

Rejection of H_0 in (26) occurs when $F_c > F(k, n-k-1)$.

A measure of the accuracy of prediction is also obtained by

$$R^2 = \frac{Q_H}{Y' (I - \frac{1}{n} 11') Y} = \frac{Q_H}{Q_H + Q_E} \qquad (31)$$

In the foregoing description of linear model theory, only general definitions were made of the dependent and independent variables; no specific variable names were given. Since suspended sediment concentrations are the quantities to be estimated, it is clear that the sediment concentrations should be taken as dependent variables. In so doing, they are grouped into three categories: sand fraction, silt-clay fraction, and the combined total concentrations. For each category, then, four variables are defined and each of them is evaluated using (14).[1] Definitions of the four dependent variables for each category and the seven independent variables are given in Table 1.

---

[1]Selection of the four dependent variables (for each category) and the seven independent variables is mainly based on the literature research.

TABLE 1

DEPENDENT AND INDEPENDENT VARIABLES FOR EMPIRICAL MODELLING OF SEDIMENT CONCENTRATIONS

Type	Category	Variable	Definition
Dependent Variables	Sand Fraction	SAND	Concentration of sand fraction (p.p.m.)
		LOGSAND	Logarithm of SAND
		CSAND	SAND divided by the reference concentration (RSAND)
		LCSAND	Logarithm of CSAND
	Silt-Clay Fraction	SILT	Concentration of silt-clay fraction (p.p.m.)
		LOGSILT	Logarithm of SILT
		CSILT	SILT divided by the reference concentration (RSILT)
		LCSILT	Logarithm of CSILT
	Total	TOTAL	Total suspended sediment concentrations (p.p.m.)
		LOGTOTAL	Logarithm of TOTAL
		CTOTAL	TOTAL divided by the reference concentration (RTOTAL)
		LCTOTAL	Logarithm of CTOTAL
Independent Variables		DISCH	Discharge (c.f.s.)
		LOGDISCH	Logarithm of DISCH
		VEL	Flow velocity (f.p.s.)
		RD	Relative depth (y/D in Equation 6)
		LOGRD	Logarithm of RD
		RSAND[1]	Reference concentration of sand fraction
		LOGRSAND[2]	Logarithm of RSAND

[1] Also RSILT and RTOTAL.

[2] Also LOGRSILT and LOGRTOTL.

Based on the initial evaluations, a dependent variable for each category is selected. The best set of independent variables (out of the seven variables) is determined based on the "max. R^2" criterion (Barr, et al., 1976) for the final estimation equations.

The crucial assumption of "linear" relationship expressed in (14) is examined by plotting the residuals (experimental errors), as illustrated by Draper and Smith (1966).

Results and Discussion

Diffusion Model

The entire 1975 data (a total of 1,984 observations) were analysed using (12) and (13), and the results are summarized in Table 2. It appears, at least from a probabilistic standpoint, that β_o in

TABLE 2

ANALYSES OF 1975 HYDROLOGICAL DATA
USING EQUATIONS (12) AND (13)

Equation†	$\hat{\beta}_0$	$\hat{\beta}_1$	$P(F>F_c)$	R^2	s_y	$\bar{y}$	c.v.(%)
Sand Fraction							
$y = \beta_1 x + \xi$		.2908**	.0001	.4141	.38	.28	135.8
$y = \beta_0 + \beta_1 x + \xi$	-.0315	.3162**	.0001	.1425	.38	.28	135.8
Silt-clay Fraction							
$y = \beta_1 x + \xi$		.0330**	.0001	.0852	.12	.03	362.9
$y = \beta_0 + \beta_1 x + \xi$	.0015	.0318**	.0001	.0169	.12	.03	363.0

†As noted in (11) and (12), $y = \log (C/C_a)$ and $x = \log (D-y/y)(a/D-a)$.

**Significance level $\alpha<.01$.

(13) is not "significantly" ($\alpha < .05$) different from zero for both grain size categories. Also notice that R^2 decreases considerably with (13), compared to (12), for both categories. These results indicate that (12), rather than (13), would be the better form of the equation for the vertical distribution of suspended sediments for each grain size category. Note, however, that accuracy of the equation (12) is only about 41% ($R^2 = .4141$) for the sand fraction and a meager 8% or so ($R^2 = .0852$) for the silt-clay fraction. Similar patterns are also shown in the analyses of the data by water stage period (Table 3). Here validity of the equation (12), again in comparison to (13), seems to be reaffirmed. Also notice that in the high water stage period accuracy of the (both) equations improves slightly for both grain size categories, yet the accuracy decreases all together in the low water stage period.

Analyses of the data by individual verticals (Table 4) reveal in general the same characteristics as noted above: the equation (12) seems more appropriate and superior in accuracy (as indicated by R^2) than (13). However, accuracy of (12) is still disappointingly low for all verticals, and it varies from about 9% to slightly over 60% for sand fraction and from almost nil to about 23% for silt-clay fraction. In the meantime, an interesting pattern revealed in Table 4 may deserve attention: while no immediate explanation seems available, $\hat{\beta}_1$ for sand fraction decreases almost consistently in one direction across the channel.[1] From a theoretical viewpoint this particular trend is rather puzzling, since there is no reason to believe that the

---

[1] Magnitudes of $\hat{\beta}_1$'s for silt-clay fraction appear to be random across the channel.

TABLE 3

ANALYSES OF 1975 HYDROLOGICAL DATA BY STAGE PERIOD

Water Stage	Equation	$\hat{\beta}_0$	$\hat{\beta}_1$	$P(F>F_c)$	R^2	s_y	$\bar{y}$	c.v.(%)
			Sand Fraction					
High	$y = \beta_1 x + \xi$		.3646**	.0001	.5510	.36	.37	99.7
	$y = \beta_0 + \beta_1 x + \xi$	.0219	.3470**	.0001	.1810	.37	.37	99.7
			Silt-clay Fraction					
	$y = \beta_1 x + \xi$		.0427**	.0001	.1261	.12	.04	283.7
	$y = \beta_0 + \beta_1 x + \xi$	.0079	.0363**	.0001	.0203	.12	.04	283.7
			Sand Fraction					
Low	$y = \beta_1 x + \xi$		.1779**	.0001	.2147	.38	.15	244.2
	$y = \beta_0 + \beta_1 x + \xi$	-.1110**	.2676**	.0001	.1110	.37	.15	242.3
			Silt-clay Fraction					
	$y = \beta_1 x + \xi$		.0182**	.0001	.0326	.11	.02	668.0
	$y = \beta_0 + \beta_1 x + \xi$	-.0081	.0247**	.0018	.0123	.11	.02	668.1

**Significance level $\alpha<.01$.

TABLE 4

ANALYSES OF 1975 HYDROLOGICAL DATA BY VERTICAL

Vertical	$y = \beta_1 x + \xi$						$y = \beta_0 + \beta_1 x + \xi$						
	$\hat{\beta}_1$	$P(F>F_c)$	R^2	s_y	$\bar{y}$	c.v.(%)	$\hat{\beta}_0$	$\hat{\beta}_1$	$P(F>F_c)$	R^2	s_y	$\bar{y}$	c.v.(%)
						Sand Fraction							
1	.4200**	.0001	.5967	.39	.44	88.8	.0905	.3485**	.0001	.1805	.39	.44	88.5
2	.4582**	.0001	.6042	.41	.45	92.2	-.0481	.4973**	.0001	.2594	.41	.45	92.3
3	.3710**	.0001	.5748	.36	.36	99.5	-.0528	.4130**	.0001	.2560	.36	.36	99.5
4	.2766**	.0001	.3733	.40	.26	150.4	-.0546	.3209**	.0001	.1350	.40	.26	150.5
5	.2513**	.0001	.4331	.32	.24	133.5	-.0547	.2956**	.0001	.1721	.32	.24	133.4
6	.2607**	.0001	.4104	.35	.25	137.1	-.0294	.2846**	.0001	.1404	.35	.25	137.2
7	.1739**	.0001	.2574	.33	.17	195.6	-.0269	.1959**	.0001	.0790	.33	.17	195.9
8	.1038**	.0001	.0962	.35	.09	387.0	-.0613	.1535**	.0012	.0436	.35	.09	386.7
						Silt-clay Fraction							
1	.0341**	.0001	.0681	.14	.03	415.0	.0012	.0332	.0606	.0145	.14	.03	415.9
2	.0552**	.0001	.2284	.11	.06	195.3	.0143	.0436**	.0030	.0347	.11	.06	195.4
3	.0362**	.0001	.1158	.11	.04	313.4	-.0017	.0375**	.0078	.0280	.11	.04	314.0
4	.0257**	.0001	.0693	.10	.03	402.3	.0022	.0239	.0883	.0124	.10	.03	403.1
5	.0441**	.0001	.1573	.11	.05	241.5	.0158	.0313*	.0356	.0181	.11	.05	241.5
6	.0322**	.0001	.1306	.09	.03	288.5	.0000	.0322**	.0070	.0288	.09	.03	289.1
7	.0355**	.0001	.1734	.08	.03	241.3	.0018	.0340**	.0021	.0362	.09	.03	241.8
8	.0000	.9980	.0000	.17	-.01	3862.3	-.0226	.0182	.4142	.0028	.17	-.01	3863.6

NOTE: For each vertical there are more than 200 observations.

*Significance level $\alpha<.05$.

**Significance level $\alpha<.01$.

shear velocity u_* varies (or increases in this particular case) almost consistently from vertical 1 to vertical 8 across the channel. However, this peculiar variation of $\hat{\beta}_1$ (for sand fraction) across the channel seems to occur in the high water stage period only (Table 5). Note that for each vertical, the accuracy of (12) seems to be considerably influenced by water stages. Note in Table 5 that R^2 (for the equation (12)) for sand fraction varies from about 33% to over 74% in the high water stage and from only .07% to about 72% in the low water stage. It appears that for the sand fraction equation (12) is much more accurate in the high water stage than in the low water stage. However, it is interesting to note that this tendency is not apparent for the finer fraction.

So far, major findings from the analyses of 1975 hydrological data have been mentioned and these results are now to be evaluated critically in the light of the diffusion model. Among the findings, of course, (prediction) accuracy of the equation (12) is of greatest interest. As mentioned previously, (12) seems to be more appropriate than (13) in accounting for the variation of suspended sediment concentrations through depth, yet the accuracy (of prediction) is remarkably low. The poor performance of the model in estimating suspended sediment concentrations can be explained as follows. One of the crucial assumptions made in order to derive equation (10) is that of a two-dimensional flow for which the relationships such as (6), (7) and (8) are postulated. Under this assumption, of course, any variation across the channel (or in X_3 direction) is not considered and therefore the relationships in (6), (7), and (8) are "assumed" to be true across the channel. Of particular interest is the vertical

TABLE 5

ANALYSES OF 1975 HYDROLOGICAL DATA BY STAGE AND VERTICAL

Water Stage	Vertical	$y = \beta_1 x + \xi$						$y = \beta_0 + \beta_1 x + \xi$						
		$\hat{\beta}_1$	$P(F>F_c)$	R^2	s_y	$\bar{y}$	c.v.(%)	$\hat{\beta}_0$	$\hat{\beta}_1$	$P(F>F_c)$	R^2	s_y	$\bar{y}$	c.v.(%)
							Sand Fraction							
	1	.4155**	.0001	.5294	.44	.44	100.7	.1143	.3246**	.0001	.1291	.44	.44	100.3
	2	.5540**	.0001	.7439	.36	.54	66.4	-.0361	.5833**	.0001	.3850	.36	.54	66.6
	3	.4624**	.0001	.6926	.35	.47	74.6	.0172	.4489**	.0001	.3087	.35	.47	74.9
High	4	.3902**	.0001	.5923	.36	.39	91.2	.0322	.3640**	.0001	.1968	.36	.39	91.5
	5	.3367**	.0001	.6236	.29	.33	87.1	-.0027	.3389**	.0001	.2477	.29	.33	87.4
	6	.3367**	.0001	.5407	.34	.34	100.5	.0424	.3022**	.0001	.1557	.34	.34	100.7
	7	.2460**	.0001	.4188	.32	.25	127.8	.0384	.2149**	.0001	.0972	.32	.25	128.0
	8	.1724**	.0001	.3354	.27	.17	160.2	-.0157	.1852**	.0001	.1015	.27	.17	160.7
							Silt-clay Fraction							
	1	.0530**	.0001	.1226	.16	.06	275.2	.0245	.0336	.1962	.0118	.16	.06	275.4
	2	.0630**	.0001	.3356	.10	.06	116.1	-.0172	.0770**	.0001	.1282	.10	.06	166.2
	3	.0408**	.0001	.1129	.13	.04	313.1	.0021	.0391	.0566	.0240	.13	.04	314.1
High	4	.0303**	.0018	.0660	.13	.03	381.7	.0158	.0175	.4218	.0045	.13	.03	382.4
	5	.0525**	.0001	.1529	.14	.06	239.1	.0270	.0306	.1849	.0120	.14	.06	239.0
	6	.0389**	.0001	.1309	.11	.04	285.2	.0019	.0374*	.0494	.0262	.11	.04	286.2
	7	.0427**	.0001	.1917	.10	.04	216.5	.0131	.0321*	.0461	.0256	.10	.04	216.9
	8	.0204*	.0348	.0300	.13	.02	655.8	-.0032	.0229	.2941	.0075	.13	.02	658.0

TABLE 5--Continued

Water Stage		$y = \beta_1 x + \xi$						$y = \beta_0 + \beta_1 x + \xi$						
		$\hat{\beta}_1$	$P(F>F_c)$	R^2	s_y	$\bar{y}$	c.v.(%)	$\hat{\beta}_0$	$\hat{\beta}_1$	$P(F>F_c)$	R^2	s_y	$\bar{y}$	c.v.(%)
							Sand Fraction							
	1	.4264**	.0001	.7184	.30	.44	69.0	.0571	.3816**	.0001	.3071	.30	.44	69.1
	2	.3131**	.0001	.3938	.43	.30	145.1	-.0680	.3682**	.0001	.1496	.43	.30	145.5
	3	.2248**	.0001	.3928	.31	.20	159.1	-.1422*	.3403**	.0001	.2316	.31	.20	156.5
Low	4	.0999**	.0059	.0805	.38	.06	609.3	-.1931*	.2563**	.0016	.1059	.37	.06	596.6
	5	.1201**	.0001	.1594	.31	.09	330.5	-.1360	.2303**	.0004	.1236	.30	.09	325.8
	6	.1505**	.0001	.2226	.31	.12	254.5	-.1287	.2551**	.0001	.1462	.31	.12	251.3
	7	.0640*	.0180	.0537	.30	.04	759.5	-.1242	.1653**	.0067	.0706	.30	.04	750.1
	8	-.0106	.7973	.0007	.43	-.04	1184.6	-.1323	.0971	.2984	.0123	.43	-.04	1180.2
							Silt-clay Fraction							
	1	.0076	.4236	.0065	.11	.00	23444.3	-.0332	.0337	.1003	.0273	.11	.00	23314.9
	2	.0434**	.0004	.1203	.13	.05	236.6	.0618*	-.0068	.7964	.0007	.13	.05	232.5
	3	.0287**	.0001	.1435	.08	.03	286.7	-.0067	.0341*	.0359	.0442	.08	.03	287.9
Low	4	.0184**	.0004	.1295	.05	.01	364.2	-.0191	.0339**	.0034	.0912	.05	.01	361.6
	5	.0312**	.0001	.2670	.06	.03	187.5	-.0016	.0325**	.0085	.0714	.06	.03	188.5
	6	.0226**	.0001	.1869	.05	.02	239.9	-.0023	.0244*	.0198	.0521	.05	.02	241.0
	7	.0245**	.0001	.1564	.06	.02	295.7	-.0150	.0367**	.0049	.0758	.06	.02	295.5
	8	-.0310	.1198	.0253	.22	-.04	520.3	-.0539	.0123	.7848	.0008	.22	-.04	519.8

NOTE: For every vertical in each stage, there are over 80 observations.

*Significance level $\alpha<.05$.

**Significance level $\alpha<.01$.

velocity distribution du/dy in (7), since du/dy largely determines the state of turbulence which in turn affects the transport of suspended sediments in a turbulent flow (Tennekes and Lumley, 1972). It is also known that du/dy takes a functional form shown in Figure 4. Indeed, one of the field samples from the Mississippi River channel plotted in Figure 5[1] reveals that the (vertical) velocity distributions for individual verticals agree reasonably well with the functional form depicted in Figure 4, even though some verticals (notably, verticals 1 and 8) show greater discrepancies than others. Note that there are only five observations for each vertical. Since only three "degrees of freedom for error" are available, no attempt was made to fit the data statistically for each vertical. Instead, the straight lines were drawn manually to enhance the visual interpretation of the (velocity) data distribution. Note further that the eight verticals do not share a single velocity distribution. In other words, the individual verticals maintain their own velocity distributions although they are similar to each other in functional form. In order to illustrate this the actual velocity distribution in the entire channel cross section on December 2, 1974 was estimated using 40 field measurements (point samples) across the channel and is shown in Figure 6. The estimation or "interpolation" was made using the SYMAP

---

[1]The velocity data plotted in Figure 5 were obtained on December 2, 1974, along with the suspended sediment samples. It may be noted that on this date a Landsat overpass took place over the river channel. Also, the sampling date (December 2, 1974) may be considered to be in the period of low water stage.

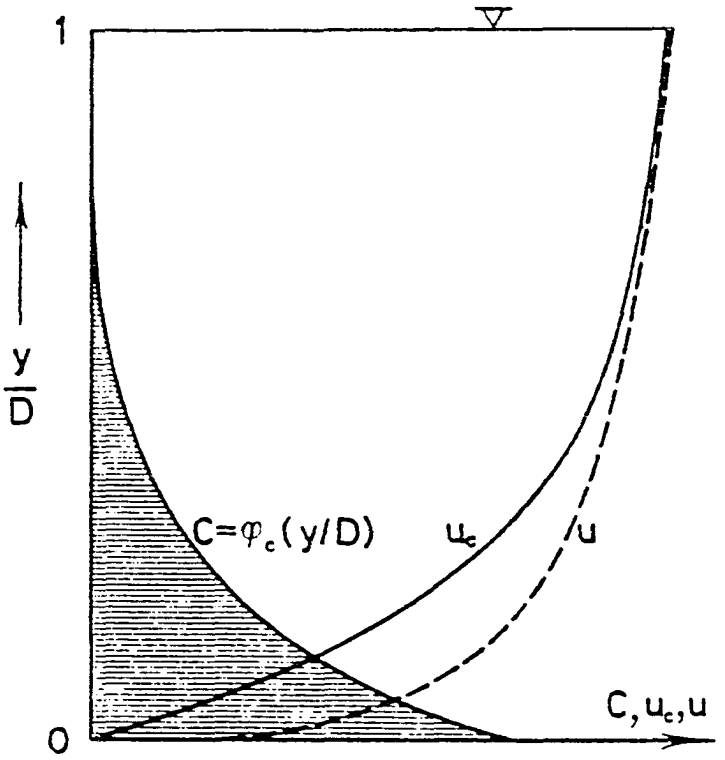

(modified from Yalin, 1977)

Fig. 4.--Vertical distributions of velocity and suspended sediments. The distributions of suspended sediment concentration (C) and the velocities of clear water (u) and sediment-loaded water (u_c) are schematically shown as a function of relative depth (y/D).

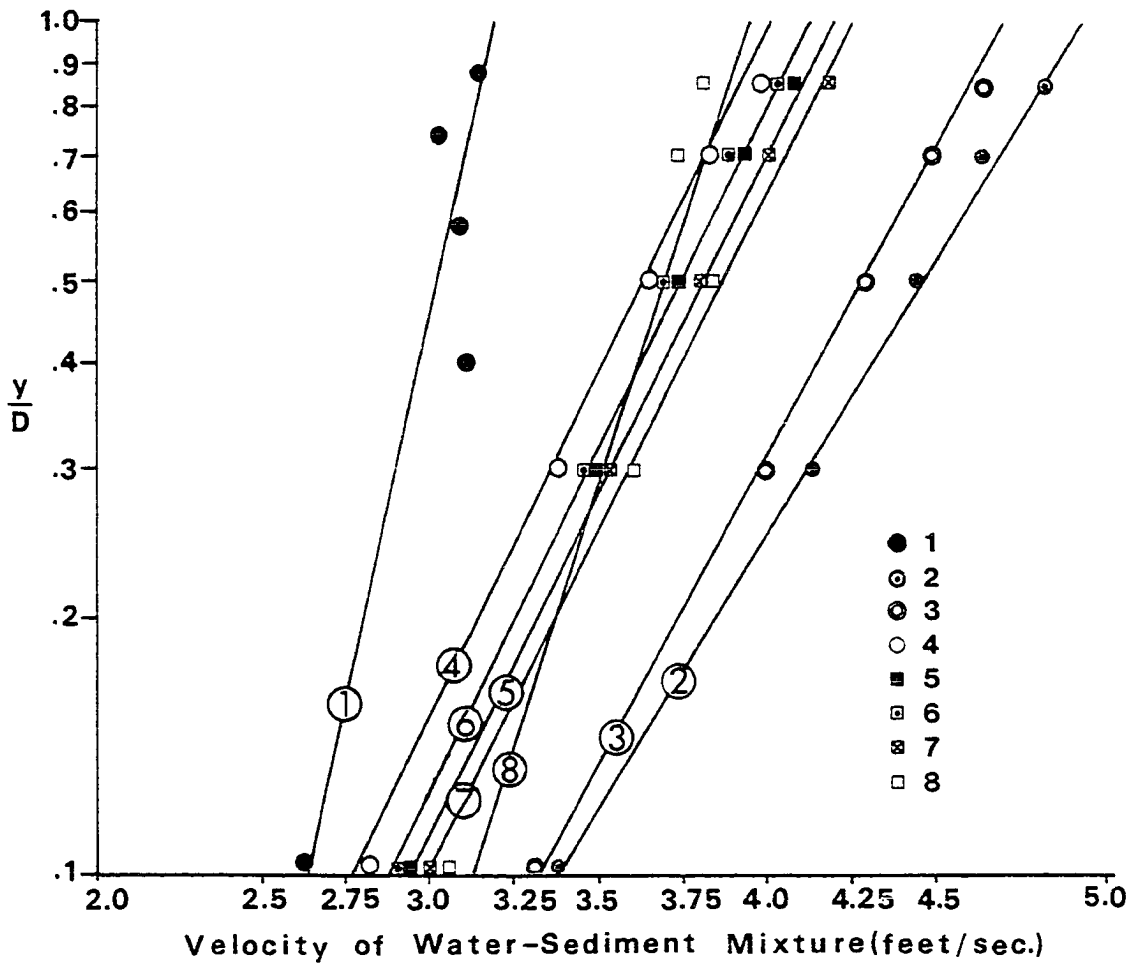

(source: U.S. Army Corps of Engineers, New Orleans District)

Fig. 5.--Velocity distribution of the Mississippi River at Tarbert Landing on December 2, 1974. The numbers indicate individual verticals. The first vertical is nearest the left bank and the eighth nearest the right bank (looking upstream).

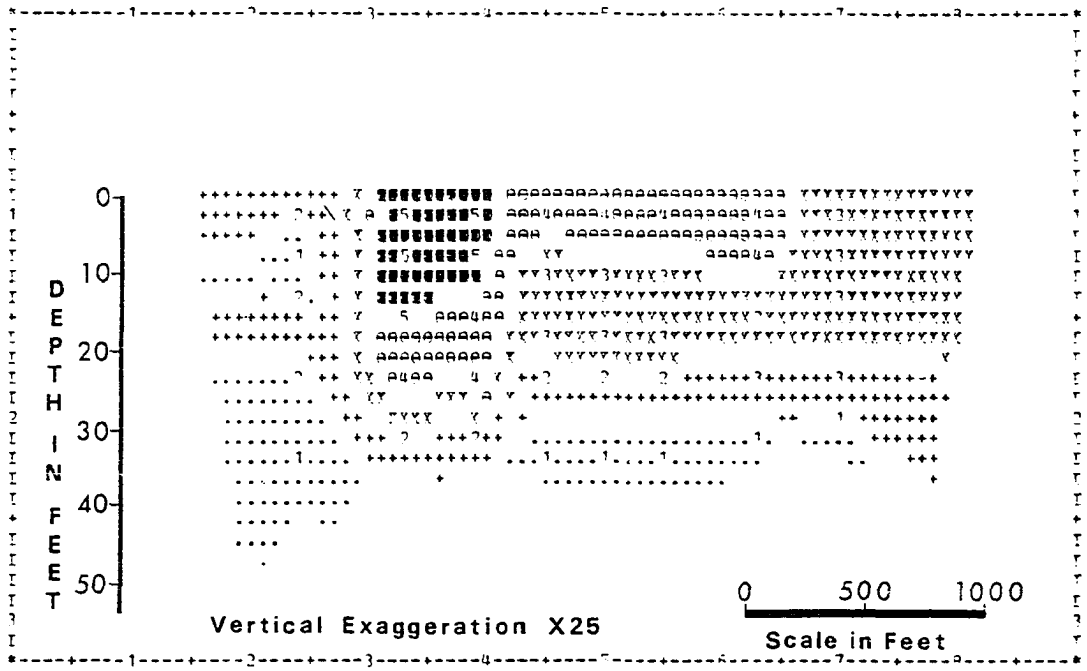

Fig. 6.--Velocity distribution in the channel cross section on December 2, 1974. The velocity varies from 2.63 f.p.s. to 4.81 f.p.s. The total velocity range (2.18 f.p.s.) is equally divided into five levels (2.63~3.07; 3.07~3.50; 3.50~3.94; 3.94~4.37; 4.37~4.81), so that the first level indicates the lowest velocity and the fifth level the highest.

computer mapping program.[1] For a detailed account of the interpolation theory see Shepard (1970). It is clearly seen that no single equation can describe the velocity distribution (du/dy) for the entire channel cross section. Mathematically, a statistical analysis indicates that a single equation for du/dy such as

$$\log \left(\frac{y}{D}\right) = \beta_0 + \beta_1 u \tag{32}$$

where β_0 and β_1 are coefficients and u is the velocity of water-sediment mixture (sediment-laden water), can account for only about 45% of the total variation (Table 6) involved in the field observations shown in Figure 5. This result, of course, reinforces the fallacy of using a single equation of du/dy for the entire channel cross section in which velocity distributions vary from one vertical to another.

According to the solution in (10), y/D and C/C_a have the relationship shown in Figure 4 (the curve denoted by $C = \varphi_c$ (y/D)) and it has been verified in the laboratory experiments (e.g., Vanoni, 1941). Mathematically, the relationship may be written as

---

[1] A standard procedure in SYMAP program is to equally divide total data value range (e.g., from 2.63 f.p.s. to 4.81 f.p.s. in Figure 6) into 5 "levels" so that each level represents 20% of the total range. On a SYMAP output, individual levels are represented by different symbols: the first level by ".", the second by "+", the third by "X", the fourth by "θ", and the fifth by "■". The numbers shown on the SYMAP output indicate the sampling locations and their data levels.

TABLE 6

SUMMARY OF REGRESSION ANALYSES FOR STREAM VELOCITY USING EQUATION (32)

Date	$\hat{\beta}_0$	$\hat{\beta}_1$	$P(F>F_c)$	R^2
Dec. 2, 1974	-1.9414**	.4170**	.0001	.4539
Apr. 16, 1975	-.6858**	.0443	.1129	.0744

**Significance level $\alpha<.01$.

TABLE 7

SUMMARY OF REGRESSION ANALYSES FOR SUSPENDED SEDIMENTS USING EQUATION (33)

Date	$\hat{\beta}_0$†	$\hat{\beta}_1$	$P(F>F_c)$	R^2
		Sand Fraction		
Dec. 2, 1974	-.3521**	-.6186**	.0001	.3535
Apr. 16, 1975	-.1203*	-.7618**	.0001	.6269
		Silt-clay Fraction		
Dec. 2, 1974	-.3158*	-1.4923**	.0013	.2404
Apr. 16, 1975	-.3641**	-.7700	.1487	.0622

†As noted in (33), $\beta_0 = \log K$.

*Significance level $\alpha<.05$.

**Significance level $\alpha<.01$.

$$\log \left(\frac{y}{D} \right) = \log K - \beta_1 \log \left(\frac{C}{C_a} \right) \tag{33}$$

where K is a constant, and the results of data "fitting" are summarized in Table 7. As expected, the relationship between y/D and C/C_a depicted in Figure 4 does not seem to be as strong as suggested by Vanoni (1941) and others, at least for this particular river channel on December 2, 1974 (Note in Table 7 that accuracy of (33) is about 35% for sand fraction and only 24% for the finer fraction). This result again illustrates the problem of assuming, among others, a consistent velocity distribution across the channel.

The difference between (10) and the "real world" is visually demonstrated in Figures 7 through 12 which depict the distribution of sediment. The actual distribution of suspended sediments in sand fraction, in the cross section looking upstream (Figure 7), reveals to some extent a pattern of lower concentration toward the surface and higher concentration near the bottom of the channel. Notable exceptions, however, can be seen toward the bank walls, especially near the right side of Figure 7 where sand-size particles show a more or less homogeneous vertical distribution. Furthermore, the asymmetric (if not random) distribution of sediment concentrations clearly indicates that the vertical distribution of shear stress, apart from the stream velocity, cannot be as simple as suggested by (6) in an ordinary river channel. For the purpose of comparison, predicted values of the sediment concentrations for the same field sampling locations were obtained using (12) and are shown in Figure 8. It is interesting to note that the "predicted" sediment distribution

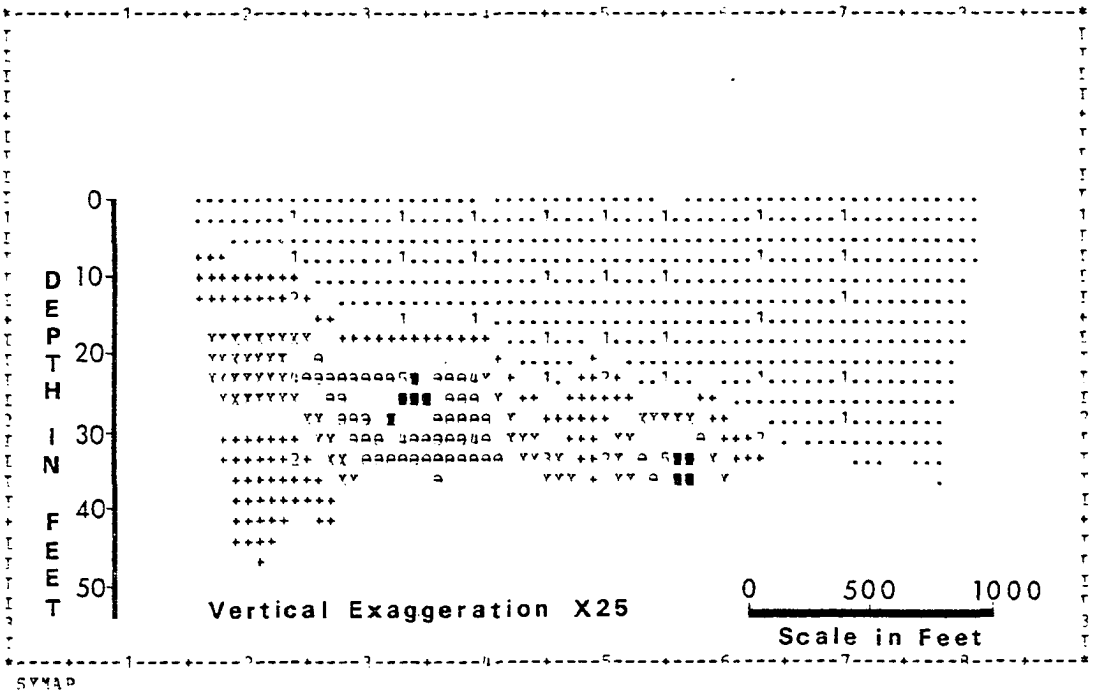

Fig. 7.--Measured suspended sediment concentration of sand fraction on December 2, 1974. The sediment concentration varies from 10.57 p.p.m. to 218.22 p.p.m. The five concentration levels are: 10.57~52.10; 52.10~93.63; 93.63~135.16; 135.16~176.69; 176.69~218.22.

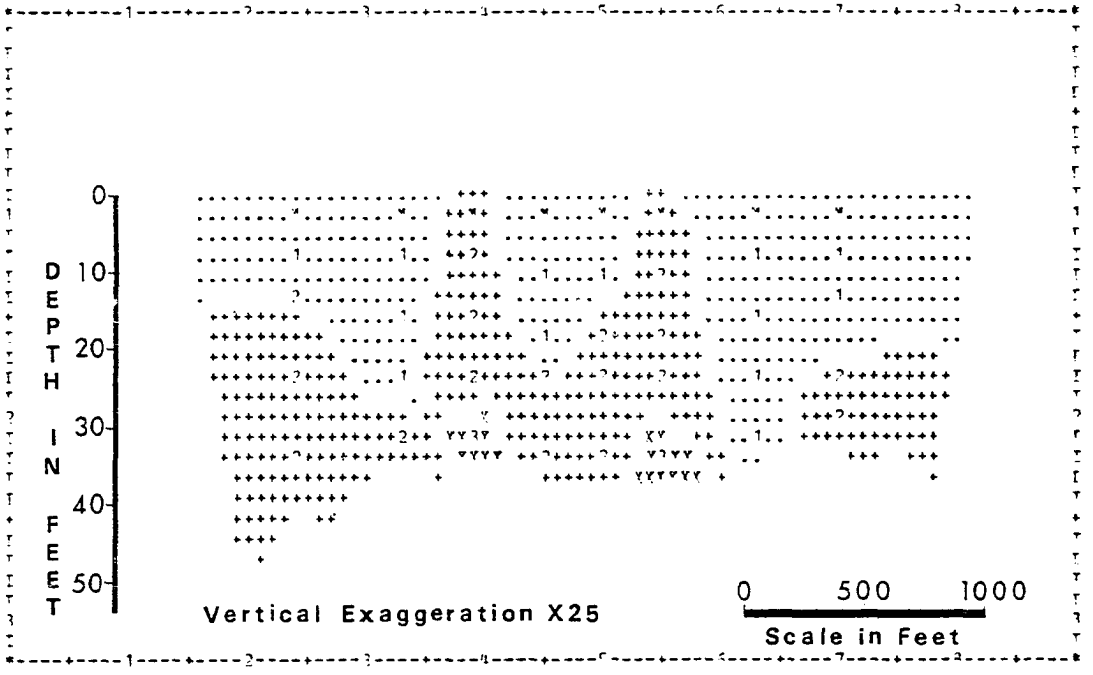

Fig. 8.--Estimated suspended sediment concentration of sand fraction on December 2, 1974. The estimated concentration varies from 22.91 p.p.m. to 104.32 p.p.m. The sediment concentration levels are same as given in Figure 7.

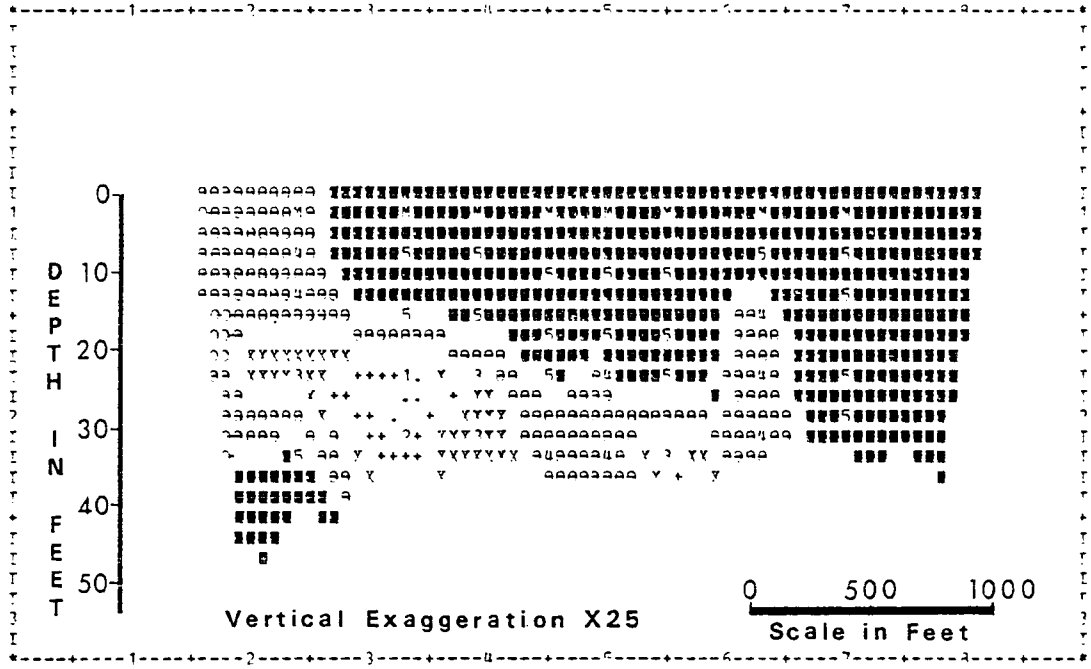

Fig. 9.--Difference between measured and estimated sediment concentrations of sand fraction on December 2, 1974. The five levels are: -171.94~-130.98; -130.98~-87.32; -87.32~-43.66; -43.66~0.00; 0.00~46.36. Since the difference is obtained by subtracting the measured concentration from the estimated concentration, the first four levels indicate underestimations and the fifth level over-estimation.

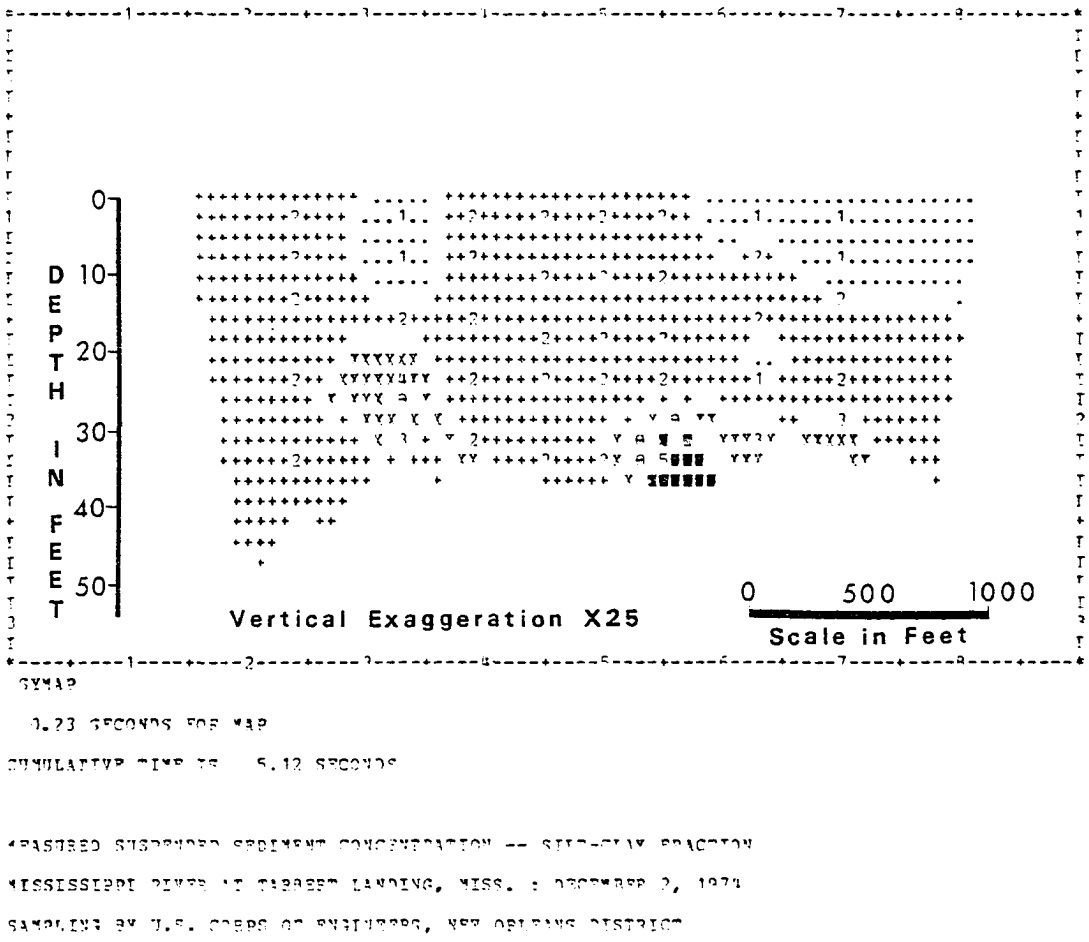

Fig. 10.--Measured suspended sediment concentration of silt-clay fraction on December 2, 1974. The sediment concentration varies from 153.56 p.p.m. to 609.66 p.p.m. The five concentration levels are: 153.56~244.78; 244.78~336.00; 336.00~427.22; 427.22~518.44; 518.44~609.66.

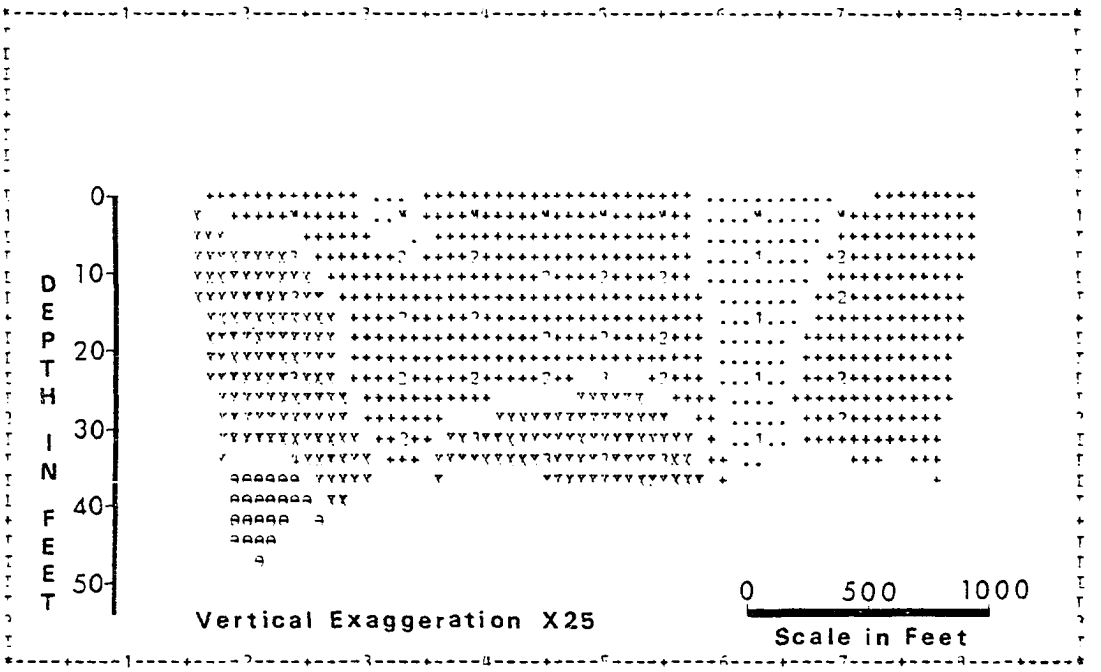

Fig. 11.--Estimated suspended sediment concentration of silt-clay fraction on December 2, 1974. The estimated concentration varies from 164.87 p.p.m. to 433.59 p.p.m. The sediment concentration levels are same as given in Figure 10.

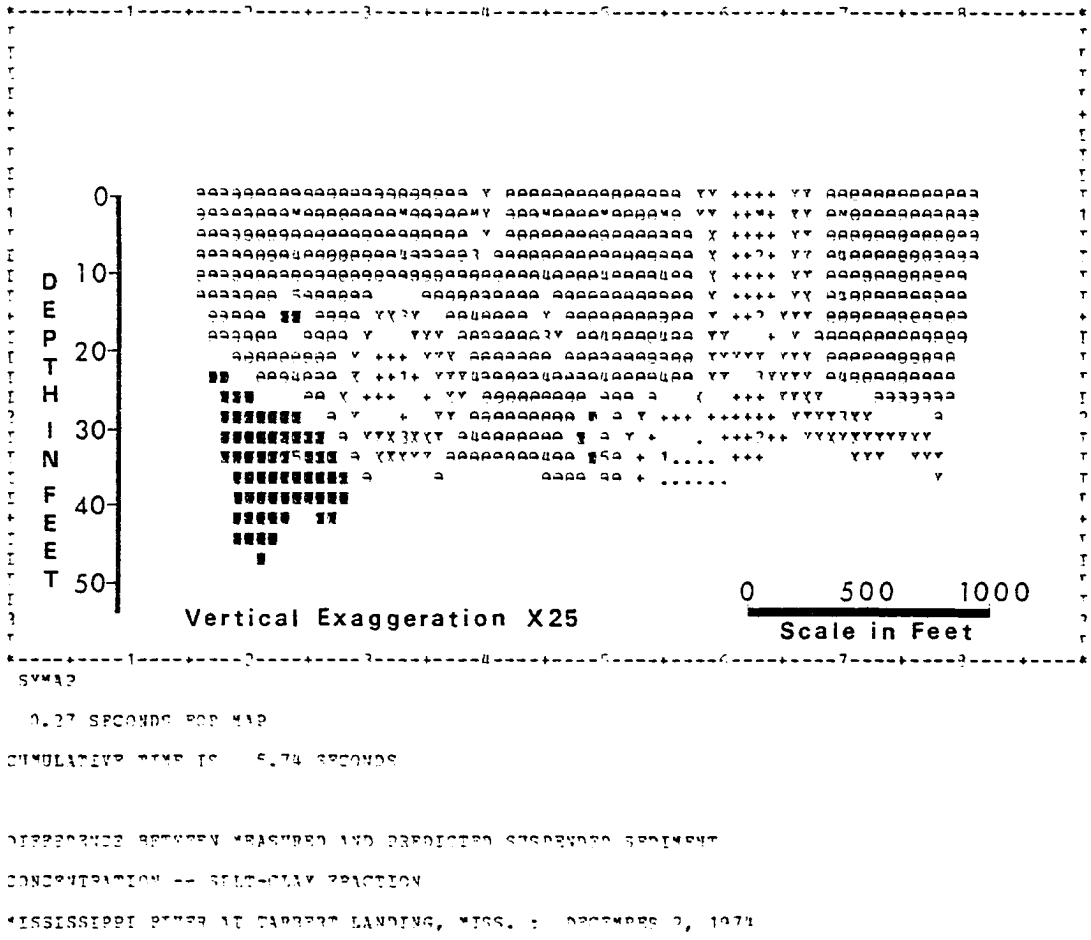

Fig. 12.--Difference between measured and estimated sediment concentrations of silt-clay fraction on December 2, 1974. The five levels are: -241.28~-157.00; -157.00~-78.50; -78.50~0.00; 0.00~78.50; 78.50~151.21. The first three levels indicate underestimations, and the fourth and the fifth levels overestimations.

in Figure 8 does not show higher sediment concentrations (higher than 135.16 p.p.m.) or the fourth and the fifth "levels" that actually occur in the channel (Figure 7).[1] Also note that the overall distribution pattern of the predicted sediment concentrations is markedly different from the actual distribution pattern shown in Figure 7. The differences between the actual and the predicted concentrations were obtained, for the individual sampling points, by subtracting the former from the latter and are shown in Figure 9. Most noticeable is the pattern of underestimating higher concentrations, notably the data (or concentration) levels 3, 4, and 5, and overestimating lower concentrations, the level 1 in particular (Figure 7). In addition, there appears to be some inverse relationship between higher concentrations and the degree of underestimation; that is, the higher the concentration, the more it is underestimated. The silt-clay fraction, on the other hand, shows a somewhat different distribution pattern in the channel as compared to the sand fraction. In Figure 10, actual distribution of the finer fraction appears to be rather uniform; the tendency of higher concentration toward the bottom is not as markedly shown as in the case of the sand fraction (Figure 7), although pockets of higher concentrations do occur near the bottom of the channel. The predicted sediment concentrations in Figure 11[2] reveal a more diversified pattern than the actual one (Figure 10), and also show no

---

[1] The same sediment concentration "levels" are applied to both Figures 7 and 8.

[2] As for the sand fraction, same sediment concentration levels are applied to both Figures 10 and 11; 5 levels for the total range (from 153.56 p.p.m. to 609.66 p.p.m.) with a range of 91.22 p.p.m. for each level.

sediment concentrations higher than 518.44 p.p.m. (level 5). The differences between the actual and the predicted concentrations were obtained in the same way as for the sand fraction and are given in Figure 12. Here, a general pattern similar to that of sand fraction (Figure 9) also seems to emerge; overestimation for the lower concentration areas (levels 1 and 2) and underestimation for the higher concentration zones (levels 3, 4, and 5). The inverse relationship (between higher concentrations and the degree of underestimation) mentioned for the sand fraction can also be seen for the levels 3, 4, and 5.

Up to this point, a major discussion has been focussed on the assumption of two-dimensional flow and subsequently the problem of applying a single velocity distribution function du/dy (as well as the shear stress distribution) to the entire channel cross section under study. Also, differences between the real world and the theory (given by (10)) have been visually demonstrated using SYMAP products. Now, attention is turned to yet another critical aspect involved in the diffusion model. Consider the velocity distribution given in Figure 13. The data used in Figure 13 were collected on April 16, 1975,[1] which is within the period of high water stage (Figure 3). Note in Figure 13 that the velocity distribution in the channel cross section is considerably different from the one shown in Figure 6. What is immediately implied, then, is that one of the assumptions required to derive (5) from (2), i.e., $\partial C/\partial t = 0$, is no longer valid.

---

[1] A Landsat overpass also took place on this date over the river channel.

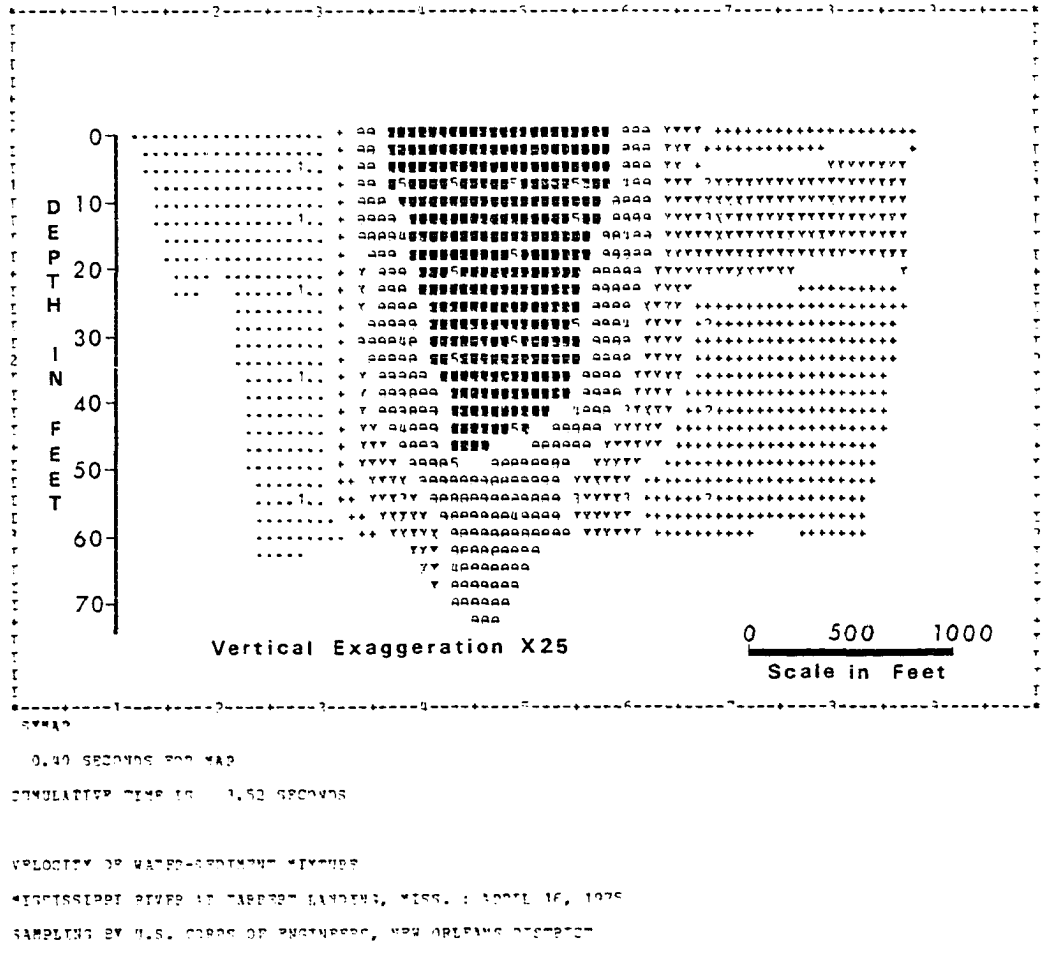

Fig. 13.--Velocity distribution in the channel cross section on April 16, 1975. The velocity varies from 2.18 f.p.s. to 9.07 f.p.s. The five velocity levels are: 2.18~3.56; 3.56~4.94; 4.94~6.31; 6.31~7.69; 7.69~9.07.

This, in turn, indicates that the solution in (10) may not be applied to the sediment data collected over a period of time for which $\partial C/\partial t \neq 0$, i.e., when sediment concentrations vary from time to time. A detailed examination of this (April 16, 1975) data, as was done for the December data previously, is given in the following.

The velocity data[1] plotted in Figure 14 show that the vertical velocity distributions, in general, agree with the functional form depicted in Figure 4. It should be noted, however, that the velocity distribution of the (first) vertical nearest to the left side of Figure 14 deviates greatly from the general pattern. A similar disagreement is, to some extent, also seen in the (seventh) vertical nearest to the right bank (looking upstream). In any event, it is again indicated from both Figures 13 and 14 that no single equation for du/dy can adequately describe the velocity distribution of the entire cross section. In fact, a statistical analysis reveals that a single equation of the form (32) can only account for some 7% of the total variation (Table 6) involved in the velocity data shown in Figure 14. Also, the relationship expressed in (32) is much less reliable ($P(F>Fc) = .1129$) in this case than the one previously considered (As seen in Table 6, $P(F>Fc) = .0001$ for the December data). Considering actual velocity distributions, however, these outcomes are not surprising at all since the vertical velocity distributions in general vary greatly across the channel (for instance, note in Figure 14 that the location nearest to the bottom in vertical 6 has greater

---

[1]Unfortunately, velocity data for the eighth vertical are missing. In Figure 14, no attempt was made to draw straight lines since the pattern of data points scatter can be readily recognized.

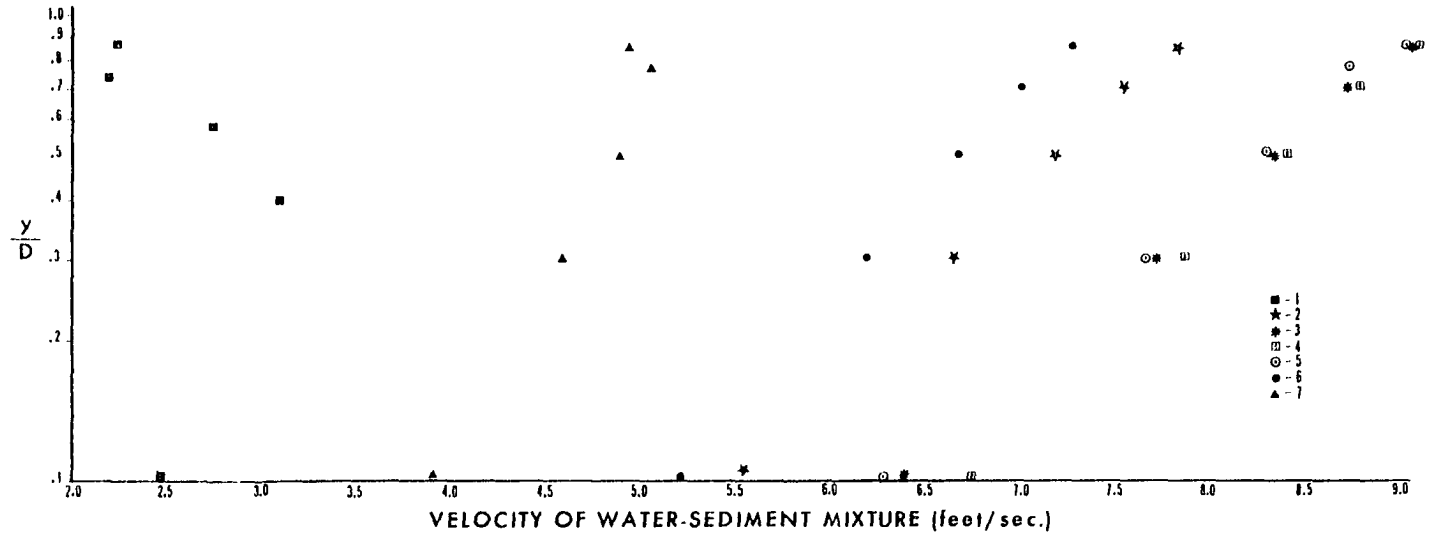

(source: U.S. Army Corps of Engineers, New Orleans District)

Fig. 14.--Velocity distribution of the Mississippi River at Tarbert Landing on April 16, 1975. The numbers (and associated symbols) represent individual verticals.

velocity than the point nearest to the surface in vertical 7).

The theoretical relationship between (relative) depth and sediment concentration, given in (33), was also examined and the result is included in Table 7. Note that the sand fraction from the April 16, 1975 data shows an accuracy of some 63%, a substantial improvement over 35% for the December data, yet the finer fraction does not reveal any (statistically) significant relationship (at $\alpha < .05$). These discrepancies are also visually illustrated in Figures 15 through 20 for both fractions from the April 16, 1975 data, as was done for the December data. In Figure 15, the actual distribution of suspended sediments in sand fraction again reveals a general tendency of lower concentration toward the surface and higher concentration near the bottom of the channel. A notable exception, however, is also seen near the left side of Figure 15 where a lower level of concentration (3.31 p.p.m. to 56.51 p.p.m.) prevails throughout the depth. The predicted sediment concentrations (Figure 16), in the meantime, seem more closely in agreement with the actual concentrations, compared to the December data, particularly in the higher concentration areas. Furthermore, note in Figure 17 that there is no apparent trend toward underestimating higher concentrations and overestimating lower concentrations, which was seen in the December data. Some major discrepancies, however, can still be noticed; for instance, an area of intermediate concentrations (109.71 p.p.m. to 162.91 p.p.m.) near the bottom is so exceedingly overestimated that the area denoted by the letter symbols "H"'s (in Figure 16) represents sediment concentrations greater than the maximum concentration (269.31 p.p.m.) observed in the field. The silt-clay fraction, on the other hand, reveals a

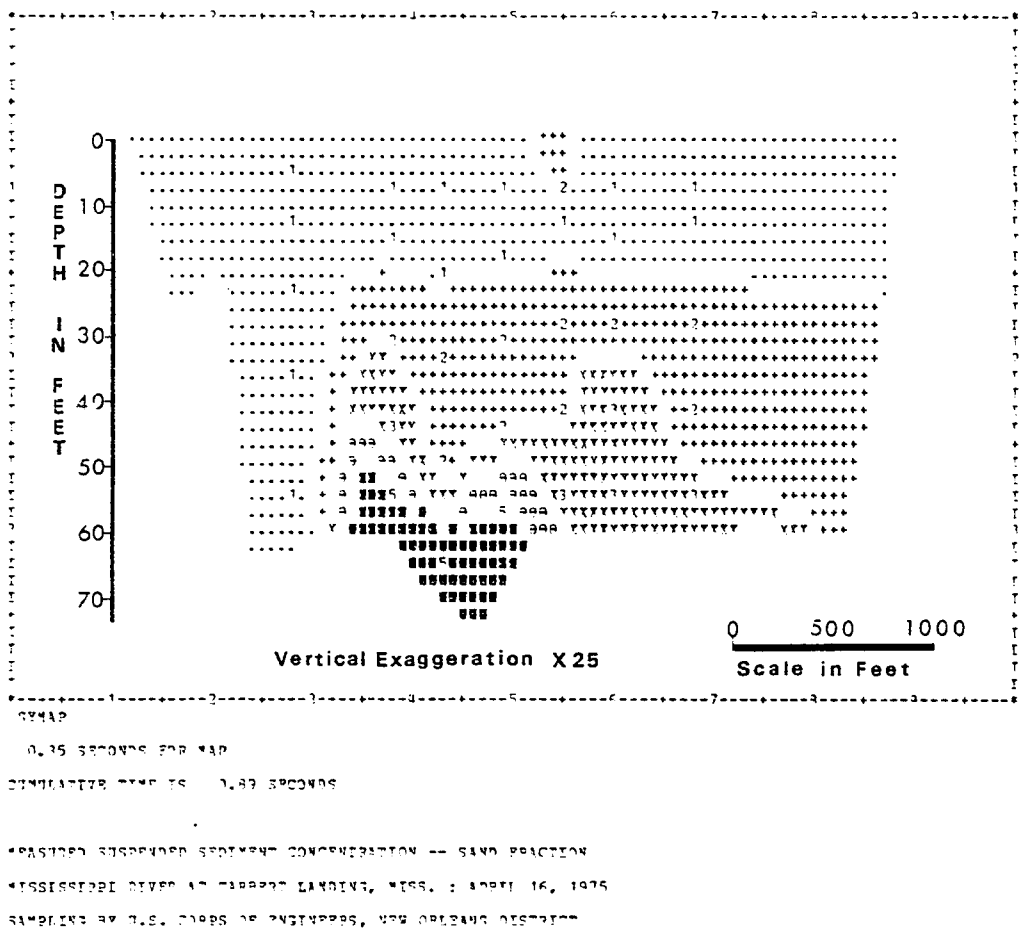

Fig. 15.--Measured suspended sediment concentration of sand fraction on April 16, 1975. The sediment concentration varies from 3.31 p.p.m. to 269.31 p.p.m. The five concentration levels are: 3.31~56.51; 56.51~109.71; 109.71~162.91; 162.91~216.11; 216.11~269.31.

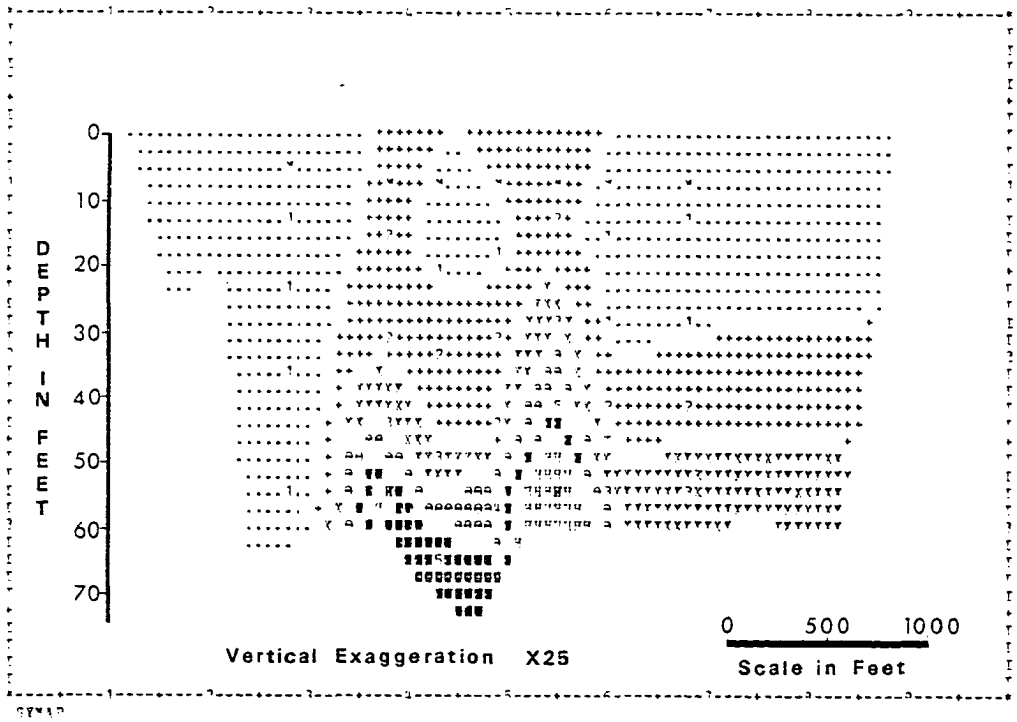

Fig. 16.--Estimated suspended sediment concentration of sand fraction on April 16, 1975. The estimated concentration varies from 5.22 p.p.m. to 429.90 p.p.m. The sediment concentration levels are same as given in Figure 15.

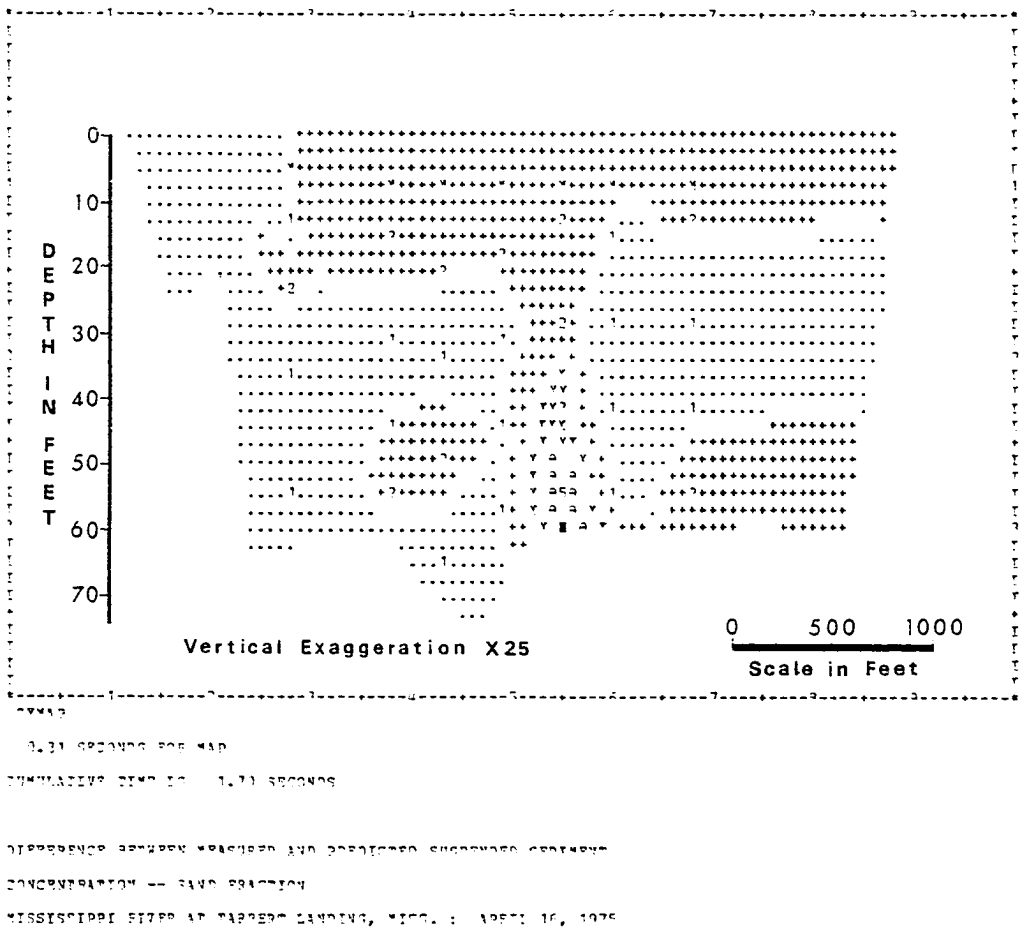

Fig. 17.--Difference between measured and estimated sediment concentrations of sand fraction on April 16, 1975. The five levels are: -82.29~0.00; 0.00~82.29; 82.29~164.58; 164.58~246.87; 246.87~279.16. The first level indicates underestimation and the next four levels overestimations.

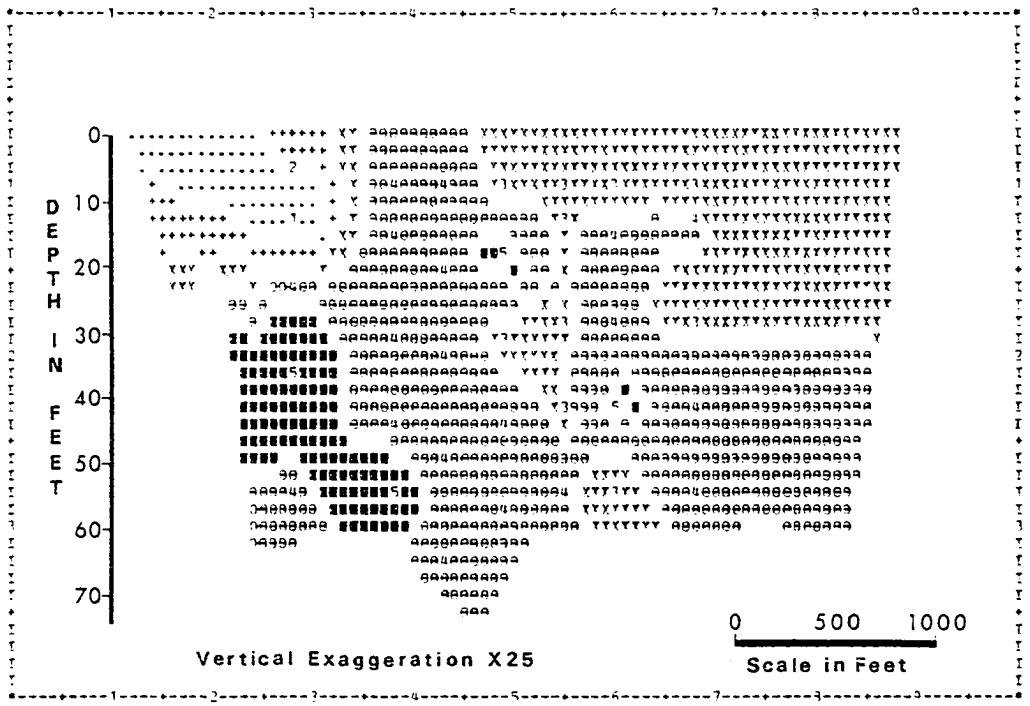

Fig. 18.--Measured suspended sediment concentration of silt-clay fraction on April 16, 1975. The sediment concentration varies from 45.88 p.p.m. to 192.90 p.p.m. The five concentration levels are: 45.88~75.28; 75.28~104.69; 104.69~134.09; 134.09~163.50; 163.50~192.90.

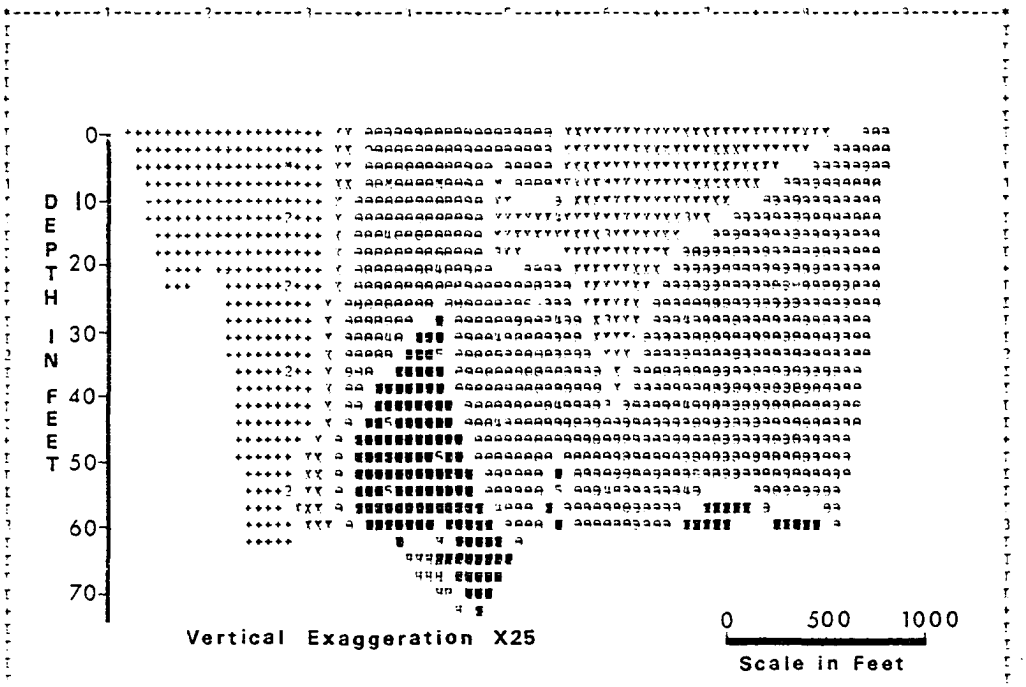

Fig. 19.--Estimated suspended sediment concentration of silt-clay fraction on April 16, 1975. The estimated concentration varies from 81.69 p.p.m. to 194.89 p.p.m. The sediment concentration levels are same as in Figure 18.

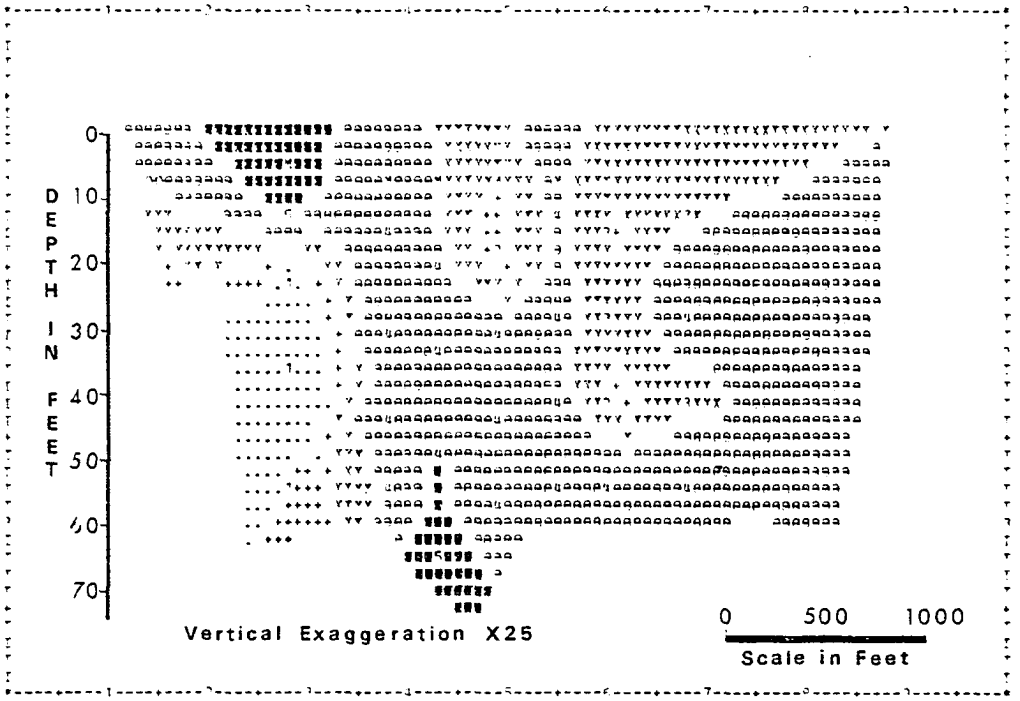

Fig. 20.--Difference between measured and estimated sediment concentrations of silt-clay fraction on April 16, 1975. The five levels are: -103.61~-60.00; -60.00~-30.00; -30.00~0.00; 0.00~30.00; 30.00~46.13. The first three levels indicate underestimations, and the fourth and the fifth levels overestimations.

considerably different distribution pattern from the sand fraction. In Figure 18, the actual distribution of the finer fraction seems to show no general pattern of higher concentration toward the channel bottom. In addition, the predicted concentration pattern in Figure 19 is grossly misleading, as expected from the low R^2 value in Table 7. As to the difference between the actual and the predicted concentrations, there are some indications of underestimating higher concentrations and vice versa (Figure 20) although the pattern is not as prominent as for the finer fraction in the December data.

To summarize, results of the analyses of 1975 hydrological data and a part of 1974 data indicate that the diffusion model cannot be used successfully in estimating suspended sediment concentrations in, at least, the natural river channel under study, even though the functional form of the model (in (10)) appears to be appropriate. The results vary widely with regard to the accuracy of the solution in (10) depending upon grain size (fraction), vertical, water stage, and combination of these factors. The only fairly consistent result is that the sand fraction appears to be estimated more accurately by the model than the finer fraction. The water stages, although arbitrarily defined, seem to have some effect on the prediction (or estimation) accuracy, however, neither theoretical grounds nor conclusive evidence are available at present. As to the problems involved in the model and in an effort to explain the poor performance of the model, two major assumptions that do not hold for the river channel under study have been discussed. These assumptions are: 1) a single velocity distribution du/dy based on a two-dimensional flow and subsequent shear stress distribution, and 2) the steady state condition of

suspended sediment concentrations, i.e., $\partial C/\partial t = 0$. It may be further pointed out that the imposed assumptions such as $\partial C/\partial x_3 = 0$ and $\partial u_2/\partial x_2 = 0$ cannot be applied to the channel under study.

Linear Model

In an attempt to find the best predictive relationships between sediment concentrations and the selected seven (independent) variables, the entire set of 1975 data was analysed using (14) and the results are given in Table 8. Note that the logarithmic transformation of original observations in sediment concentrations gives rise to the highest R^2 values for each fraction as well as the total concentration. From this result, it seems appropriate to choose LOGSAND, LOGSILT, and LOGTOTAL as the dependent variables representing the concentrations of sand fraction, silt-clay fraction, and the combined total, respectively. For each of the three dependent variables so obtained, Table 9 shows the models that provide the maximum R^2 for a given number of independent variables included in the linear model (14). Suppose, for instance, that the sediment concentrations are to be estimated by means of y/D and C_a (the "reference" concentration or the surface concentration in this case). As seen in Table 9, the linear model[1]

$$\log C = \beta_0 + \beta_1 \frac{y}{D} + \beta_2 \log C_a + e \qquad (34)$$

would provide a predictive accuracy of about 46% ($R^2 = .4634$) and 41%

---

[1]Notations compatible with those in the diffusion model are used in (34) and other linear equations that follow. For example, log C for LOGSAND (or LOGSILT, or LOGTOTAL), y/D for RD, C_a for RSAND (or RSILT, or RTOTAL), etc.

TABLE 8

SUMMARY OF REGRESSION ANALYSES FOR SUSPENDED SEDIMENT CONCENTRATIONS

y_i	$\hat{\beta}_0$	$\hat{\beta}_1$	$\hat{\beta}_2$	$\hat{\beta}_3$	$\hat{\beta}_4$	$\hat{\beta}_5$	$\hat{\beta}_6$	$\hat{\beta}_7$	$P(F>F_c)$	R^2
Sand Fraction										
SAND	-664.25**	-.00**	141.49**	14.23**	9.99	-132.02**	.17	58.88**	.0001	.3647
CSAND	-28.03**	-.00**	8.30**	.46**	.61	-5.33**	.01	-4.02**	.0001	.1986
LOGSAND	-3.32**	-.00**	.99**	.05**	-.38**	-.30**	-.00**	.78**	.0001	.5499
LCSAND	-3.32**	-.00**	.99**	.05**	-.38**	-.30**	-.00**	-.22**	.0001	.3038
Silt-clay Fraction										
SILT	-90.35	-.00**	103.23**	1.22	-60.12*	10.91	1.20**	-121.09**	.0001	.5742
CSILT	2.96**	-.00**	.75**	-.00	-.30*	.08	.00**	-2.19**	.0001	.1302
LOGSILT	.48**	-.00**	.18**	.00	-.09*	.02	.00**	.48**	.0001	.5947
LCSILT	.48**	-.00**	.18**	.00	-.09*	.02	.00**	-.52**	.0001	.0898
Total										
Total	-1057.89**	-.00**	330.05**	18.25**	-117.16	-89.70	1.11**	-74.38	.0001	.1976
CTOTAL	-1.54	-.00**	1.57**	.08**	-.50	-.39	.00	-1.47**	.0001	.1076
LOGTOTAL	-.52*	-.00**	.35**	.02**	-.14*	-.10**	.00	.66**	.0001	.4713
LCTOTAL	-.52*	-.00**	.35**	.02**	-.14*	-.10**	.00	-.34**	.0001	.2114

NOTE: The independent variables used in the analyses for DISCH (X_1), LOGDISCH (X_2), VEL (X_3), RD (X_4), LOGRD (X_5), RSAND (or RSILT, or RTOTAL) (X_6), and LOGRSAND (or LOGRSILT, or LOGRTOTL) (X_7). See Table 1 for their definitions.

*Significance level $\alpha<.05$.

**Significance level $\alpha<.01$.

TABLE 9

THE "BEST" MODELS (BASED ON MAX. R^2)
FOR THE SEDIMENT CONCENTRATIONS

Dependent Variable	No. of Variables in the Model (14)	R^2	Independent Variables in the Model
LOGSAND (N = 1975)	1	.3760	LOGRSAND
	2	.4634	RD LOGRSAND
	3	.5244	LOGDISCH LOGRD LOGRSAND
	4	.5333	LOGDISCH VEL LOGRD LOGRSAND
	5	.5431	DISCH LOGDISCH VEL LOGRD LOGRSAND
	6	.5477	DISCH LOGDISCH VEL LOGRD RSAND LOGRSAND
	7	.5499	DISCH LOGDISCH VEL RD LOGRD RSAND LOGRSAND
LOGSILT (N = 1982)	1	.5702	LOGRSILT
	2	.5794	RSILT LOGRSILT
	3	.5871	RD RSILT LOGRSILT
	4	.5886	DISCH RD RSILT LOGRSILT
	5	.5945	DISCH LOGDISCH RD RSILT LOGRSILT
	6	.5946	DISCH LOGDISCH VEL RD RSILT LOGRSILT
	7	.5947	DISCH LOGDISCH VEL RD LOGRD RSILT LOGRSILT
LOGTOTAL (N = 1982)	1	.3513	LOGRTOTL
	2	.4179	RD LOGRTOTL
	3	.4525	VEL LOGRD LOGRTOTL
	4	.4560	LOGDISCH VEL LOGRD LOGRTOTL
	5	.4690	DISCH LOGDISCH VEL LOGRD LOGRTOTL
	6	.4708	DISCH LOGDISCH VEL RD LOGRD LOGRTOTL
	7	.4713	DISCH LOGDISCH VEL RD LOGRD RTOTAL LOGRTOTL

(R^2 = .4179) for the sand fraction and the total concentrations, respectively. Given the information y/D and C_a, the concentration of the silt-clay fraction could also be estimated with an accuracy of 58% (R^2 = .5871) by using the model

$$\log C = \beta_0 + \beta_1 \frac{y}{D} + \beta_2 C_a + \beta_3 \log C_a + e \tag{35}$$

Now, further suppose that additional information on the flow, such as velocity, is available and therefore the discharge data are also available. In Table 9, it is found that for the sand fraction, the accuracy increases to about 55% (R^2 = .5499) by using a 7-variable model such that

$$\log C = \beta_0 + \beta_1 Q + \beta_2 \log Q + \beta_3 u + \beta_4 \frac{y}{D} + \beta_5 \log \left(\frac{y}{D}\right)$$

$$+ \beta_6 C_a + \beta_7 \log C_a + e \tag{36}$$

where Q is the discharge and u the flow velocity. Similarly, the silt-clay fraction and the total concentrations can also be estimated with an accuracy of 59% (R^2 = .5947) and 47% (R^2 = .4713), respectively, by employing the 7-variable models shown in Table 9. However, note in Table 8 that for LOGSILT $\hat{\beta}_3$ and $\hat{\beta}_5$ are not (statistically) significant, implying that the velocity u (or VEL) and log (y/D) (or LOGRD) do not seem to affect the concentration of silt-clay fraction. Furthermore, evaluation of the Mallow's statistic (Cp) (Hocking, 1976) indicates that the 5-variable model in Table 9 may be used instead of the 7-variable one without any major loss of information (C_5 = 1.9085

and $C_6 = -.3944$ while MSE $\simeq .0134$ for both cases). In fact, R^2 decreases very little (from .5947 to .5945) for the reduced (5-variable) model (Table 9). Therefore, for the silt-clay fraction, the suggested equation is

$$\log C = \beta_0 + \beta_1 Q + \beta_2 \log Q + \beta_3 \frac{y}{D} + \beta_4 C_a + \beta_5 \log C_a + e \quad (37)$$

It should be noted in (37) that information on the depth (y/D) is included in the equation but the velocity itself is not. In the meantime, similar inspection of the 7-variable model for the total concentrations indicates that the 6-variable model (without C_a or RTOTAL)

$$\log C = \beta_0 + \beta_1 Q + \beta_2 \log Q + \beta_3 u + \beta_4 \frac{y}{D} + \beta_5 \log \left(\frac{y}{D}\right) + \beta_6 \log C_a + e \quad (38)$$

can be utilized without seriously affecting the accuracy of estimation.

One of the basic assumptions for the empirical models discussed here is the "linear" relationship between sediment concentrations and the independent variables defined in Table 1. In order to evaluate this assumption, experimental errors (or residuals) of the 7-variable models (for each of the 3 dependent variables in Table 9) were plotted against the individual variables involved in the models. For the dependent variables, there appears to be a tendency of positive (and increasing) residuals with higher values of the dependent variables and vice versa (Figures 21, 22, and 23), and this is particularly noticeable for LOGTOTAL (Figure 23). Suppose, however, that those

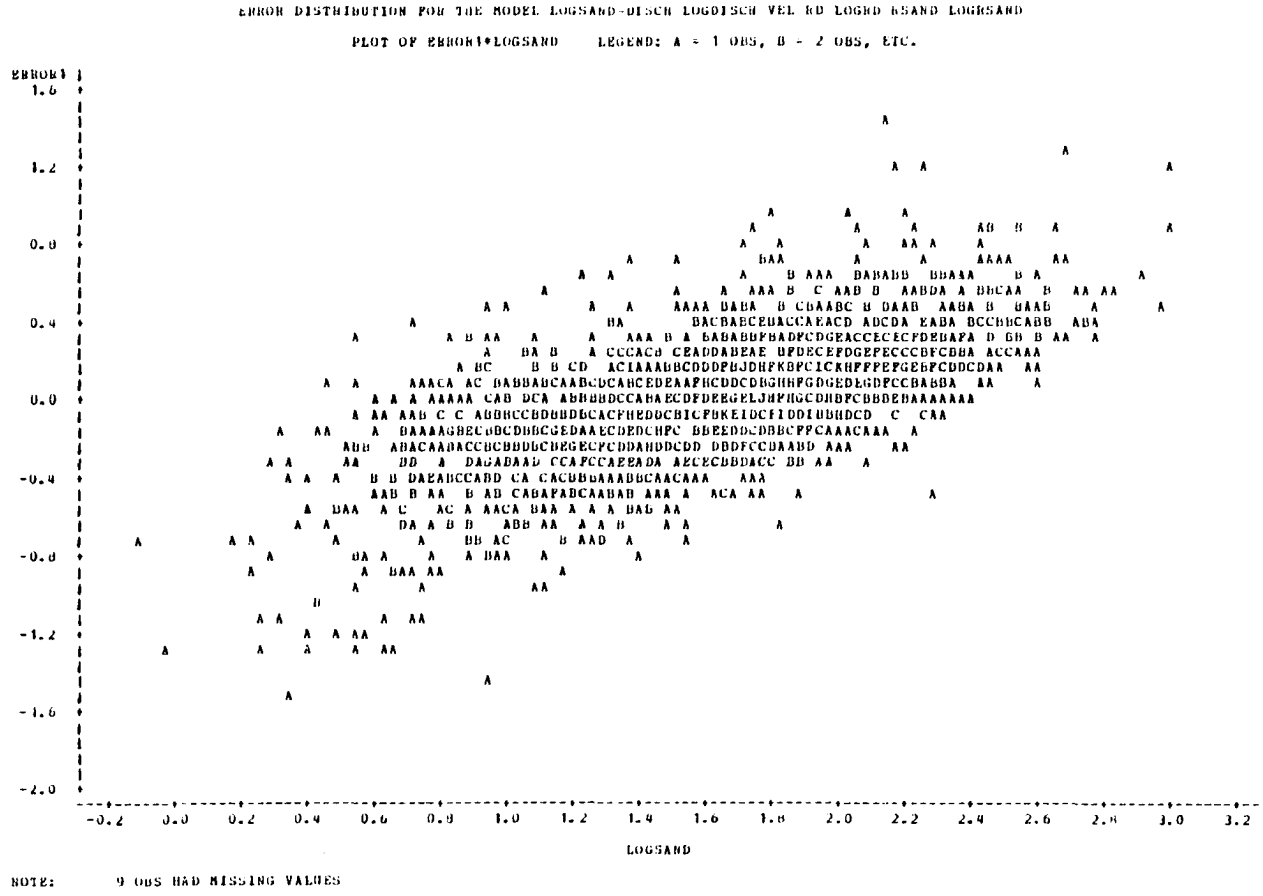

Fig. 21.--Plot of the residuals against LOGSAND for the "best" 7-variable model for sand fraction.

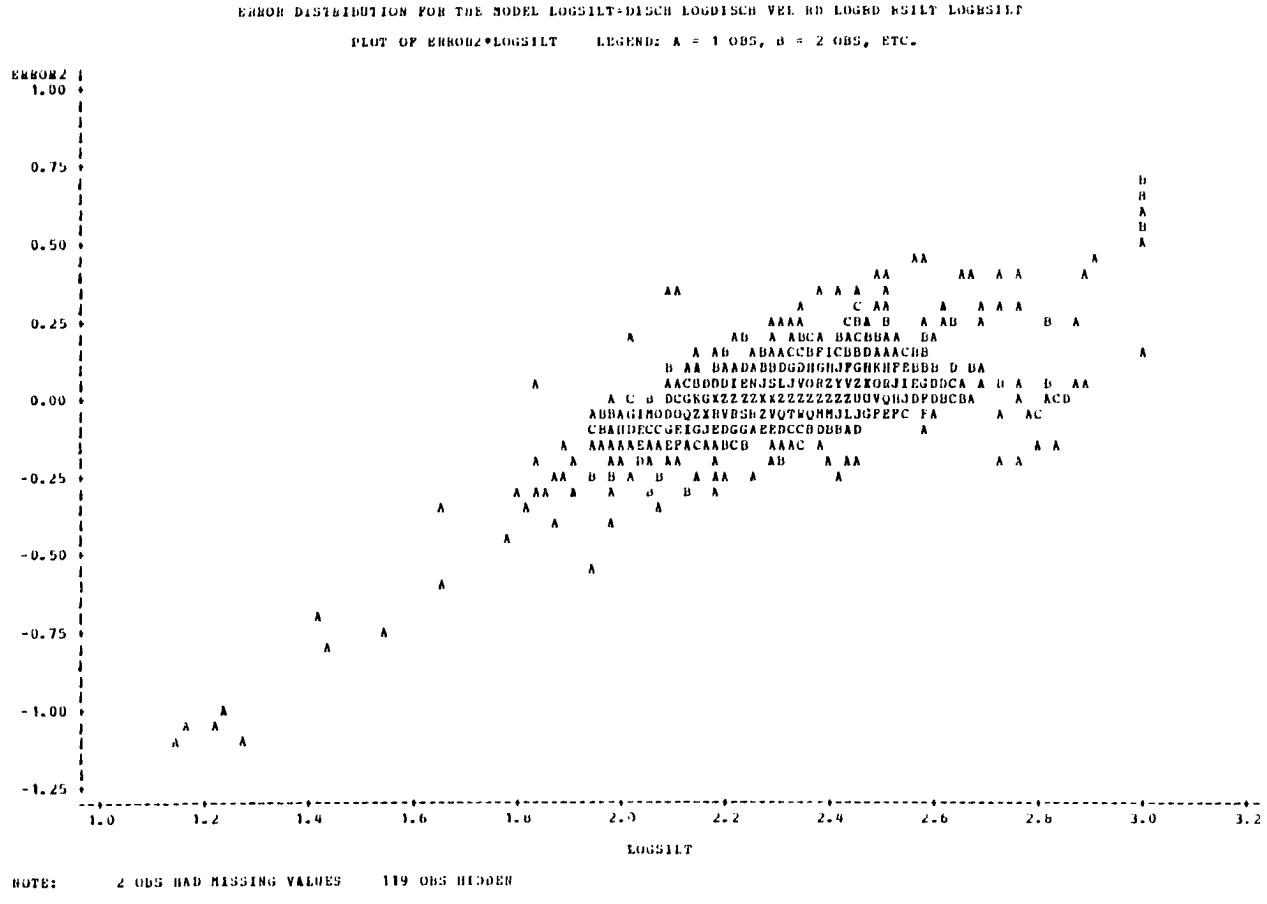

Fig. 22.--Plot of the residuals against LOGSILT for the "best" 7-variable model for silt-clay fraction.

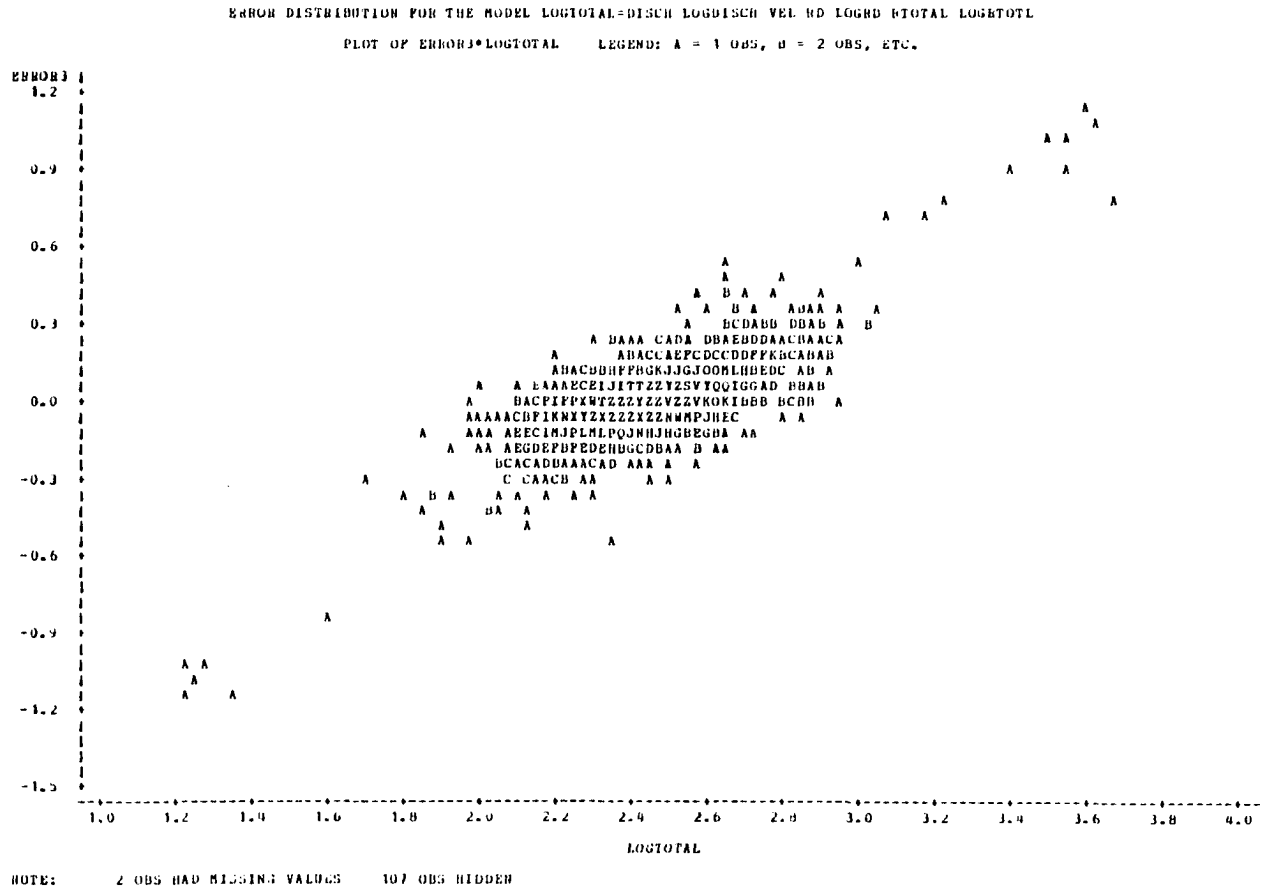

Fig. 23.--Plot of the residuals against LOGTOTAL for the "best" 7-variable model for total sediment concentration.

observations with LOGTOTAL values greater than, say, 3.1 and less than 1.8 were not considered in the analysis. Then, the tendency noted above (Figure 23) would disappear considerably. At this point, it is difficult to determine whether these "outliers" are the result of errors that occurred during the sampling and/or subsequent laboratory analysis procedures. Error distributions for the independent variables[1] generally show no signs of abnormality, i.e., a general pattern of a horizontal band of residuals may be seen on each plot against the independent variables. These results indicate that the basic assumption of "linear" relationship do not seem to be invalid.

In summary, given the two types of information (the "reference" or surface concentration C_a and the depth y/D), linear models such as (34) and (35) produce prediction accuracies of 46% for the sand fraction, 58% for the silt-clay fraction, and about 41% for the total concentrations. With additional information, such as the velocity (and subsequently the discharge), accuracy would increase to 55% for the sand fraction, 59% for the finer fraction, and 47% for the total, by utilizing the linear models (36), (37), and (38), respectively. It appears that information on the velocity as well as the discharge does not seem to significantly improve the accuracy of predicting (or estimating) concentrations of the finer fraction. Distributions of the residuals indicate that the assumption of a "linear" relationship between sediment concentrations and the independent variables (defined in Table 1) appears to be valid.

---

[1]The residual plots against the independent variables may be found in Appendix 3.

CHAPTER III

ESTIMATION OF SUSPENDED SEDIMENT CONCENTRATIONS IN SURFACE LAYER VIA LANDSAT REFLECTANCE DATA

It was pointed out earlier that one of the most significant assets of Landsat is the capability of monitoring physical processes on the earth's surface on a multi-temporal basis. This particular functional characteristic of Landsat has been widely recognized (e.g., Everett and Simonett, 1976; Rabchevsky, 1977; Polcyn and Lyzenga, 1979). Subsequently, many researchers have focussed on the use of Landsat in monitoring physical processes through time.

The purpose of this chapter is to evaluate, using a statistical model, the feasibility of monitoring sediment concentrations in the surface layers of a natural river by means of successive Landsat overpasses, particularly without concurrent surface truth collection at each time of the overpass. To this end, an attempt is made to develop a transformation method to remove the environmental effects from Landsat radiance data. Also, statistical characteristics of the MSS radiance data, in relation to the surface sediment concentrations, will be examined in detail.

Methods

Apart from the literature review, a study of this nature requires three steps in the procedure: quantitative data collection,

transformation of raw spectral data to remove the environmental effects, and statistical analysis of the relationship between the river sediments and the spectral signature represented by the transformed spectral data. Each step followed in this study will be elaborated in the following.

Data Collection

The basic quantitative Landsat data utilized in this study are the Multispectral Scanner's 4-channel (band) radiance values recorded in the Computer Compatible Tapes (CCT's). The radiance values from the CCT's form a set of raw spectral data which are to be transformed into a new spectral data set. The CCT's from three cloud-free Landsat overpasses (frame ID 1718-15595, 1862-15545, and 2084-15562) of the study area were processed through the computer facility at NASA's Earth Resources Laboratory[1] in Slidell, Louisiana.

In an attempt to remove the effect of uneven detector efficiencies (USGS, 1979) for each of the four MSS channels, the three Landsat scenes were destripped using a method developed by Forbes and Pearson (1977). With this method an entire Landsat scene is viewed as a composite of six-element by six-scan line areas with each area containing 36 picture elements (or pixels). For each six by six area an overall mean radiance value is computed. Then, for areas of the same overall mean radiance, adjusted mean radiance values are obtained for the individual scan lines in those areas. In so doing, cumulative number of pixels are used; for example, the

---

[1]Presently at National Space Technology Laboratory in Bay St. Louis in Mississippi.

number of pixels used to compute the adjusted mean radiance values of the scan lines in the first area is 6, that for the second area is 12, and so on. For each of the areas for which more than 300 pixels were used to compute the adjusted mean radiances of the scan lines, an adjusted overall mean radiance is obtained by taking the arithmetic mean of the six adjusted mean radiances of the scan lines in the area. Some of the scan lines may show adjusted mean radiances much higher than the adjusted overall mean radiance of the area. Therefore, the adjusted overall mean radiance of the area is further modified to take into account the unusual "brightness" of a particular scan line(s). For areas having less than 300 pixels, on the other hand, adjusted mean radiances of the scan lines are computed as "weighted" mean values based on the number of pixels used and the adjusted overall mean radiance of the particular area. The final adjusted mean radiances of the scan lines for the entire Landsat scene are computed using the (finally) adjusted overall mean radiances and weight coefficients for the individual six-element by six-scan areas. The foregoing procedure is repeated for each of the four MSS channels. A mathematical version of the computational procedure is given in Appendix 4. For further details, see Forbes and Pearson (1977).

In order to identify the surface truth sampling locations on the Landsat scenes, the following procedure was applied: An area of 1.992 km x 3 km that includes the channel cross section was delineated on a map of 1:24,000. The same area was then identified on the Landsat scenes and the accuracy was evaluated by measuring the lengths (or distances) of the area boundaries. The distance

measurements on the image utilized the pixel dimensions (57.5 m x 79 m) and the lower left-hand corner of the area as a reference point. The X and Y coordinates of the individual ground sampling points were obtained on the map and these points were transferred on to the image using the X-Y coordinates. Then, the pixels containing the sampling points were identified in terms of scan line and element numbers. An illustration of the pixel locations so identified is given in Figure 24.

Raw radiance values of the three vertically juxtaposed pixels (Figure 25) were averaged because the geographical accuracy of locating the pixel for each sampling location was ±1 scan line. Therefore, the average radiance values so obtained constitute the raw radiance data.

The surface truth data consist of a portion of the U.S. Corps of Engineers' data, i.e., suspended sediment concentrations on the surface layer[1] of the Mississippi River at Tarbert Landing, Mississippi. Eight observations on the river's surface layer are available for each of the three Landsat overpasses or a total of 24 observations (Table 10). The time lapse between the water sampling and the satellite overpass is approximately 1.5 to 4 hours.

Transformation of the CCT MSS Radiance Data

In order to construct a new set of spectral data, free from the environmental effects such as sun angles and atmospheric

---

[1]The surface layer samples are taken from approximately 1.2 to 3 meters below the water surface.

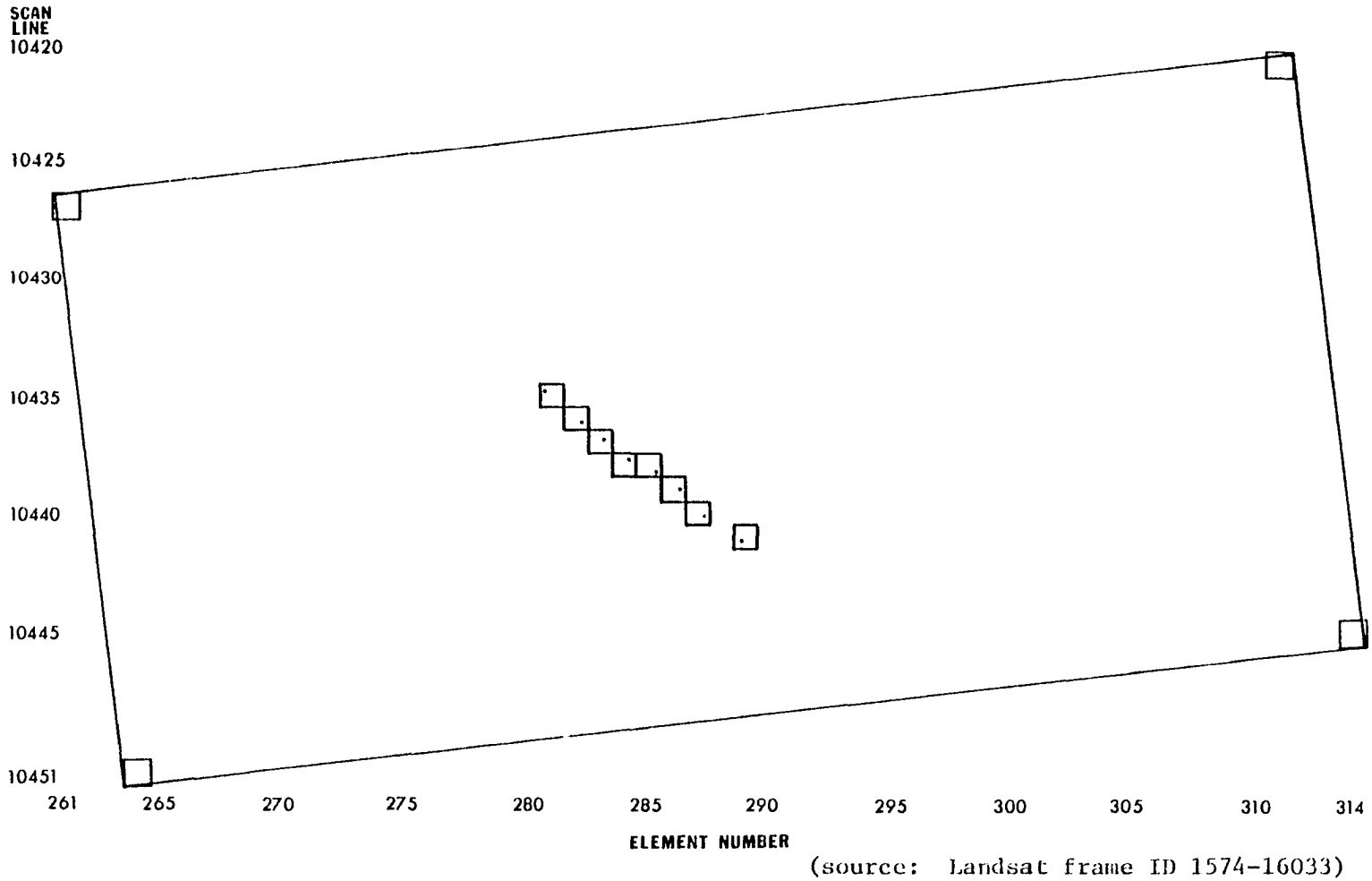

(source: Landsat frame ID 1574-16033)

Fig. 24.--Location of water samples in the Landsat-based coordinate system.

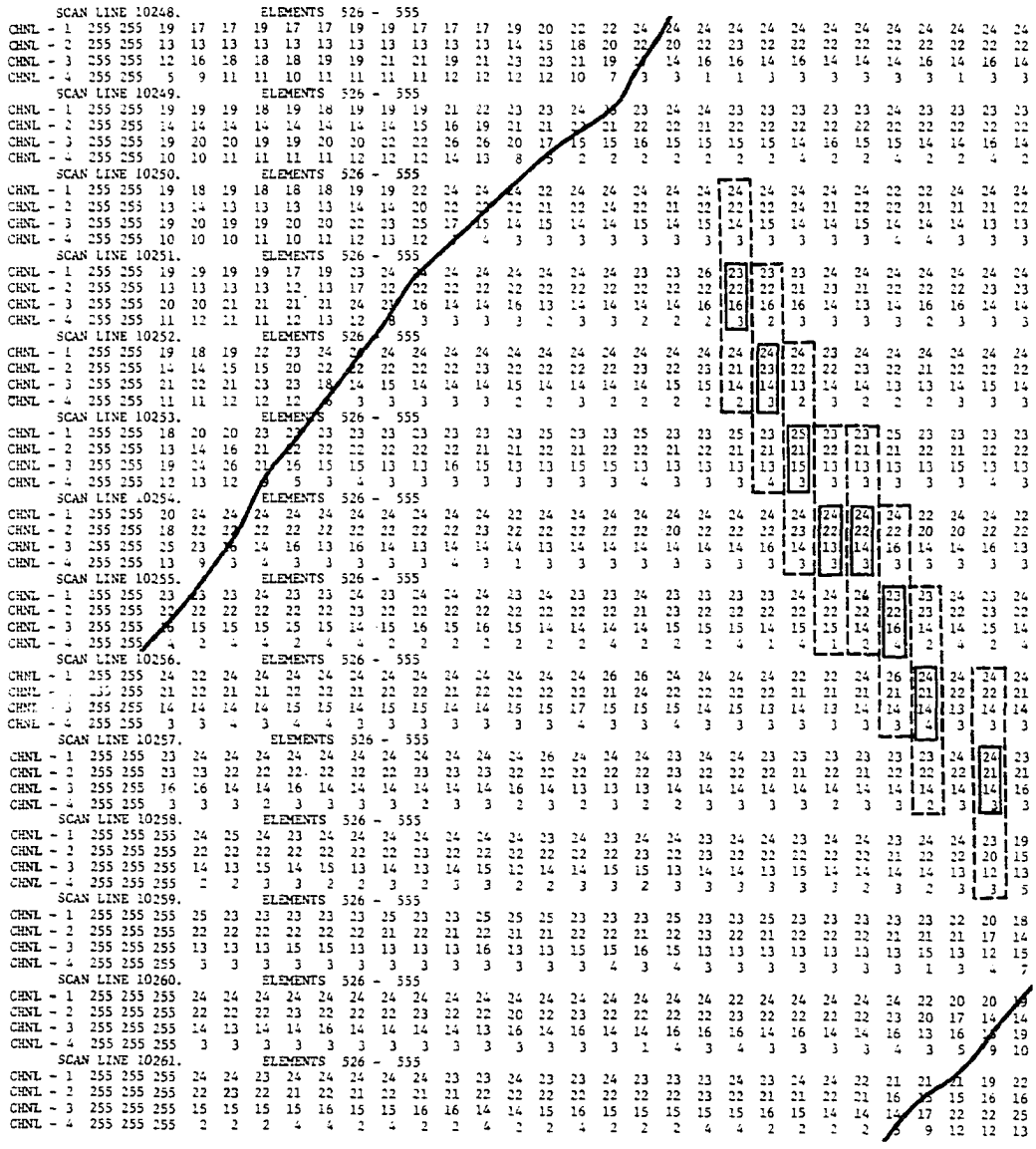

(source: Landsat frame ID 1862-15545)

Fig. 25.--Three vertically juxtaposed pixels averaged for each sampling location (center pixel). The solid diagonal lines represent approximate positions of the river banks. The element number increases from the left side (element 526) to the right side (element 555) of the figure.

TABLE 10

THE SURFACE TRUTH AND LANDSAT RADIANCE DATA

Overpass Date	Ground Sample Location	Suspended Sediments (p.p.m.)	Raw Radiance Data								Transformed Radiance Data			
			River Water				Reference Target				River Water			
			MSS-4	MSS-5	MSS-6	MSS-7	MSS-4	MSS-5	MSS-6	MSS-7	MSS-4	MSS-5	MSS-6	MSS-7
7/11/74	1	380.74	33.7	32.0	24.7	6.0	77	83	76	29	.44	.39	.32	.21
	2	328.23	32.7	32.0	25.3	6.0					.42	.39	.33	.21
	3	368.13	33.7	33.0	24.7	5.7					.44	.40	.32	.20
	4	344.57	33.3	32.3	24.0	6.0					.43	.39	.32	.21
	5	308.68	33.3	31.3	24.7	6.0					.43	.38	.32	.21
	6	326.82	33.7	31.7	24.3	5.7					.44	.38	.32	.20
	7	350.47	33.7	30.7	24.3	6.0					.44	.37	.32	.21
	8	367.20	31.7	30.7	25.7	6.3					.41	.37	.34	.22
12/2/74	1	351.07	23.7	21.7	14.7	2.7	46	48	47	22	.51	.45	.31	.12
	2	257.51	23.3	22.0	14.3	3.0					.51	.46	.30	.14
	3	307.00	24.3	22.0	14.0	2.7					.53	.46	.30	.12
	4	300.00	23.6	22.0	13.7	2.3					.51	.46	.29	.11
	5	316.32	23.6	21.7	13.7	2.6					.51	.45	.29	.12
	6	321.15	24.3	21.7	15.3	3.3					.53	.45	.33	.15
	7	173.10	23.3	22.0	14.0	2.6					.51	.46	.30	.12
	8	270.49	23.7	21.0	13.3	3.0					.51	.44	.28	.14
4/16/75	1	80.38	28.3	36.3	24.0	2.7	52	71	77	33	.54	.51	.31	.08
	2	184.72	28.7	35.0	24.3	2.7					.55	.49	.32	.08
	3	183.70	27.7	35.3	25.3	2.3					.53	.50	.33	.07
	4	156.06	28.0	35.3	22.3	2.3					.54	.50	.29	.07
	5	194.94	27.7	35.3	23.7	2.7					.53	.50	.31	.08
	6	133.65	28.7	36.3	23.0	2.3					.55	.51	.30	.07
	7	150.13	28.3	36.3	23.0	3.3					.54	.51	.30	.10
	8	--	27.0	33.7	23.7	3.3					.52	.47	.31	.10

conditions, linear transformations of the CCT radiance data were utilized and are described in the following section.

Suppose that there is a "reference" target in the Landsat scene (185 x 185 kilometers) whose physical properties remain relatively constant throughout the year (e.g., a concrete structure of size greater than four pixels). Let W_{ij} be the radiance value obtained from the reference target for the ith Landsat overpass and the jth MSS channel. It should be pointed out that for the jth channel the radiance value W_{ij} varies from one overpass to another due to the effects of different sun angles, atmospheric conditions, etc. on each overpass.

For any given MSS channel, the radiance values U_i obtained from the target (sediment-laden river water) may be represented by

$$U_i = f(s_i, e_i) \tag{39}$$

for the ith Landsat overpass, where s_i denote suspended sediment concentrations in the water and e_i represent the combined effects of the environmental factors (i.e., sun angles, atmospheric conditions, etc.) and the sensor system's noise. If the effects on the radiance values, U_i, of sediment concentrations, s_i, and environmental factors are functionally independent, then (39) can be written

$$U_i = f(s_i, e_i) = f_1(s_i)\, f_2(e_i) \tag{40}$$

Similarly, provided that a reference target mentioned earlier is available, the radiance values W_i from the reference target may be represented by

$$W_i = g(k, e_i) \tag{41}$$

where k denotes a constant physical property of the reference target (e.g., a concrete structure). If the physical property, k, and the environmental properties, e_i, are independent, then (41) can be written as

$$W_i = g(k, e_i) = g_1(k)\ g_2(e_i) \tag{42}$$

For a given overpass, it may be reasonable to assume that $f_2(e_i) = g_2(e_i)$. This reflects the assumption that the environmental effects are the same for various targets on a particular MSS channel. Under these assumptions,

$$\frac{U_i}{W_i} = \frac{f(s_i, e_i)}{g(k, e_i)} = \frac{f_1(s_i)\ f_2(e_i)}{g_1(k)\ g_2(e_i)} = \frac{f_1(s_i)}{g_1(k)} \tag{43}$$

Now, the fact that $g_1(k)$ is constant from overpass to overpass means that the ratio U_i/W_i depends only on s_i.

Now consider the transformations

$$X_{ijk} = a_{ij}\ C_{ijk} \qquad \begin{matrix} i = 1,\ldots,m \\ j = 1,\ldots,4 \\ k = 1,\ldots,n \end{matrix} \tag{44}$$

where k denotes the number of the observation in the jth channel and the ith overpass. X_{ijk} is a new variable and C_{ijk} is the Landsat MSS's jth spectral channel. Then, by defining $a_{ij} = 1/W_{ij}$ for the ith overpass and the jth channel, a new set of radiance data is obtained.

In order to acquire W_{ij}, a reference target (the runway at Ryan Airport in Baton Rouge) was selected on the Landsat scene and the radiance values were obtained from the reference target (Table 10). As a result, a set of new data was created by the transformation in (44) and the new spectral data set was utilized in the prediction model which follows.

Linear Model

In attempting to relate the observed suspended sediment concentration with the MSS (transformed) radiance values, a basic assumption is made, as in (14), that there is a linear relationship of the form

$$Y = \beta_0 + \beta_1 X_1 + \beta_2 X_2 + ... + \beta_4 X_4 + e \qquad (45)$$

between the suspended sediment concentration (a dependent variable) Y and the four Landsat MSS channels (independent variables) $X_1, \ldots, X_4$. The observations are then represented as

$$\begin{bmatrix} y_1 \\ y_2 \\ . \\ . \\ . \\ y_n \end{bmatrix} = \begin{bmatrix} 1 & x_{11} & x_{12} & x_{13} & x_{14} \\ 1 & x_{21} & x_{22} & x_{23} & x_{24} \\ . & . & . & . & . \\ . & . & . & . & . \\ . & . & . & . & . \\ 1 & x_{n1} & x_{n2} & x_{n3} & x_{n4} \end{bmatrix} \begin{bmatrix} \beta_0 \\ \beta_1 \\ \beta_2 \\ \beta_3 \\ \beta_4 \end{bmatrix} + \begin{bmatrix} e_1 \\ e_2 \\ . \\ . \\ . \\ e_n \end{bmatrix} \tag{46}$$

for n = 24, or

$$\underset{(24x1)}{Y} = \underset{(24x5)}{X} \quad \underset{(5x1)}{B} + \underset{(24x1)}{E} \tag{47}$$

where

$$E(Y) = X B \quad \text{and} \quad \text{var}(Y) = \sigma^2 I \tag{48}$$

Analysis of the data follows the procedure outlined in (18) through (31).

Results and Discussion

Linear Transformation Method

In the development of the transformation procedure described earlier, an assumption was made that the "error" functions are multiplicative, i.e., $f(s_i, e_i) = f_1(s_i)\, f_2(e_i)$ and $g(k, e_i) = g_1(k)\, g_2(e_i)$. While it may be subject to the argument whether or not the particular assumption holds, it will be discussed from a statistical standpoint in the following paragraph.

Suppose that u_i in (39), in fact, represent the observed values of the random variable U and that U has the probability density

function (p.d.f.) h(u). Furthermore, suppose it is reasonable to assume that the random variables S and E, with their respective p.d.f.'s $f_1(s)$ and $f_2(e)$, have the joint p.d.f. f(s,e) and are stochastically independent. If u = f(s,e), as implied by (39), then by theorem $u = f_1(s)\, f_2(e)$ (Hogg and Craig, 1970, p. 77). The same argument may be applied to the assumption that $g(k, e_i) = g_1(k)\, g_2(e_i)$.

A rather critical argument is the assumption that $f_2(e_i) = g_2(e_i)$, i.e., the combined effects of the environmental effects and the sensor system's noise are the same for both the target under investigation and the "reference" target. In fact, atmospheric conditions will not be the same particularly at the lower level atmosphere near ground, unless the targets are immediately juxtaposed. For instance, the location of the reference target (Baton Rouge's Ryan Airport) in this study is approximately 60 km southeast of the Mississippi River channel at Tarbert Landing. In addition to the fact that no other suitable reference target is available in the Landsat scene, it was felt that the differences in atmospheric paths for both targets may be negligible as long as cloud-free conditions are maintained. This assumption is valid considering the large vertical distance between the ground and the sensor (920 km) as compared to the relatively small horizontal distance (60 km) between the target and the reference.

Relationship between Landsat Radiance
and the Suspended Sediments

Results of the test of hypothesis in (26) are shown in Table 11, in that "Regression" sum-of-squares and "Error" sum-of-squares correspond to (29) and (30), respectively. Note that the null hypothesis $H_0: B^* = 0$ is rejected at $\alpha \leq .0001$ significance level. That is, it can be ascertained based on the evidence from our data that observations on suspended sediments are significantly regressed on the joint set of variables, namely, the four Landsat spectral channels. It is then immediately implied that the actual suspended sediment concentrations y_i can be predicted (or estimated) with the observed spectral radiances in the 4 MSS channels, by using the equation

$$\hat{y}_i = 609.05 + 1803.75x_{i1} - 3058.19x_{i2} + 368.49x_{i3} + 59.65x_{i4} \quad (49)$$

where x_{ij} denotes observed radiance values (after the transformation) in the jth channel[1] for i = 1,2,..., n, and the equation is mathematically equivalent to (23).

When a prediction equation is formed, it is of primary interest to see how well the equation describes (or approximates) the "real world." It is seen in Table 11 that R^2=.800, which was computed by (31). Since the squared multiple correlation coefficient R^2 is the portion of the total variance of Y accounted for by the regression

---

[1] In equation (49) the independent variables X_1, X_2, X_3, and X_4 represent the MSS channels 4, 5, 6, and 7, respectively.

TABLE 11

RESULTS OF THE TEST OF NULL HYPOTHESIS B*=0 AND THE PARAMETER ESTIMATION

Source	d.f.	Sum of Squares	Mean Square	F	$P(F>F_c)$	R^2	s_y	$\bar{y}$	c.v.(%)
Regression	4	141,452.69	35,363.17	18.03	.0001	.800	44.3	267.6	16.5
Error	18	35,309.89	1.961.66						
Total	22	176,762.58							

Parameter	Estimate	t	$P(\|t\|>\|t_c\|)$	Standard Error of Estimate
β_0	609.05	1.08	.2944	563.92
β_1 (for MSS-4)	1803.75	2.29	.0340	786.34
β_2 (for MSS-5)	-3058.19	-3.11	.0061	983.84
β_3 (for MSS-6)	368.49	.44	.6622	829.57
β_4 (for MSS-7)	59.65	.07	.9440	837.46

of Y on X's, it is clearly indicated that the R^2 represents "a measure of the accuracy of prediction" (Timm, 1975, p. 275). Therefore, it can be stated that the accuracy of the prediction equation obtained from our data is about 80%.

Besides the accuracy measure of the prediction equation, attention is also given to the estimated regression coefficients $\hat{\beta}_j$. Note that in (49) the estimates of actual observations in sediment concentrations are describable in terms of the four Landsat MSS channels. Geometrically, the observations are represented by a set of points in a five-dimensional Euclidean space. Then, it is suggested that the sizes of the regression coefficients indicate relative contributions of the respective spectral channels to the estimated individual observations in sediment concentrations. In other words, the estimated value $\hat{y}_i$ is more influenced by the channels with greater $\hat{\beta}$. This should not, however, be interpreted as a "causal" effect of the spectral channels on $\hat{y}$. In fact, it is rather actual sediment concentrations that "cause", to a large extent, the spectral signatures as recorded in the MSS channels. Thus, it should simply be understood that the greater changes in $\hat{y}_i$ result from the changes in the spectral signatures of the channels that have greater regression coefficients.

Note in (49) that the MSS channel 5 has the largest (estimated) regression coefficient and channel 7 the smallest.[1] Channels 4 and 6

---

[1] The sizes of regression coefficients are expressed in terms of absolute values.

maintain the second and the third, respectively, in the size of regression coefficients (Table 11). As pointed out earlier, this result indicates that the estimated sediment concentrations $\hat{y}_i$ are to a greater extent affected by the spectral signatures in the MSS channels 4 and 5, and to the much less extent by those in the channels 6 and 7. In order to further investigate the relationship between suspended sediments and each of the four MSS channels, the conventional (Pearson product-moment) and the partial correlations among the variables will be examined in the following paragraphs.

Table 12 shows that the four MSS channels maintain pairwise "statistically significant" (conventional) correlations. This implies that the correlations between suspended sediments and each of the four channels (see first column in Table 12) are rather difficult to interpret. Note, for instance, that a negative relationship is shown between suspended sediments and channel 4 ($r = -.76$). However, channel 4 is also highly correlated with channel 5 ($r = .96$), and channel 5 in turn has a rather strong negative relationship with suspended sediments ($r = -.86$). Consequently, even if channel 4 was not directly related to suspended sediments, its high correlation with channel 5 would probably have resulted in a negative relationship of some magnitude. Of course, multiple effects of channels 6 and 7 on channel 4 as well as suspended sediments should also be taken into account in evaluating the direct relationship between suspended sediments and channel 4.

Unlike a conventional (Pearson product-moment) correlation, a partial (or conditional) correlation reveals the degree of

TABLE 12

CORRELATIONS AMONG THE VARIABLES

	Sediments	MSS-4	MSS-5	MSS-6	MSS-7
Sediments	1.00				
MSS-4	-.76**	1.00			
MSS-5	-.86**	.96**	1.00		
MSS-6	.42*	-.63**	-.55**	1.00	
MSS-7	.82**	-.95**	-.97**	.59**	1.00

*Significance level $\alpha<.05$.

**Significance level $\alpha<.01$.

TABLE 13

PARTIAL CORRELATIONS BETWEEN SUSPENDED SEDIMENTS AND MSS CHANNELS

	Sediments
MSS-4	.48*
MSS-5	-.59**
MSS-6	.10
MSS-7	.02

*Significance level $\alpha<.05$.

**Significance level $\alpha<.01$.

association between two variables after removing the effects of other variables on them.[1] That is, a partial correlation coefficient between two variables is obtained while holding other variables constant. As a result, another aspect of the relationship between the two variables can be evaluated.

The partial correlations between suspended sediments and each of the four MSS channels are shown in Table 13 and illustrate strikingly different relationships among them, as compared to those in the first column of Table 12. It is found that channel 4 alone is in fact positively related to suspended sediments, at the significance level $\alpha = .05$, which is in contrast to the highly significant ($\alpha = .01$) negative relationship in Table 12. In the meantime, it is noted that channel 5 shows a highly significant negative relation with suspended sediments. Channels 6 and 7, however, show very little relation with suspended sediments, again, as contrasted to those revealed in the conventional correlation analysis (Table 12). Therefore the regression and the partial correlation analyses clearly indicate that most of the information on suspended sediments is contained in the MSS channels 4 and 5. In addition, the (two-channel) prediction equation employing the MSS channels 4 and 5 achieves an accuracy of 79.77%, whereas with the addition of channels 6 and 7 the accuracy increases less than 1% to 80.03% (Table 14).

The poor relationship between the sediments and the infrared channels is in accordance with what would have been theoretically

---

[1] Theory of the partial correlation is usually found in many advanced statistical textbooks. See, for instance, Timm (1975).

TABLE 14

THE "BEST" 1-, 2-, 3-, AND 4-CHANNEL PREDICTION EQUATIONS

# of MSS Channels	$\hat{\beta}_0$	$\hat{\beta}_1$	$\hat{\beta}_2$	$\hat{\beta}_3$	$\hat{\beta}_4$	$P(F_c \geq F)$	R^2(%)
1	936.91		-1508.85**			.0001	73.68
2	800.20	1637.67*	-3026.64**			.0001	79.77
3	640.37	1793.39*	-3107.77**	381.80		.0001	80.02
4	609.05	1803.75*	-3058.19**	368.49	59.65	.0001	80.03

NOTE: The term "best" is based on the maximum R^2 criterion for the variable selection methods. For further details, see Barr, et al. (1976).

*Significance level $\alpha<.05$.

**Significance level $\alpha<.01$.

TABLE 15

INTERVAL ESTIMATES FOR β_j

	95% - Confidence Interval		Length
	lower limit	upper limit	
β_1 (for MSS-4)	151.65	3455.85	3304.20
β_2 (for MSS-5)	-5125.24	-991.14	4134.10
β_3 (for MSS-6)	-1374.44	2111.42	3485.86
β_4 (for MSS-7)	-1699.85	1819.15	3519.00

anticipated; the near infrared spectrum of MSS channels 6 and 7 is strongly absorbed by the water molecules. Therefore, there is very little diffuse reflectance (or backscattered upwelling radiance) from the water. As documented by Maul and Gordon (1975), Atwell (1976), and McCluney (1976), it is the backscattered upwelling radiance that escapes the water surface and reaches the (satellite) sensor. Information on the conditions beneath the water surface, such as suspended sediment concentration is contained in the backscattered upwelling radiance. Hence, in the present case lack of strong backscattered upwelling radiance from the water in the near infrared spectral region (0.7 - 1.1μ) means that very little information on the suspended sediments in the river water is received by channels 6 and 7. In this regard, Table 13 shows that the relationship of the sediments with channel 7 is much weaker than it is with channel 6. This can be accounted for by the greater absorption by the water molecules at channel 7 wavelengths (0.8 - 1.1μ) than channel 6 (0.7 - 0.8μ) (Maul and Gordon, 1975).

In the spectral region of MSS channels 4 (0.5 - 0.6μ) and 5 (0.6 - 0.7μ) the diffuse reflectance from water molecules and suspended particles in the water increases considerably. This phenomenon is not noticeable at the wavelengths of channel 4. This is due to the decreased absorption of the downwelling radiance by the water molecules (Maul and Gordon, 1975). Theoretically, therefore, channels 4 and 5 should be superior to channels 6 and 7 in providing information on the suspended sediment concentration. It is perhaps for this reason that some investigators (e.g., McKeon, et al., 1977)

completely excluded the Landsat radiance data from channels 6 and 7 from their studies on suspended sediment concentrations. The results obtained in this study seem to agree with the theoretical prediction, i.e., the "best" two-channel equation for estimating suspended sediments includes both channels 4 and 5. As mentioned earlier the "best" three-channel equation, using channels 4, 5, and 6, did not result in any significant improvement in the accuracy of the estimation (Table 14).

It should be pointed out, however, that there are rather persistent arguments for the use of channel 6 wavelengths in suspended sediment studies. Holyer (1978), for instance, measured upwelling spectra related to suspended sediments with a boat-mounted spectroradiometer in Lake Mead water. Instead of using the diffuse reflectance, Holyer calculated the volume spectral reflectance from the measured upwelling spectra and related it to actual sediment concentrations and nephelometric turbidity. It is interesting that Holyer's best one-wavelength equation used the 0.782μ wavelength. His two-wavelength model includes wavelengths of 0.652μ and 0.782μ. Furthermore, Holyer reported that his one-wavelength model using the 0.782μ wavelength is almost as good as the two-wavelength model in accurately estimating the nephelometric turbidity. Even though his method of evaluating prediction accuracy seems somewhat misleading, this result apparently challenges the readily accepted idea of the past few years, i.e., the red portion of the spectrum is most suitable for studies of suspended sediment concentrations (Maul and Gordon, 1975; McCluney, 1976). More recently, a report by Ritchie and Schiebe

(1979) used the optimal wavelength region of 0.7 - 0.8μ for suspended sediment studies. Unfortunately, Ritchie and Schiebe did not include critical details of their data analysis, yet they argued that the same results were obtained in the past at other test sites. The upwelling spectra obtained from the Gulf of Mexico by Maul and Gordon (1975) is also interesting in this regard. It appears that the two water types, Gulf Stream and Coastal, can be differentiated just as well at ≈0.78μ as at ≈0.65μ. Maul and Gordon failed to comment on that, nor did they attempt to examine the theoretical spectra in the spectral region of 0.7 - 1.1μ, as they had for the 0.4 - 0.7μ region.

So far, the discussion has been focussed on the accuracy of the prediction equation and the contribution of each of the four MSS channels to the estimation of suspended sediments by the prediction equation. Attention is now turned to the variability of the estimates in the prediction equation, namely, sample variance of the regression coefficients and that of the estimated suspended sediments quantities. It should be noted from (23) that the regression coefficients $\hat{\beta}_j$ for each of the four MSS channels, as well as the suspended sediment quantities $\hat{y}_i$, are merely estimated values from a limited amount of observed data which consists of a "statistical" sample. Obviously, both $\hat{\beta}_j$ and $\hat{y}_i$ vary from one sample to another and greater variability is not desirable for the estimates.

The standard errors and interval estimates ($\alpha = .05$) for each $\hat{\beta}_j$ are given in Tables 11 and 15, respectively. Table 11 shows that $\hat{\beta}_2$ has the largest variance and $\hat{\beta}_1$ the smallest. Of particular interest, however, are the interval estimates of β_1 and β_2 for the

channels 4 and 5, respectively. As noted in Table 15, the interval estimates indicate that the suspended sediment concentrations may have a positive relationship with channel 4 yet a negative one with channel 5. The negative relationship between sediment concentrations and channel 5 is rather puzzling and apparently in contradiction to (human) photo interpretation. In fact, however, this negative relationship between sediment concentrations and channel 5 (or the red portion of the spectrum) has been reported by several investigators (Maul and Gordon, 1975; Holyer, 1978; Khorram, 1979; Whitlock and Kuo, 1979). In Maul and Gordon's work, the upwelling spectra observed with a spectroradiometer show that the coastal water has lower reflectance in the 0.6 - 0.7μ region than does the Gulf Stream. Presumably, the coastal water contains more suspended sediments than the Gulf Stream; therefore, a higher red reflectance in the coastal waters would be expected. However, no explanation of this "reversed" situation was given by the investigators. A negative relationship between the suspended sediments and the red spectrum has also been found in Khorram's Ocean Color Scanner data obtained in the San Francisco Bay area; Holyer's spectroradiometer data from Lake Mead; and Whitlock and Kuo's multispectral data simulated in the laboratory. None of the investigators, however, provided an explanation for this negative relationship.

A close examination of the data (Table 10) used in this study reveals some interesting features. In the April 16, 1975 data the raw radiance values of the river water are higher for channel 5 than for channel 4. Furthermore, the suspended sediment

concentrations in the water are much lower on April 16 than on July 11. Yet, the raw radiance values of the water for channel 5 are consistently higher on April 16 than on July 11. It is very difficult understanding what appears to be an abnormal spectral response of the water body in the 0.6 - 0.7μ spectral region on April 16. The sun's angle (above the horizon) on April 16 is lower than that on July 11. Thus, the sun's angle cannot be considered a possible cause of the abnormality.

Ignoring the April 16 data and considering only the December 2 and the July 11 data, it appears that the spectral behavior of the river water in each MSS channel is as expected as related to the changes in sediment concentration and sun angle. However, in channel 5 the transformed radiance values of the water are still considerably higher on December 2 than on July 11, despite the decreased sediment concentrations. In fact, the same pattern occurs in channel 4. These results led directly to the recognition of a negative relationship between the sediment concentrations and both channels 4 and 5 in a conventional correlation analysis (Table 12). It immediately comes to mind that some extraordinary spectral response of the reference target might have inflated the transformed radiance values of the water for channel 5. Equation (44) and the definition of the transformation coefficient a_{ij} indicate that the transformed radiance values of the water are influenced by the radiance values of the reference target. Unfortunately, no data are available that examine the spectral behavior of the reference target and the extent of its influence on the transformed radiance

data. However, a previous investigation of the data (Table 10), together with additional radiance data for the river water obtained from another Landsat overpass on February 17, 1974 showed a negative relationship between the sediments and the raw radiance values of the water for channel 5 (Kim and Smith, 1979). The particular transformation procedure used in this study may not necessarily be the only factor that has contributed to the negative relationship being discussed.

Holyer (1978) noted that the volume reflectance of silt-size particles (average diameter 0.004 mm) at 0.652 μ wavelength was affected by the degree of sediment concentration up to 350 mg/l. His spectroradiometer data indicated the maximum volume reflectance at ≈300 mg/l with a gradual decrease from 300 - 350 mg/l. However, Khorram (1979) and Whitlock and Kuo (1979) demonstrated a negative relationship at much lower sediment concentrations (up to 80 mg/l and 173 p.p.m., respectively). Therefore, the degree of sediment concentration alone does not seem to explain the cause of the negative relationship between the sediments and the red spectrum.

The foregoing discussion on the subject of negative relationship between the sediments and channel 5 now leads to the remaining question of the spectral response of a sediment-laden water body in the red portion of the spectrum. With the limited information available, no immediate answer to this question can be found.

In the meantime, the interval estimates of β_3 and β_4 (for the channels 6 and 7, respectively) do not seem to reveal any consistent relationship with suspended sediments. Note in Table 15

that both intervals include 0 with the negative lower limits and the positive upper limits. Based on the probability of 95%, it is only certain that the intervals (-1374.44, 2111.42) and (-1699.85, 1819.15) most likely include β_3 and β_4, respectively. Yet, it cannot be determined whether the true values β_3 and β_4 are negative or positive. Although the point estimates $\hat{\beta}_3$ and $\hat{\beta}_4$ turned out to be both positive from our data, they are of course subject to change from one sample to another. It appears that further experimentation (or much more information) is required to identify the nature of the relationships between the MSS channels 6 and 7 and suspended sediment concentrations.

Finally, it should be indicated that the size of the variances of $\hat{\beta}$'s (hence, the lengths of the interval estimates for β's) are influenced by the variance of Y, σ^2, as indicated by (20). Also influenced by σ^2 are the variances of estimated sediment concentrations $\hat{y}_i$. Therefore, every effort should be made to get a reliable estimate for σ^2 in order to better understand the relationship between suspended sediment concentrations and the spectral signatures in the MSS channels.

CHAPTER IV

SUMMARY AND CONCLUSIONS

Despite its limitations (such as relatively poor resolution, insufficient overpass intervals and weather dependence), Landsat provides a unique method of collecting information over a large area through time. However, varying results obtained from this study indicate that the accurate monitoring of suspended sediment concentrations in a river channel by utilizing Landsat digital data appears far from operational. More specific findings and their implications resulted from this study are summarized in the following paragraphs.

Analyses of the suspended sediment data used in this study showed that the diffusion model does not adequately describe the relationship between suspended sediment concentrations in surface and subsurface layers of the river water. Consequently, accuracy of estimating sediment concentrations at a depth by means of surface concentrations varied considerably (from nearly zero to about 74%), depending upon grain-size (fraction), locations across the channel, water stage, and combinations of these factors. It appears that the diffusion model estimates the sand fraction more accurately than the silt-clay fraction. In addition, water stages seem to affect the performance of the model to some extent, for example, estimation of the sand fraction was considerably more accurate in the high water stage than in the low water stage. Yet, the silt-clay

fraction did not reveal the same trend. It was also found in this study that the accuracy of the estimation varies widely from one location (or vertical) to another across the channel.

Apparently, poor performance of the diffusion model is attributable to the oversimplifying assumptions applied to the model. Most critical is the assumption of a two-dimensional flow, which does not account for the variations of velocity and sediment concentrations across the channel. Other crucial assumptions, such as constant sediment concentrations through time ($\partial C/\partial t = 0$) and constant upward velocity through depth ($\partial u_2/\partial x_2 = 0$), also render the diffusion model unrealistic for the Mississippi River channel under study.

Utilizing the same two types of information (surface concentration and depth) as for the diffusion model, the full rank linear model produced estimation accuracies of 46% for sand fraction, 58% for silt-clay fraction, and 41% for the total concentrations. However, it should be noted that these results are better, particularly for the finer fraction, than those of the diffusion model which resulted in estimation accuracies of 41% for sand fraction and 8% for silt-clay fraction. The addition of other variables, such as velocity and discharge, to the linear model did not improve the estimation accuracy enough to warrant their inclusion in the model. While the assumption of a "linear" relationship between sediment concentrations and the independent variables seems to be valid, the proposed linear model suffers from large sample variances. This, of course, indicates that a new model should be sought so as to reduce the sample variance and thereby increasing accuracy of the estimation.

Based on the evidence extracted from the data used in this study, the following statements can be made concerning the relationship between suspended sediment concentrations and the spectral signatures received by the Landsat Multispectral Scanner. First, it appears that the actual suspended sediment concentrations in the surface layers of a natural river can be estimated with better than 80% accuracy when using all four MSS channels in the full rank linear model. A further improvement in accuracy would be achieved by refining the estimate of σ^2 and increasing sample size, via a carefully devised experimental plan. The improved estimate of σ^2 should also make the estimates of the β's, as well as the estimated values of sediment concentrations, more reliable.

Second, it was found that the estimated sediment concentrations are largely influenced by the spectral signatures in MSS channels 4 and 5, and to a much smaller amount by those in channels 6 and 7. The "best" (based on the maximum R^2 criterion) one-channel prediction equation used channel 5 with an accuracy of 73.68%. The best two-channel equation included both channels 4 and 5 with an accuracy of 79.77%. With the addition of channels 6 and 7, however, the accuracy increased less than 1% to 80.03%. These results may well indicate that most of the information on suspended sediments is contained in the MSS channels 4 and 5. In fact, these findings are in accordance with the theoretical prediction of optimal spectral region for studies of suspended sediments in the water.

The negative relationship between channel 5 and suspended sediments is suspect and indicates that a better understanding of

spectral behavior of a (naturally) sediment-laden water body in the MSS spectral region (0.5 - 1.1μ) is necessary. Otherwise, interpretation of the empirically determined relationship between the suspended sediments and the four Landsat MSS channels will at best be difficult if not impossible. Until there is a better understanding of spectral behavior of sediment-laden water, inconsistent findings from empirical studies on the subjects such as the relationship between sediment concentrations and the red spectrum, the optimal spectral region for the suspended sediment studies, and the accuracy of the prediction equation will continue. Therefore, it is recommended that carefully planned field experiments be conducted to obtain the spectra of a sediment-laden water body so as to evaluate the individual radiance components, i.e., upwelling diffuse reflectance, water surface (or specular) reflectance, atmospherically scattered radiance, etc.

The transformation method developed in this study to eliminate the environmental effects should prove to be very useful. One major drawback of the method is that a suitable reference target must be available near the target area under investigation. It may be also pointed out that the accuracy of the estimation equation may be influenced by the types of reference targets utilized, provided that they are available in the study area. At present, this possible effect of the reference targets on the estimation results is not known and further studies on this subject are recommended.

Finally, it should be indicated that the transformation method, defining random variables representing the MSS spectral

signatures, is not necessarily limited to the estimation of suspended sediments via Landsat. The basic principles involved in the transformation should be readily applicable to any other type of investigations that deal with monitoring surface physical phenomena through successive Landsat overpasses (e.g., monitoring or mapping crop maturity in the growing season). The application may also be extended to multispectral scanner data obtained from other sensors and/or platforms (e.g., Ocean Color Scanner).

SELECTED BIBLIOGRAPHY

Anderson, A. T., et al., 1977, "Landsat Imagery for Surface-Mine Inventory," Photogr. Eng. and Remote Sensing, vol. 43, no. 8, pp. 1027-1036.

Ashley, M. D. and J. Rea, 1975, "Seasonal Vegetation Differences from ERTS Imagery," Photogr. Eng. and Remote Sensing, vol. 41, no. 6, pp. 713-719.

Atwell, B. H., 1976, "Remote Sensing of Chlorophyll Concentration State-of-the-Art-1975," Report No. 156, NASA Earth Resources Laboratory, Lyndon B. Johnson Space Center, Houston, Tex., 26 p.

Barr, A. J., et al., 1976, A User's Guide to the Statistical Analysis System, SAS Inst., Inc., Raleigh, N.C., 329 p.

Bartolucci, L. A., B. F. Robinson, and L. F. Silva, 1977, "Field Measurements of the Spectral Response of Natural Waters," Photogr. Eng. and Remote Sensing, vol. 43, no. 5, pp. 595-598.

Blatt, H., G. Middleton, and R. Murray, 1972, Origin of Sedimentary Rocks, Prentice-Hall, Inc., Englewood Cliffs, N.J., 634 p.

Bogárdi, J. L., 1972, "Fluvial Sediment Transport," In: Advances in Hydroscience, vol. 8, V. T. Chow, ed., Academic Press, New York, N.Y., pp. 184-254.

Brooks, D. J., 1975, "LANDSAT Measures of Water Clarity," Photogr. Eng. and Remote Sensing, vol. 41, no. 10, pp. 1269-1272.

Chirieleison, J. P., Jr., 1974, "Suspended Sediment Load Computer Program--Program Number 723-F3-A2-070," Unpublished Report, USGS Water Resources Division, Baton Rouge, La., 35 p.

Colby, B. R., 1964, "Discharge of Sands and Mean Velocity Relationships in Sand-Bed Streams," USGS Professional Paper, 462-A, 47 p.

Dacey, M. F., 1975, "Model of Recurring Random Walks for Sediment Transport," In: Quantitative Studies in the Geological Sciences, E.H.T. Whitten, ed., Geol. Soc. Am., Inc., Boulder, Colo., pp. 105-119.

Draper, N. and H. Smith, 1966, Applied Regression Analysis, John Wiley & Sons, Inc., New York, N.Y., 407 p.

Einstein, H.A., 1950, "The Bed-Load Function for Sediment Transportation in Open Channel Flows," USDA Technical Bulletin, No. 1026, 78 p.

_____, 1964, "River Sedimentation," In: Handbook of Applied Hydrology, V. T. Chow, ed., McGraw-Hill, New York, N.Y., pp. 35-67.

Everett, J. and D. S. Simonett, 1976, "Principles, Concepts, and Philosophical Problems in Remote Sensing," In: Remote Sensing of Environment, J. Lintz, Jr. and D. S. Simonett, eds., Addison-Wesley Pub. Co., Inc., Reading, Mass., pp. 85-127.

Fischer, W. A., et al., 1975, "History of Remote Sensing," In: Manual of Remote Sensing, R. G. Reeves, ed., Am. Soc. Photogr., Falls Church, Va., pp. 27-50.

Forbes, J. and R. Pearson, 1977, "Program Destripe," Unpublished Report, NASA/Lockheed Electronic Co., Inc., Earth Resources Laboratory, Slidell, La.

Graf, W. H., 1971, Hydraulics of Sediment Transport, McGraw-Hill, New York, N. Y., 513 p.

Hocking, R. R., 1976, "The Analysis and Selection of Variables in Linear Regression," Biometrics, vol. 32, pp. 1-49.

Hogg, R. V. and A. T. Craig, 1970, Introduction to Mathematical Statistics, 3rd ed., Macmillan Publishing Co., New York, N.Y., 415 p.

Holyer, R. J., 1978, "Toward Universal Multispectral Suspended Sediment Algorithms," Remote Sensing of Environment, 7, pp. 323-338.

Johnson, J. M., P. Cressy, and W. C. Dallam, 1975, "Utilization of LANDSAT Data for Water Quality Surveys in the Choptank River," Proc. of the NASA Earth Resources Survey Symposium, vol. I-D, Lyndon B. Johnson Space Center, Houston, Tx., pp. 2325-2350.

Johnson, R. W., 1975, "Quantitative Sediment Mapping from Remotely Sensed Multispectral Data," paper presented at the 4th Annual Remote Sensing of Earth Resources Conference, March, 1975, Tullahoma, Tenn.

Khorram, S., 1979, "Remote Sensing Analysis of Water Quality in the San Francisco Bay-Delta," Proc. of the 13th International Symp. on Remote Sensing of Environment, Ann Arbor, Mich., pp. 1591-1602.

Kim, S. T. and D. W. Smith, 1979, "Elimination of Environmental Effects from Landsat Radiance Data," Proc. of Am. Soc. Photogr. 45th Annual Meeting, Washington, D.C., pp. 694-699.

Klemas, V., J. F. Borchardt, and W. M. Treasure, 1973, "Suspended Sediment Observations from ERTS-1," Remote Sensing of Environment, vol. 2, pp. 205-221.

_____, et al., 1974, "Correlation of Coastal Water Turbidity and Circulation with ERTS-1 and Skylab Imagery," 9th International Sym. on Remote Sensing of Environment, University of Michigan, Ann Arbor, Mich.

Kritikos, H., L. Yorinks, and H. Smith, 1974, "Suspended Solids Analysis Using ERTS-A Data," Remote Sensing of Environment, vol. 3, pp. 69-78.

Maul, G. A. and Gordon, H. R., 1975, "On the Use of the Earth Resources Technology Satellite (LANDSAT-1) in Optical Oceanography," Remote Sensing of Environment, 4, pp. 95-128.

McCluney, W. R., 1976, "Remote Measurement of Water Color," Remote Sensing of Environment, vol. 5, pp. 3-33.

McKeon, J. B., et al., 1977, "Production of a Water Quality Map of Saginaw Bay by Computer Processing of Landsat-2 Data," Proc. of the 11th International Symp. on Remote Sensing of Environment, Ann Arbor, Mich., pp. 1045-1054.

McNeil, W. R. and K. P. B. Thomson, 1974, "Remote Measurement of Water Colour and Its Application to Water Quality Surveillance," Remote Sensing of Earth Resources, vol. 3, pp. 117-146.

Middleton, G. V. and J. B. Southard, 1977, "Mechanics of Sediment Movement," Soc. Eco. Paleon. Mineralogists Short Course No. 3, Binghamton, N.Y.

Nordin, C. F., Jr., 1963, "A Preliminary Study of Sediment Transport Parameters Rio Duerco Near Bernardo New Mexico," USGS Professional Paper, 462-C, 21 p.

_____ and G. R. Dempster, Jr., 1963, "Vertical Distribution of Velocity and Suspended Sediment, Middle Rio Grande, N. Mexico," USGS Professional Paper, 462B, 20 p.

Polcyn, F. C. and D. R. Lyzenga, 1979, "Landsat Bathymetric Mapping by Multitemporal Processing," Proc. of the 13th International Symp. on Remote Sensing of Environment, Ann Arbor, Mich., pp. 1269-1276.

Rabchevsky, G. A., 1977, "Temporal and Dynamic Observations from Satellites," Photogr. Eng. and Remote Sensing, vol. 43, no. 12, pp. 1515-1518.

Ritchie, J. C., et al., 1974, "The Relationship of Reflected Solar Radiation and the Concentration of Sediment in the Surface Water of Reservoirs," Remote Sensing of Earth Resources, vol. 3, pp. 57-71.

_____ and F. R. Schiebe, 1979, "Remote Sensing of Suspended Surface Sediments in Lake Chicot, Arkansas," Proc. of Am. Soc. Photogr. 45th Annual Meeting, Washington, D.C., pp. 29-39.

Rogers, R. H., et al., 1975, "Computer Mapping of Turbidity and Circulation Patterns in Saginaw Bay, Michigan (Lake Huron) from ERTS Data," Proc. of Am. Soc. Photogr. 41st Annual Meeting, Washington, D.C., pp. 415-429.

Rouse, H., 1937, "Modern Conceptions of the Mechanics of Turbulence," Trans. Am. Soc. Civil Engrs., vol. 102, pp. 463-543.

Scheidegger, A. E., 1970, Theoretical Geomorphology, 2nd ed., Springer, Berlin, 435 p.

Schuburt, J., 1973, "Digital Analysis of Potomac River Basin ERTS-1 Imagery," Symp. on Significant Results Obtained from ERTS-1, pp. 659-664.

Searle, S. R., 1971, Linear Models, John Wiley & Sons, New York, N.Y., 532 p.

Shepard, D. S., 1970, "SYMAP Interpolation Characteristics," Computer Mapping as an Aid in Air Pollution Studies Project, vol. 2, report L, Cambridge, Mass., 49 p.

Tennekes, H. and J. L. Lumley, 1972, A First Course in Turbulence, MIT Press, Cambridge, Mass., 300 p.

Thomas, V. L., 1975, "Generation and Physical Charcteristics of the LANDSAT 1 and 2 MSS Computer Compatible Tapes," NASA/Goddard Space Flight Center, X-563-75-223, Greenbelt, Md., 28 p.

Timm, N. H., 1975, Multivariate Analysis with Applications in Education and Psychology, Brooks/Cole Publishing Co., Monterey, Calif., 689 p.

Trexler, P. L. and J. L. Barker, 1975, "LANDSAT-1 Data As It Has Been Applied for Land Use and Water Quality Data by the Virginia State Water Control Board," Proc. of the NASA Earth Resources Survey Symposium, vol. I-A, Lyndon B. Johnson Space Center, Houston, Tx., pp. 371-418.

U. S. Army Corps of Engineers, Unpublished Data File on Suspended Sediment Observation Mississippi River at Tarbert Landing, Miss., 1974-75, New Orleans District, New Orleans, La.

U. S. Geological Survey, 1979, Landsat Data Users Handbook, revised edition, Arlington, Va.

U. S. Geological Sruvey Water Resources Division, 1973, "Test Procedure for Sediment Analysis," Unpublished Report, Baton Rouge, La.

Vanoni, V. A., 1941, "Some Experiments on the Transportation of Suspended Loads," Trans. Am. Geophys. Union, pp. 608-631.

Vennard, J. K., 1961, Elementary Fluid Mechanics, 4th ed., John Wiley & Sons, Inc., New York, N.Y.

Vincent, R. K., 1972, "An ERTS Multispectral Scanner Experiment for Mapping Iron Compounds," Proc. of the 8th Int'l Sym. on Remote Sensing of Environment, Ann Arbor, Mich., pp. 1239-1243.

Weismiller, R. A., et al., 1977, "Change Detection in Coastal Zone Environments," Photogr. Eng. and Remote Sensing, vol. 43, no. 12, pp. 1533-1539.

Whitlock, C. H. and C. Y. Kuo, 1979, "A Regression Technique for Evaluation and Quantification for Water Quality Parameters from Remote Sensing Data," Proc. of the 13th International Symp. on Remote Sensing of Environment, Ann Arbor, Mich., pp. 1351-1365.

Williamson, A. N. and W. E. Grabau, 1973, "Sediment Concentration Mapping in Tidal Estuaries," Third Earth Resources Tech. Satellite - 1 Sym., vol. I, Sect. B, NASA/Goddard Space Flight Center, Washington, D.C., pp. 1347-1386.

Yalin, M. S., 1977, Mechanics of Sediment Transport, 2nd ed., Pergamon Press, Oxford.

_____ and G. D. Finlayson, 1972, "On the Velocity Distribution of the Flow Carrying Sediment in Suspension," In: Sedimentation, H. W. Shen, ed., Fort Collins, Colo., pp. 8-1-18.

Yarger, H., 1973, "Water Turbidity Detection Using ERTS-1 Imagery," Symp. on Significant Results Obtained from ERTS-1, pp. 651-658.

Yarger, H. L. and J. R. McCauley, 1975, "Quantitative Water Quality with LANDSAT and SKYLAB," Proc. of the NASA Earth Resources Survey Symposium, vol. I-A, Lyndon B. Johnson Space Center, Houston, Tx., pp. 347-370.

Yuan, S. W., 1967, Foundations of Fluid Mechanics, Prentice-Hall, Inc., Englewood Cliffs, N.J., 608 p.

APPENDIX 1

A SAMPLE OF HYDROLOGICAL DATA COMPILED BY THE U.S. ARMY CORPS OF ENGINEERS, NEW ORLEANS DISTRICT

U.S. ARMY ENGINEER DISTRICT
NEW ORLEANS CORPS OF ENGINEERS

SUSPENDED SEDIMENT OBSERVATION
MISSISSIPPI RIVER AT TARBERT LANDING MISS.

ADPS CODE	DATE MO-DA-YR	GAGE READING FEET	TIME FROM TO	TYPE SAMPLER	TYPE SAMPLES	# OF VERTICALS	WATER TEMPERATURE (DEG C)	DEPTH FEET	DISCHARGE C.F.S.
1100	1/18/74	45.1	1540 1710	P 46	AP	8	5.3	10.0	1012686.

FIELD SAMPLE NUMBER	DISTANCE FROM REF. POINT FEET	TOTAL STATION DEPTH FEET	DEPTH OF SAMPLE FEET	PORTION OF CROSS SECTION REPRESENTED BY SAMPLE DISCHARGE C.F.S.	VELOCITY F.P.S.	AREA SQ.FT.	SUSP. SED. CONCENTRATION US 230 SIEVE 0.0625 M.M. RETAINED P.P.M.	PASSED P.P.M.	TOTAL P.P.M.	GRAIN SIZE ANALYSIS OF RETAINED MATERIAL = CUMULATIVE % FINER PARTICAL DIAMETER IN M.M. 1.00	.500	.250	.125	.0625
81	1398	51.0	6.1	21644	2.26	9572	86.18	229.90	316.08	100.0	100.0	96.5	91.5	72.7
82	1398	51.0	13.3	18029	2.20	7293	118.02	216.67	334.68	100.0	99.7	99.5	91.9	64.7
83	1398	51.0	21.4	16075	3.15	5102	93.85	222.20	316.04	100.0	100.0	100.0	92.3	70.4
84	1398	51.0	30.6	22934	3.55	6464	95.10	212.11	307.22	100.0	100.0	99.7	93.1	69.0
85	1398	51.0	45.9	19762	3.23	6119	144.81	226.93	371.74	100.0	100.0	99.9	88.8	61.0
86	1900	58.0	8.7	41654	8.50	4900	65.85	190.69	256.54	100.0	99.8	99.8	90.0	74.3
87	1900	58.0	17.4	31243	8.20	3811	57.94	163.55	221.49	100.0	100.0	99.8	95.0	82.9
88	1900	58.0	29.0	34130	7.84	4355	150.77	182.64	333.41	100.0	99.4	99.3	78.1	54.8
89	1900	58.0	40.6	31648	7.27	4355	171.77	186.43	358.21	100.0	100.0	99.7	75.9	52.0
90	1900	58.0	52.2	24151	6.10	3960	528.00	191.56	719.56	100.0	99.9	99.4	46.2	28.6
91	2149	58.0	8.7	31820	8.93	3562	63.11	178.44	241.56	100.0	99.7	99.1	87.9	73.9
92	2149	58.0	17.4	23895	8.62	2770	100.44	188.67	289.11	100.0	99.8	98.9	81.8	65.3
93	2149	58.0	29.0	28155	8.26	3408	117.70	188.50	306.19	100.0	100.0	98.6	76.3	61.8
94	2149	58.0	40.6	24378	7.70	3166	224.32	180.45	404.77	100.0	100.0	97.9	63.2	44.0
95	2149	58.0	52.2	21512	6.47	3327	262.11	173.54	435.65	100.0	99.7	98.9	58.8	39.8
96	2446	56.0	8.4	31046	8.16	3805	66.30	169.36	235.68	100.0	100.0	98.0	86.0	71.4
97	2446	56.0	16.8	23349	7.89	2959	66.23	161.59	227.81	100.0	100.0	99.5	86.7	70.4
98	2446	56.0	28.0	25549	7.55	3382	122.72	186.64	309.35	100.0	99.7	96.0	77.0	60.3
99	2446	56.0	39.2	23498	7.07	3362	115.17	167.86	283.03	100.0	100.0	97.5	76.8	59.7
100	2446	56.0	50.4	22466	5.89	3811	229.02	170.76	399.78	100.0	99.8	95.6	58.4	42.7
101	2753	53.0	7.9	26670	8.11	3290	107.94	172.95	280.89	100.0	100.0	95.4	76.6	61.6
102	2753	53.0	15.9	20105	7.82	2571	66.35	160.50	226.85	100.0	100.0	97.8	85.4	70.1
103	2753	53.0	26.5	21944	7.49	2930	131.77	156.82	288.59	100.0	100.0	95.2	73.2	54.3
104	2753	53.0	37.1	20459	6.98	2930	179.00	183.33	362.34	100.0	100.0	89.7	66.3	50.6
105	2753	53.0	47.7	18485	5.87	3147	145.13	187.61	332.74	100.0	100.0	89.9	70.2	56.4
106	2999	57.0	8.5	27370	6.88	3980	67.78	182.44	250.22	100.0	100.0	96.6	84.0	72.9
107	2999	57.0	17.1	20665	6.63	3110	105.49	168.88	274.37	100.0	100.0	94.8	75.6	61.6
108	2999	57.0	28.5	22527	6.35	3545	116.19	186.21	302.41	100.0	100.0	92.0	76.6	61.6
109	2999	57.0	39.9	21019	5.93	3545	162.87	189.36	352.23	100.0	100.0	84.6	66.7	53.8
110	2999	57.0	51.3	17906	4.95	3619	180.27	166.16	346.43	100.0	100.0	90.5	70.2	53.7
111	3375	50.0	7.5	24504	8.11	4855	55.16	174.94	230.25	100.0	100.0	96.8	86.8	70.0
112	3375	50.0	15.0	21247	5.91	3605	72.70	170.33	243.03	100.0	100.0	91.5	81.1	70.1
113	3375	50.0	25.0	23265	5.65	4120	77.49	163.42	240.91	100.0	100.0	94.0	82.6	67.6
114	3375	50.0	35.0	21774	5.29	4120	128.50	187.92	316.43	100.0	100.0	81.9	70.5	59.4
115	3375	50.0	45.0	21981	4.53	4851	136.56	168.94	305.51	100.0	100.0	78.4	67.3	55.3
116	3823	53.0	7.9	41119	4.61	8925	47.16	173.70	220.85	100.0	100.0	96.7	89.4	78.6
117	3823	53.0	15.9	30975	4.56	6786	43.06	206.07	249.13	100.0	100.0	99.7	93.6	82.7
118	3823	53.0	26.5	37273	5.10	7304	63.50	188.50	251.99	100.0	100.0	97.6	89.5	74.6
119	3823	53.0	37.1	32051	4.75	6752	65.67	188.48	254.15	100.0	99.3	94.4	85.5	74.1
120	3823	53.0	47.7	24155	3.98	6072	110.64	203.16	314.00	100.0	95.7	84.3	75.9	64.7
STRAIGHT NUMERICAL AVERAGES							122.58	185.21	307.79	100.0	99.8	95.3	79.2	63.0
TOTALS				1012686.		179118.								
DISCHARGE WEIGHTED AVERAGES					5.65		116.85	184.54	301.39	100.0	99.8	95.7	80.1	64.2

APPENDIX 2

A SAMPLE OF THE U.S. GEOLOGICAL SURVEY WATER QUALITY LABORATORY DATA

EXAMPLE #2 LABORATORY DATA

SEDIMENT ANALYSIS

BY SIEVE AND BOTTOM WITHDRAWAL METHODS

ADPS CODE: 04800

LOCATION NAME: RED RIVER ABOVE OLD RIVER OUTFLOW CHANNEL LA.

DATE	GAGE ROD (FT)	FROM	TIME	TO	TYPE SAMPLER	TYPE SAMPLES	NO VERT	PTS/VERT	WATER TEMP (°C)	DEPTH (FT)	DISCHARGE (1000 CFS)
030474	9.37	1540		1625	P 46	AP	3	5	18.6	1.00	1.08222
DATE SAMPLED					SAMPLE NO		BW TUBE NO	TYPE OF BW		DATE TESTED	TESTED BY

BEAKER NO	853	854	855	856	857	858	859	860	861	862
GROSS	547309	540468	536992	558323	538216	540434	547467	538200	548275	535212
TARE	546751	540087	536648	557988	537924	540165	547224	537958	548053	535048
NET WT SED	0.558	3.81	3.44	3.35	2.92	2.69	2.43	2.42	2.22	1.64

WASH CORP BEAKER NO 863: 548229 548213 0016

SUS SOLIDS CORP BEAKER NO 864: 536712 536674 0038

TOTAL VOLUME (cc): 522

TEMP (Deg C): 24.5

BED MATERIAL	2.54	1.91	1.27	0.88	0.76	0.36	0.20	0.141	0.100	0.050	0.035	0.0250	0.0177	0.0125	0.0088	0.0078	0.0062	PAN
% PASSED	100.0	100.0	100.0	100.0	100.0	100.0	100.0	100.0	100.0	99.8	99.4	98.4	94.2	86.0	77.6	66.8	64.4	63.8	0.0

BEAKER NO	LAB SAMPLE NO	WET SIEVE GROSS	WET SIEVE TARE	WET SIEVE NET	DRY SIEVE ANALYSIS (CUM WT RETAINED) US 18	US 35	US 60	US 120	US 230	BEAKER NO	HALF FINES GROSS	HALF FINES TARE	HALF FINES NET	TOTAL VOLUME (cc)	DISTANCE FROM REF PT	DEPTH AT STATION	DEPTH OF SAMPLE	CODE 1	CODE 2	CODE 3	
973	1366	529000	528890	1.10	...	0.000	0.000	0.007	0.075	685	563918	563717	2.01	0.358	3.50	5.2	1.52	1			0096
974	1367	537874	537795	7.79	...	0.000	0.000	0.000	0.446	686	542405	542182	2.23	0.446	3.50	5.2	1.30	2			0053
975	1368	538909	538818	2.91	...	0.000	0.033	0.082	0.263	687	538007	537774	2.33	0.463	3.50	5.2	2.60	3			0274
976	1369	538818	530902	79.16	...	0.000	1.047	4.690	7.904	688	546603	546278	3.25	0.439	3.50	5.2	1.20	4			2464
977	1370	547719	547559	3.60	...	0.000	0.013	0.072	0.329	689	543228	542973	2.55	0.454	3.50	5.2	4.68	5	1		0355
978	1371	522165	522090	0.98	...	0.000	0.024	0.037	0.094	690	523458	523230	2.28	0.459	5.50	5.4	.54	1			0098
979	1372	534058	533934	1.24	...	0.000	0.000	0.018	0.103	691	545010	544777	2.33	0.451	5.50	5.4	1.95	2			0113
980	1373	545915	545834	1.55	...	0.000	0.000	0.029	0.141	692	521687	521451	2.36	0.458	5.50	5.4	2.70	3			0165
981	1374	542662	540484	21.78	...	0.000	0.111	0.783	2.109	693	519073	518861	2.12	0.456	5.50	5.4	4.05	4			2161
982	1375	534506	534254	2.52	...	0.000	0.004	0.055	0.237	694	519489	519246	2.43	0.457	5.50	5.4	4.86	5	1		0245
983	1376	537592	537492	1.00	...	0.000	0.000	0.028	0.079	695	540457	540245	2.12	0.398	7.50	6.0	.60	1			0093
984	1377	564276	564189	0.87	...	0.000	0.017	0.036	0.078	696	516253	516039	2.14	0.412	7.50	6.0	1.50	2			0081
985	1378	542672	542493	1.79	...	0.000	0.008	0.042	0.155	328	530042	529829	2.13	0.463	7.50	6.0	3.00	3			0164
986	1379	532212	532058	1.54	...	0.000	0.006	0.034	0.135	329	541814	541599	2.15	0.445	7.50	6.0	4.50	4			0151
987	1380	535524	535245	2.79	...	0.000	0.033	0.109	0.277	330	543252	543041	2.11	0.455	7.50	6.0	5.40	5	1	1	0279

PAGE 20

APPENDIX 3

RESIDUAL PLOTS ACAINST THE INDEPENDENT VARIABLES

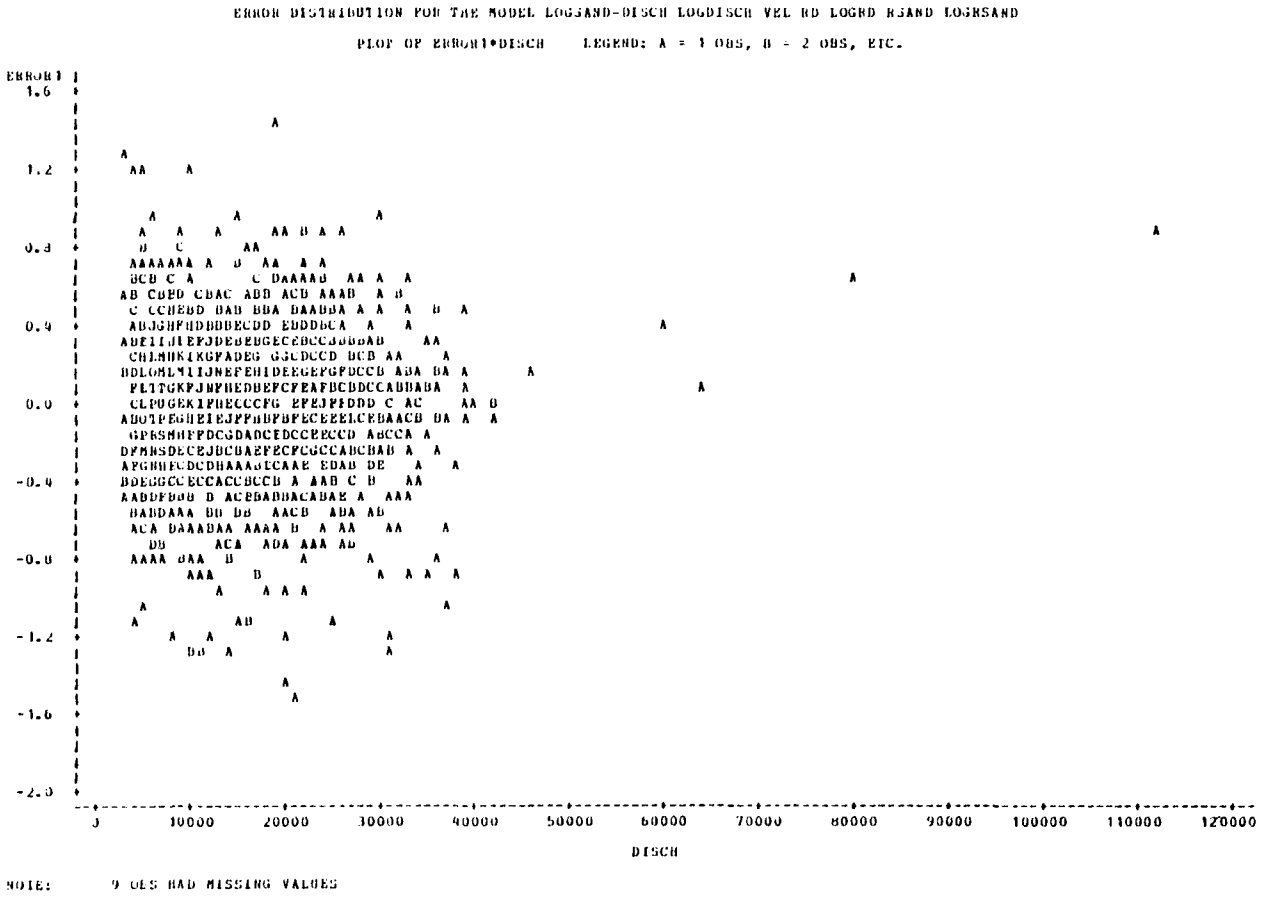

NOTE: 9 OBS HAD MISSING VALUES

APPENDIX 3--Continued

APPENDIX 3--Continued

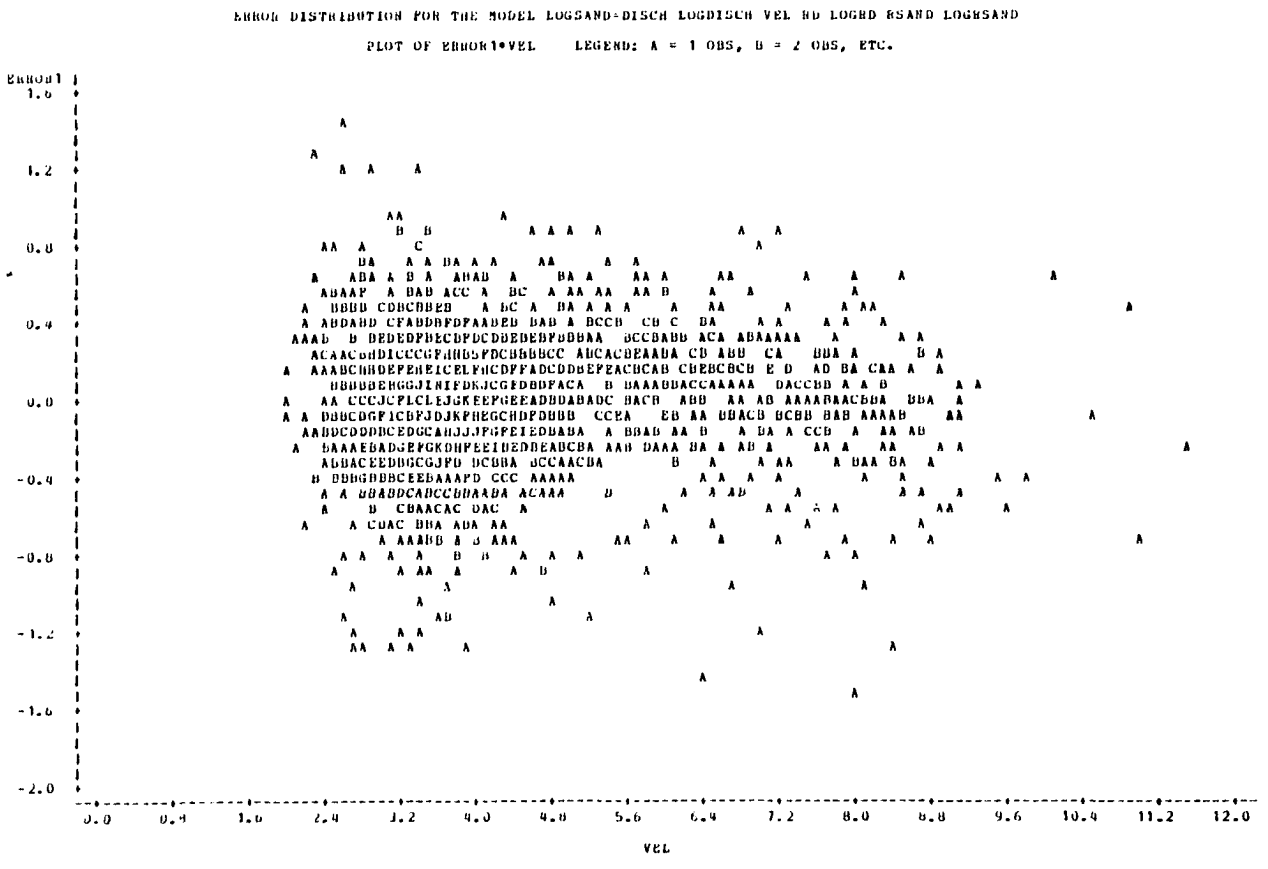

NOTE: 3 OBS HAD MISSING VALUES

APPENDIX 3--Continued

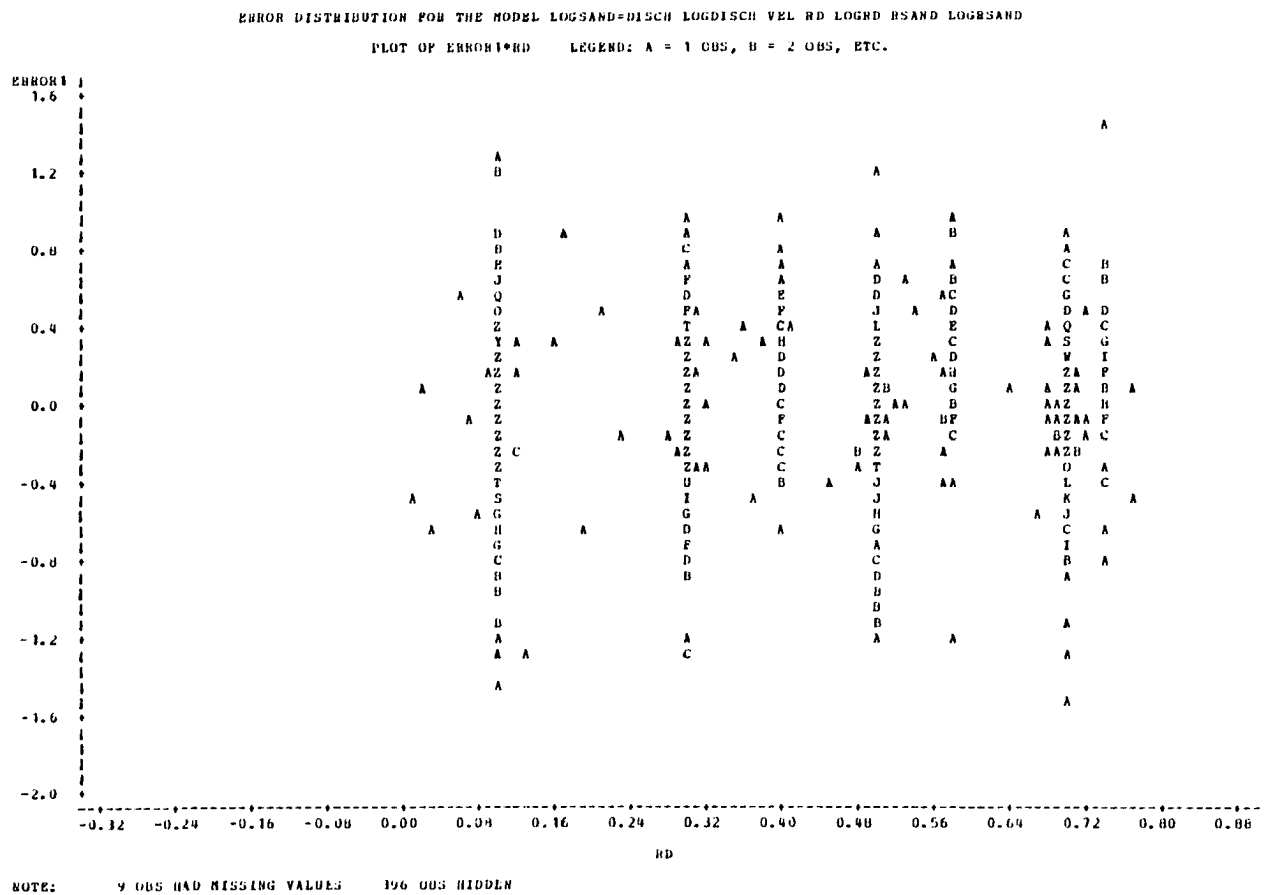

APPENDIX 3--Continued

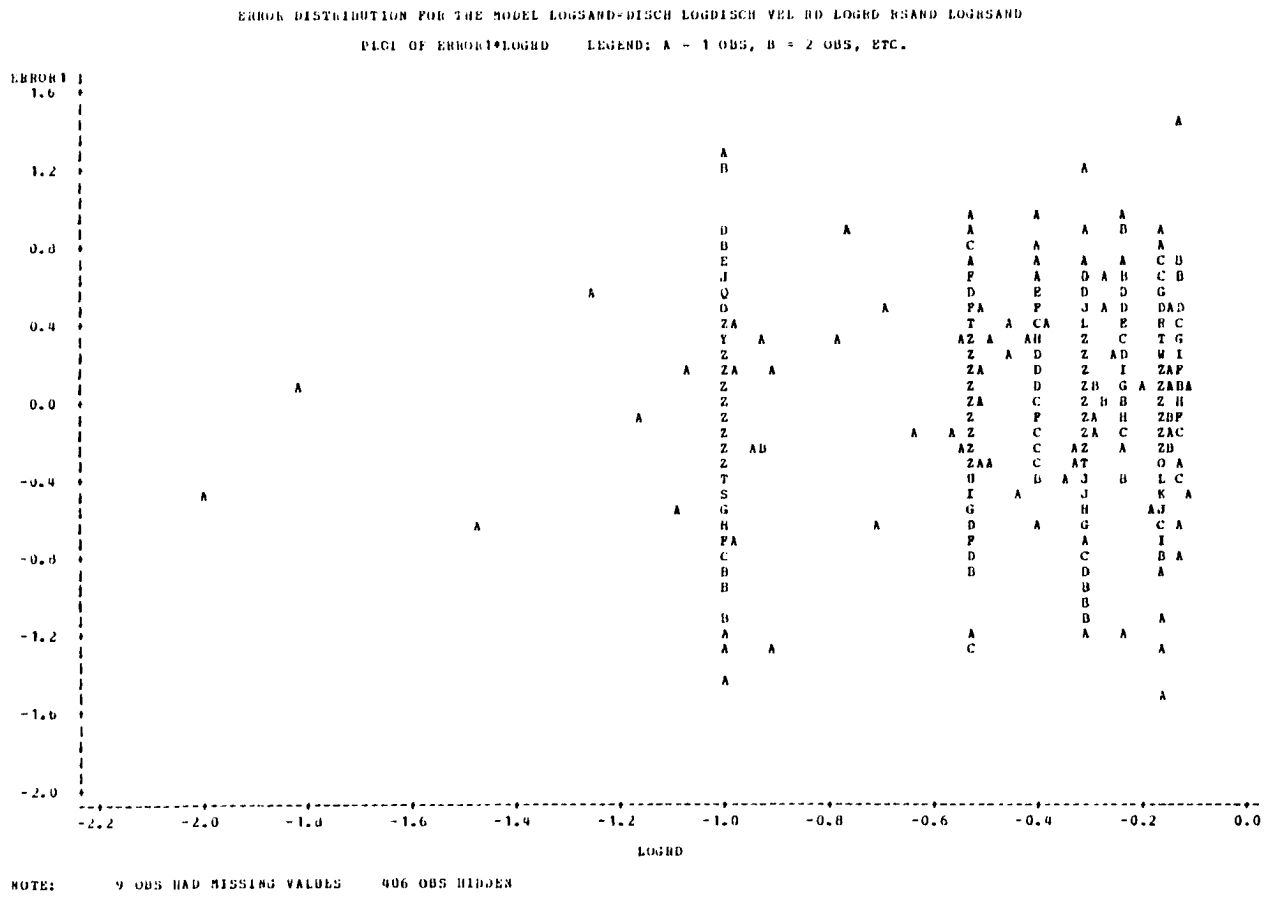

APPENDIX 3--Continued

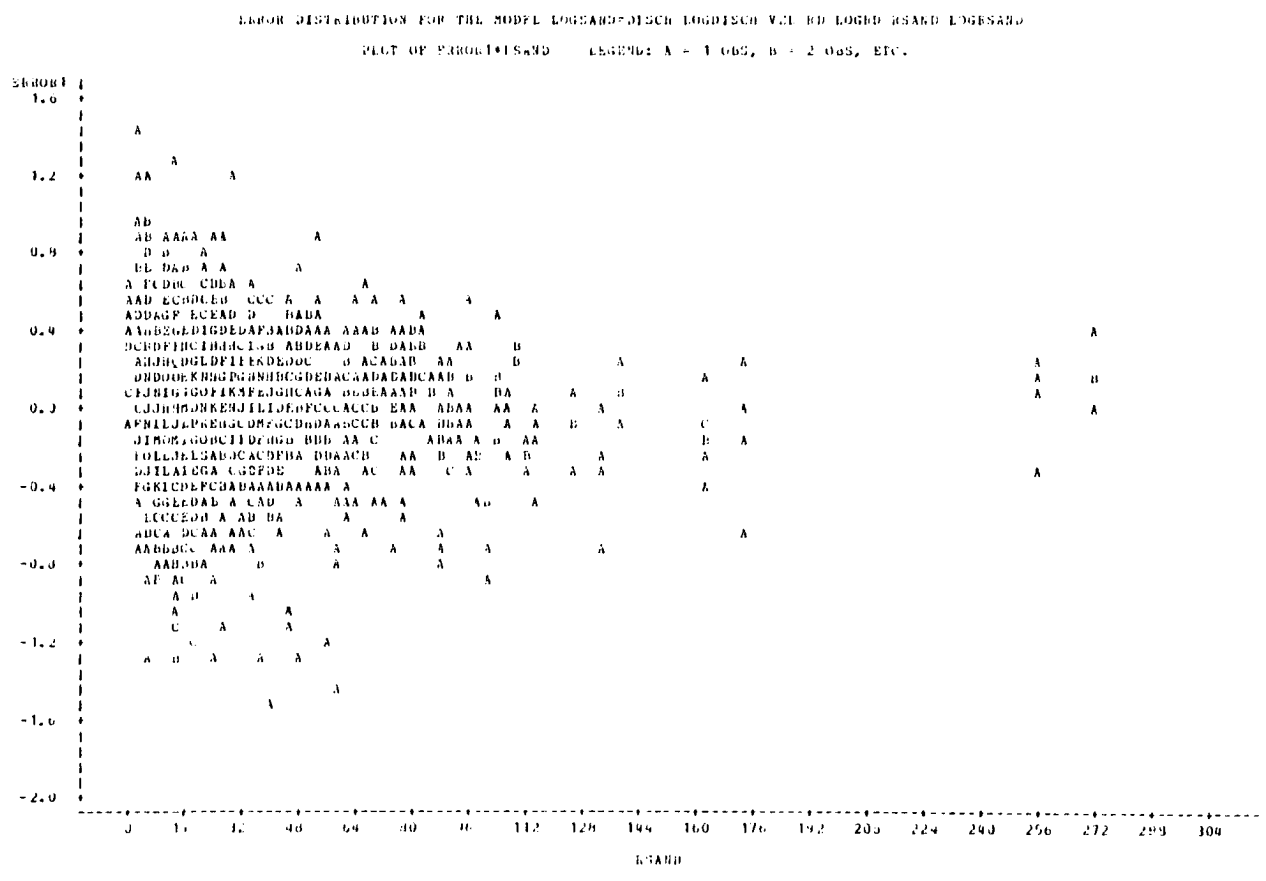

NOTE: 9 OBS HAD MISSING VALUES

APPENDIX 3--Continued

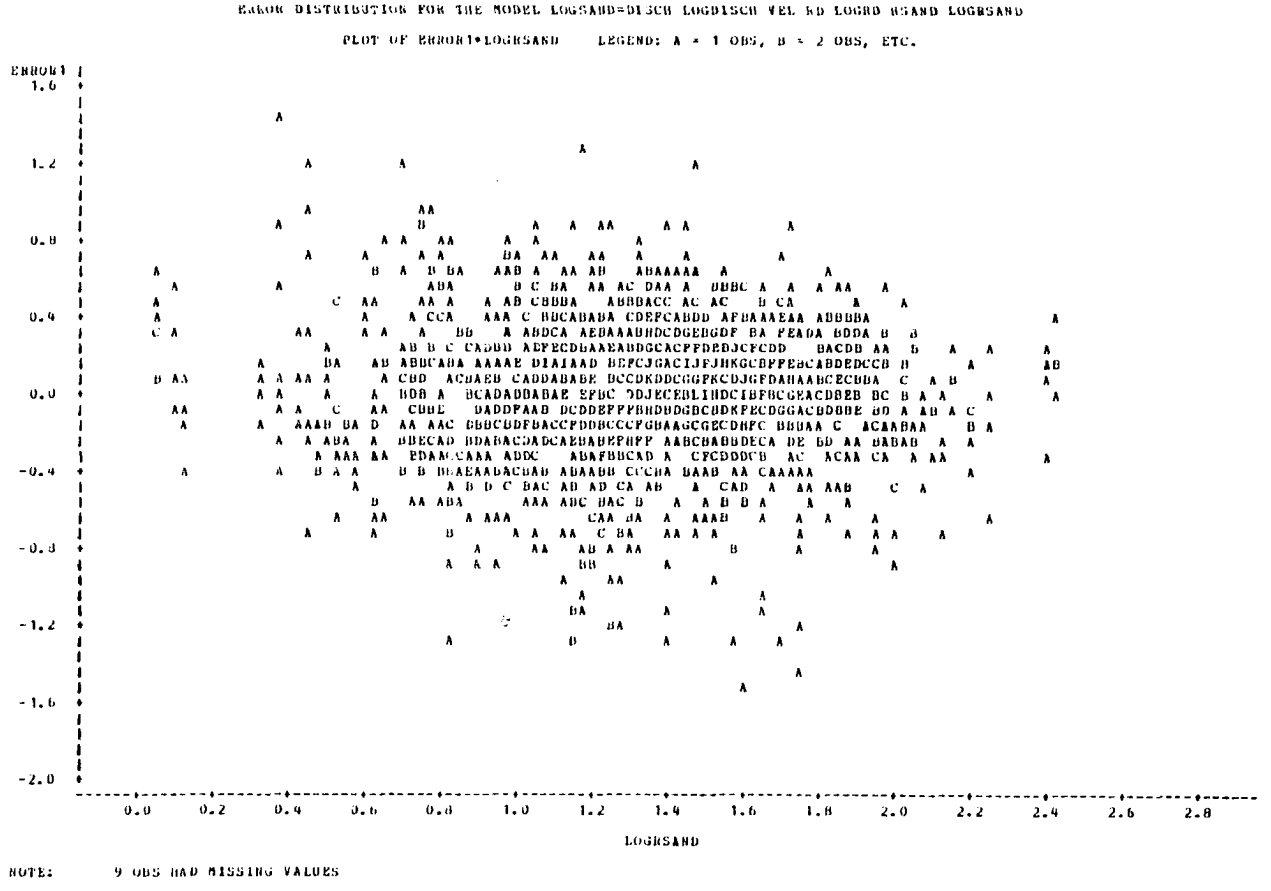

NOTE: 9 OBS HAD MISSING VALUES

APPENDIX 3--Continued

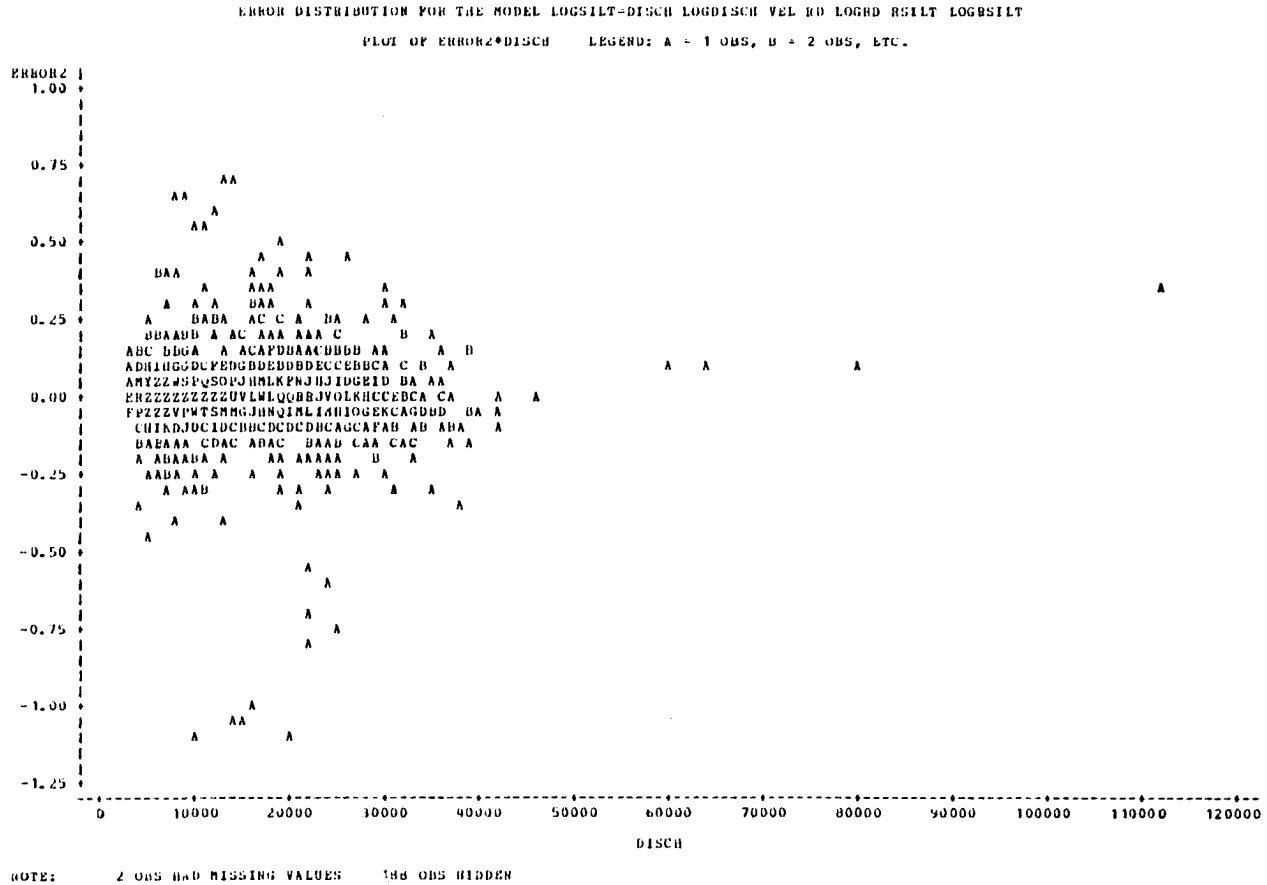

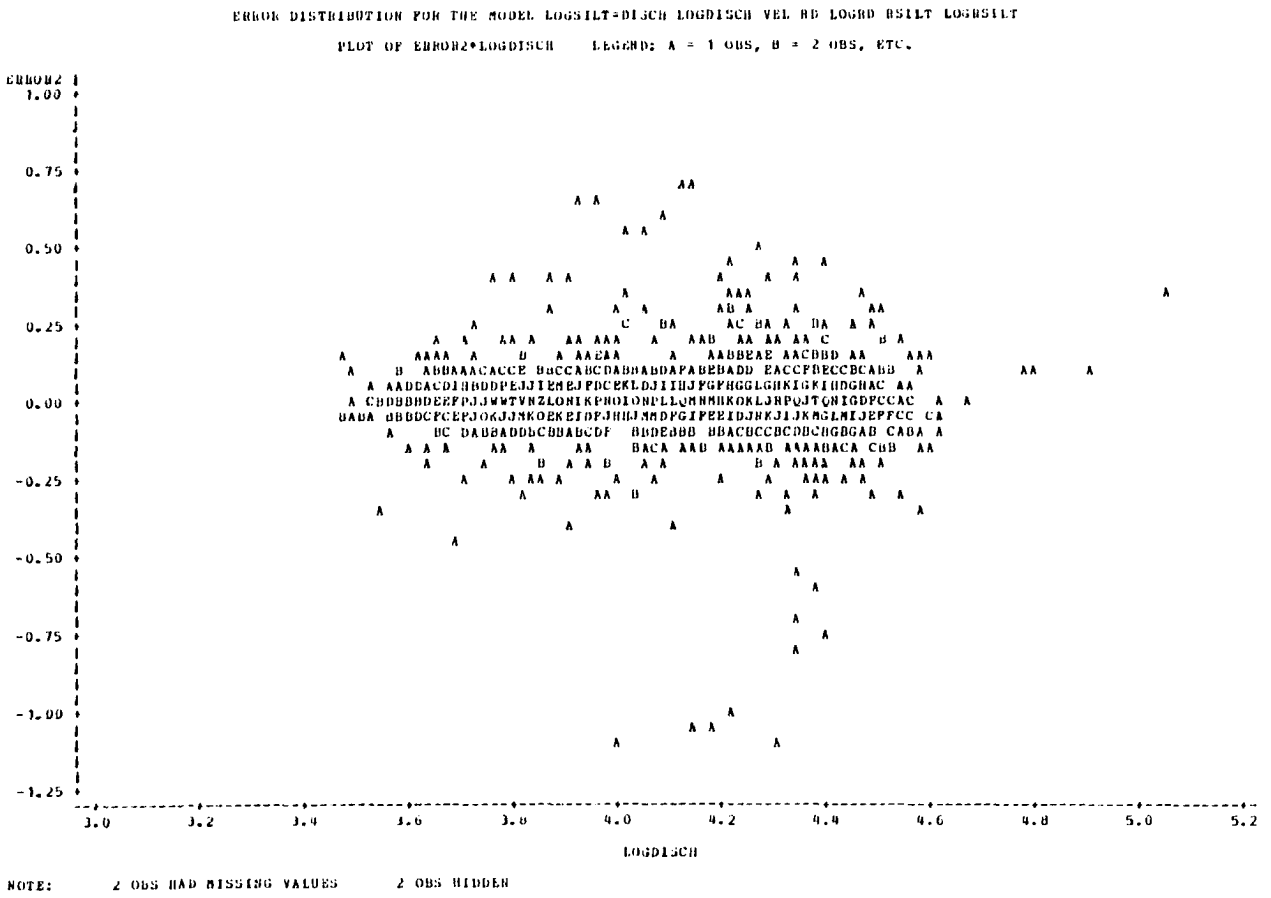

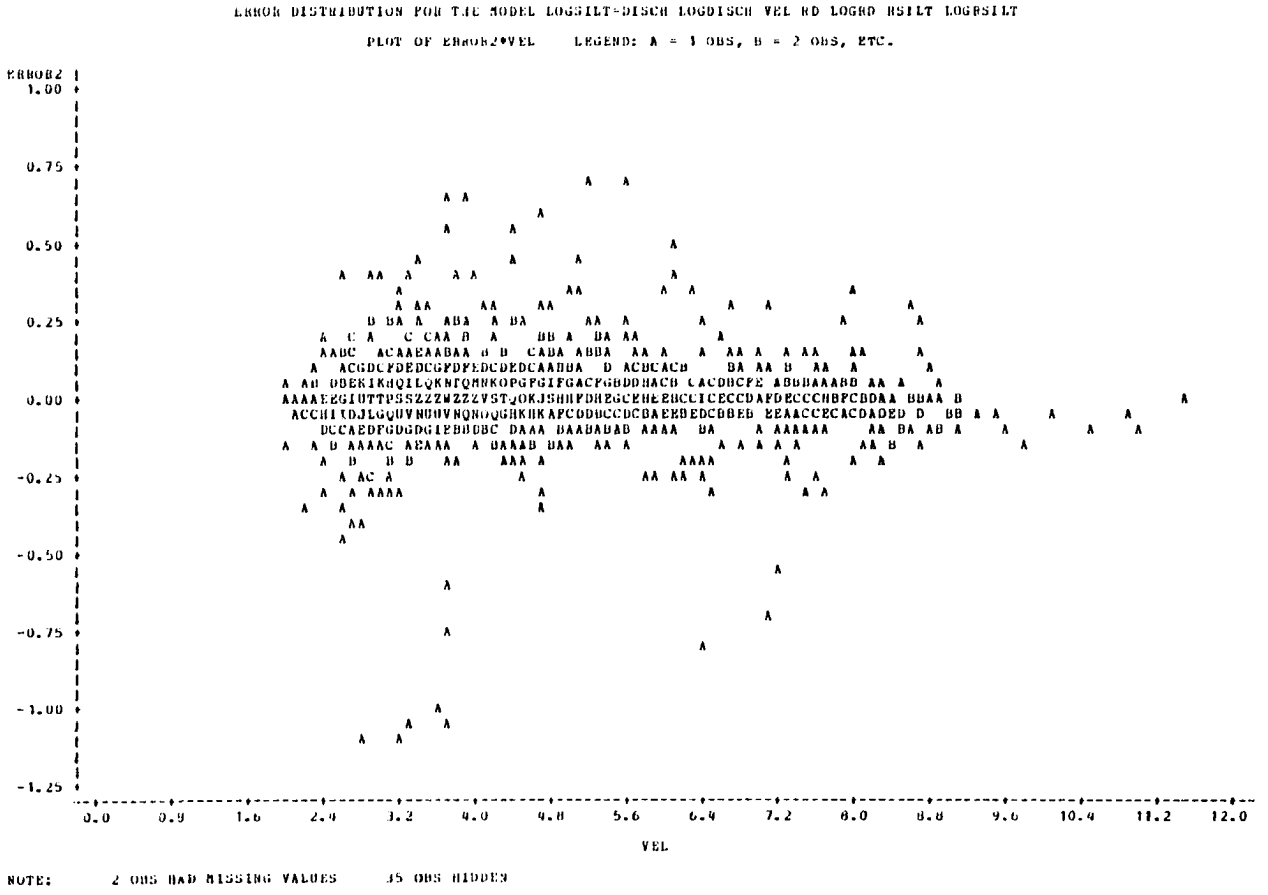

NOTE: 2 OBS HAD MISSING VALUES 35 OBS HIDDEN

APPENDIX 3--Continued

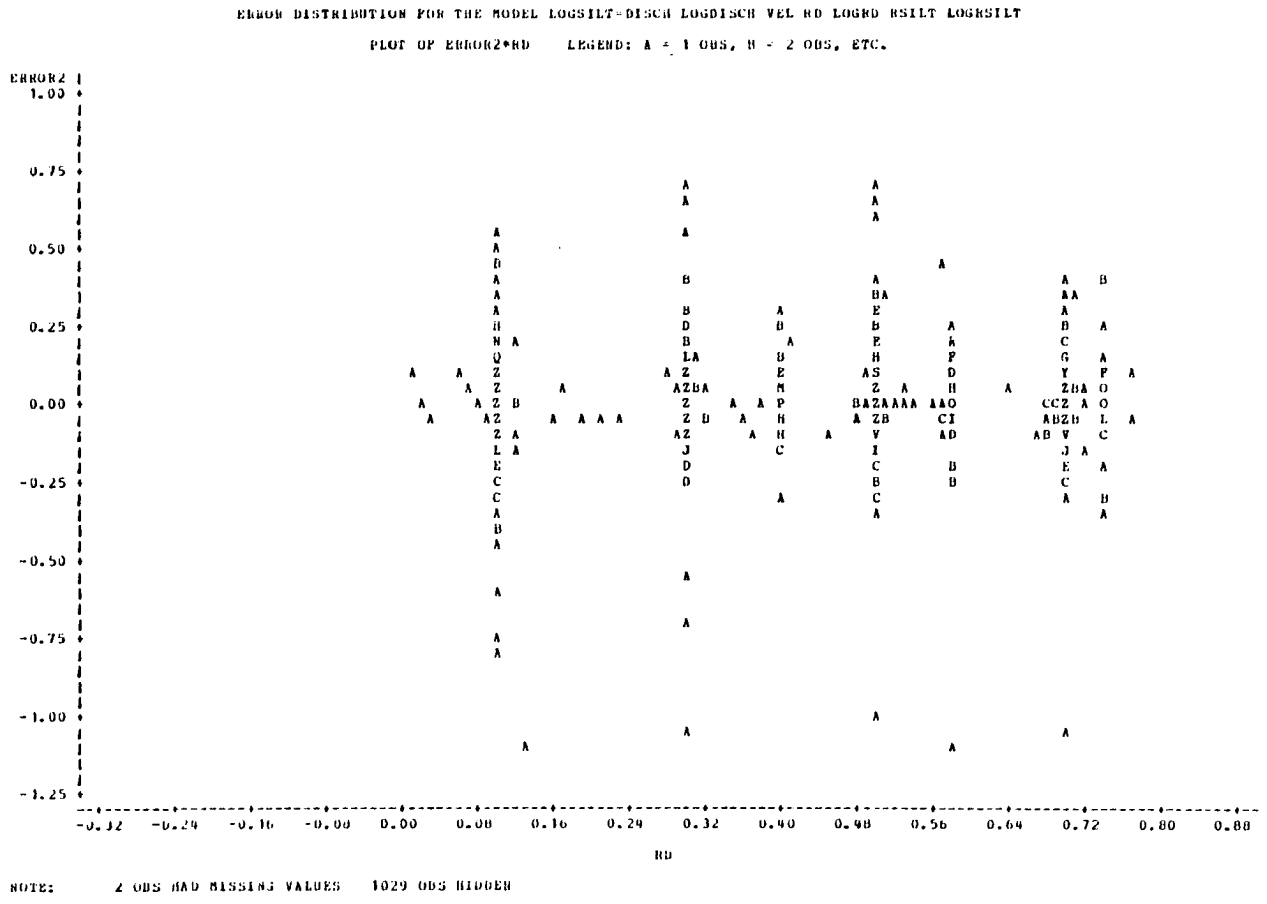

APPENDIX 3--Continued

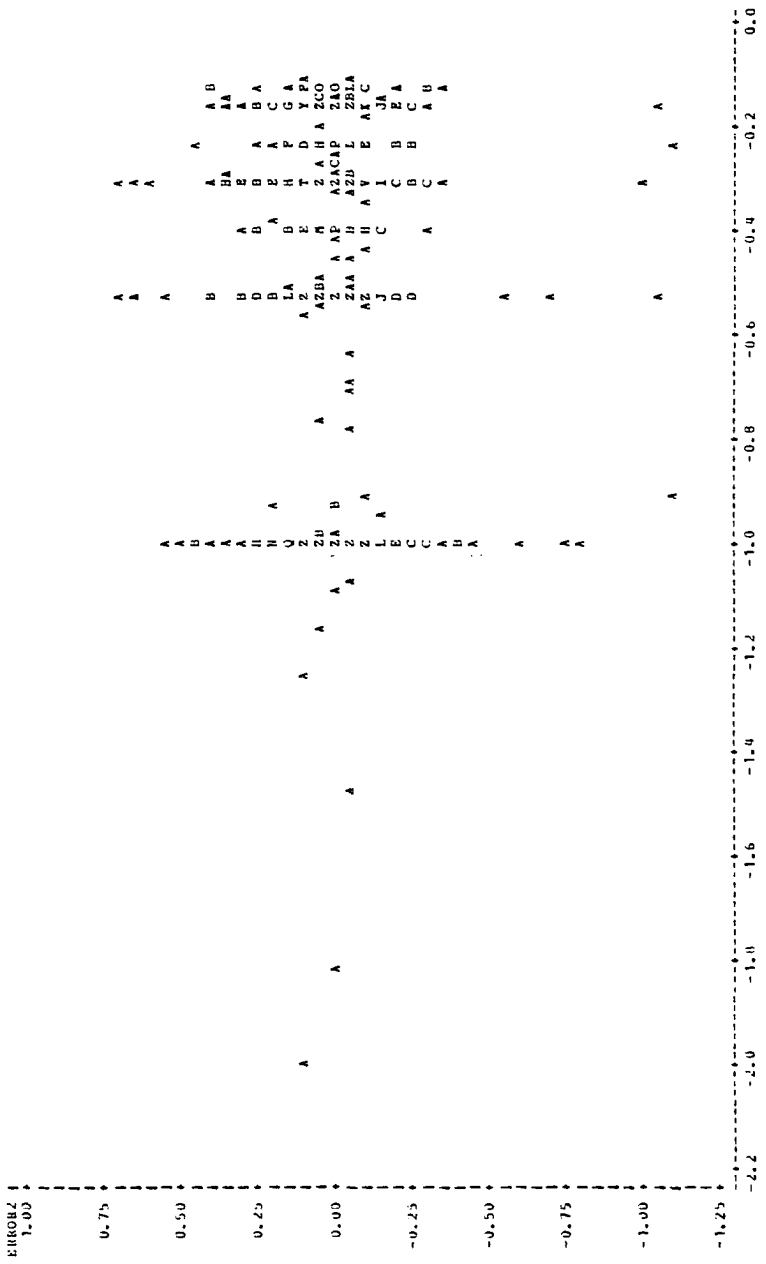

APPENDIX 3--Continued

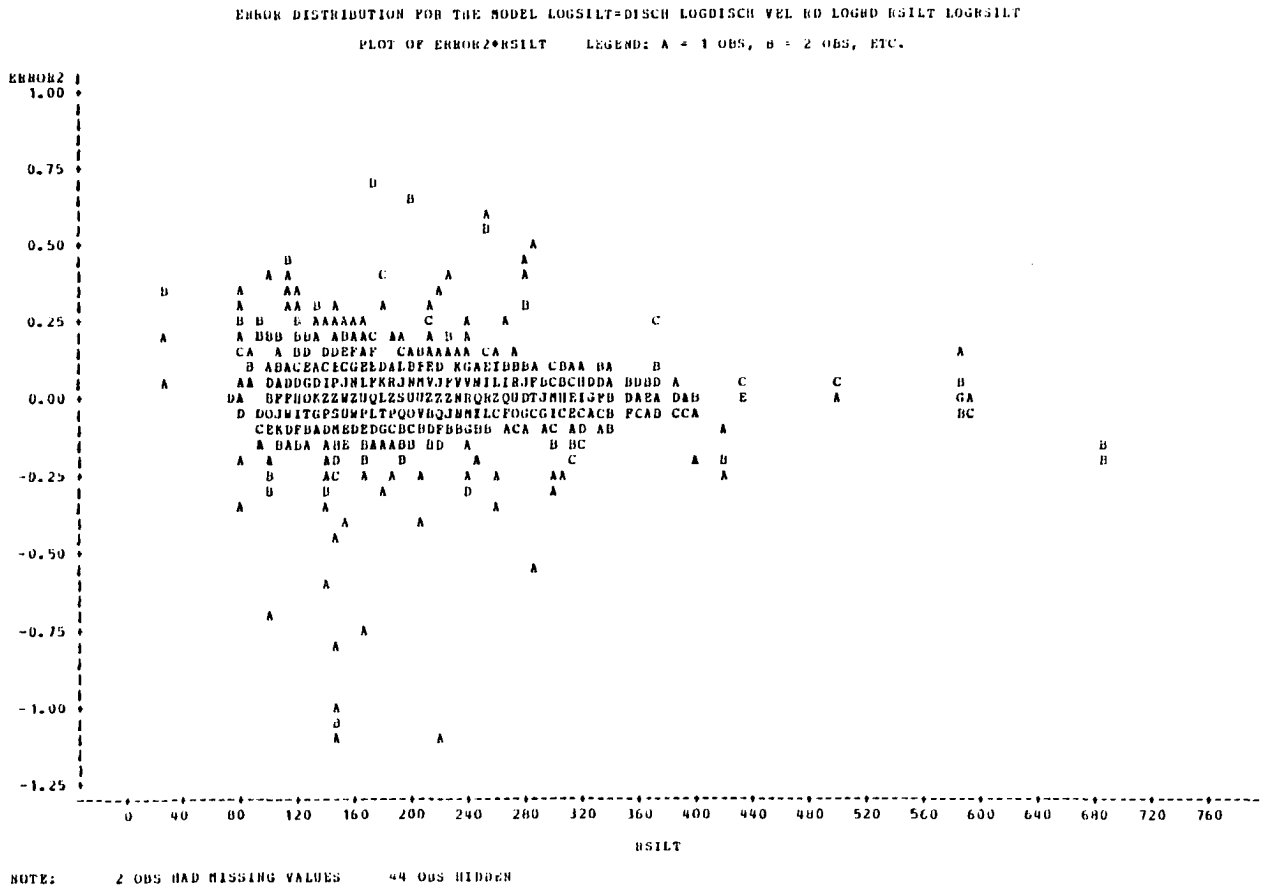

APPENDIX 3--Continued

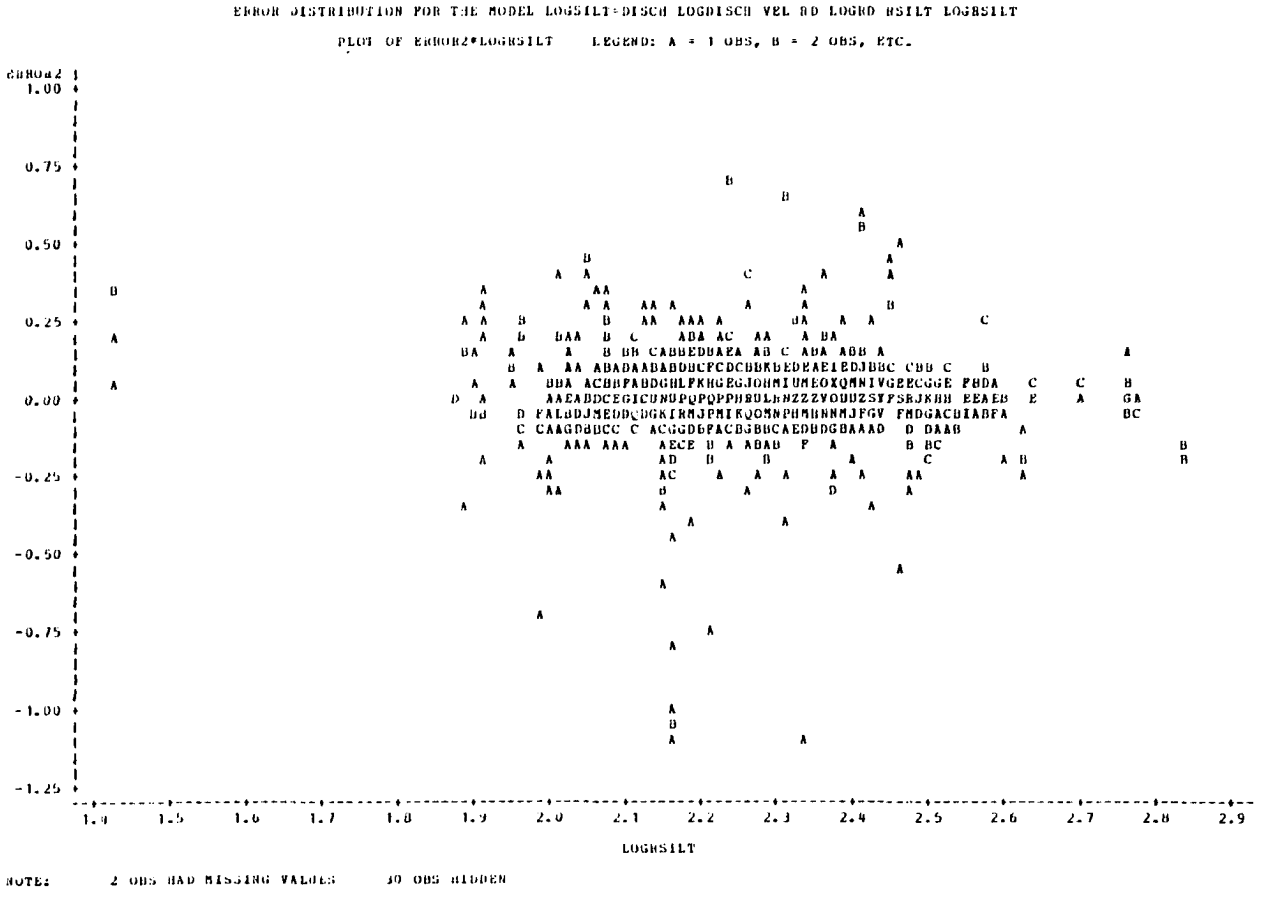

APPENDIX 3--Continued

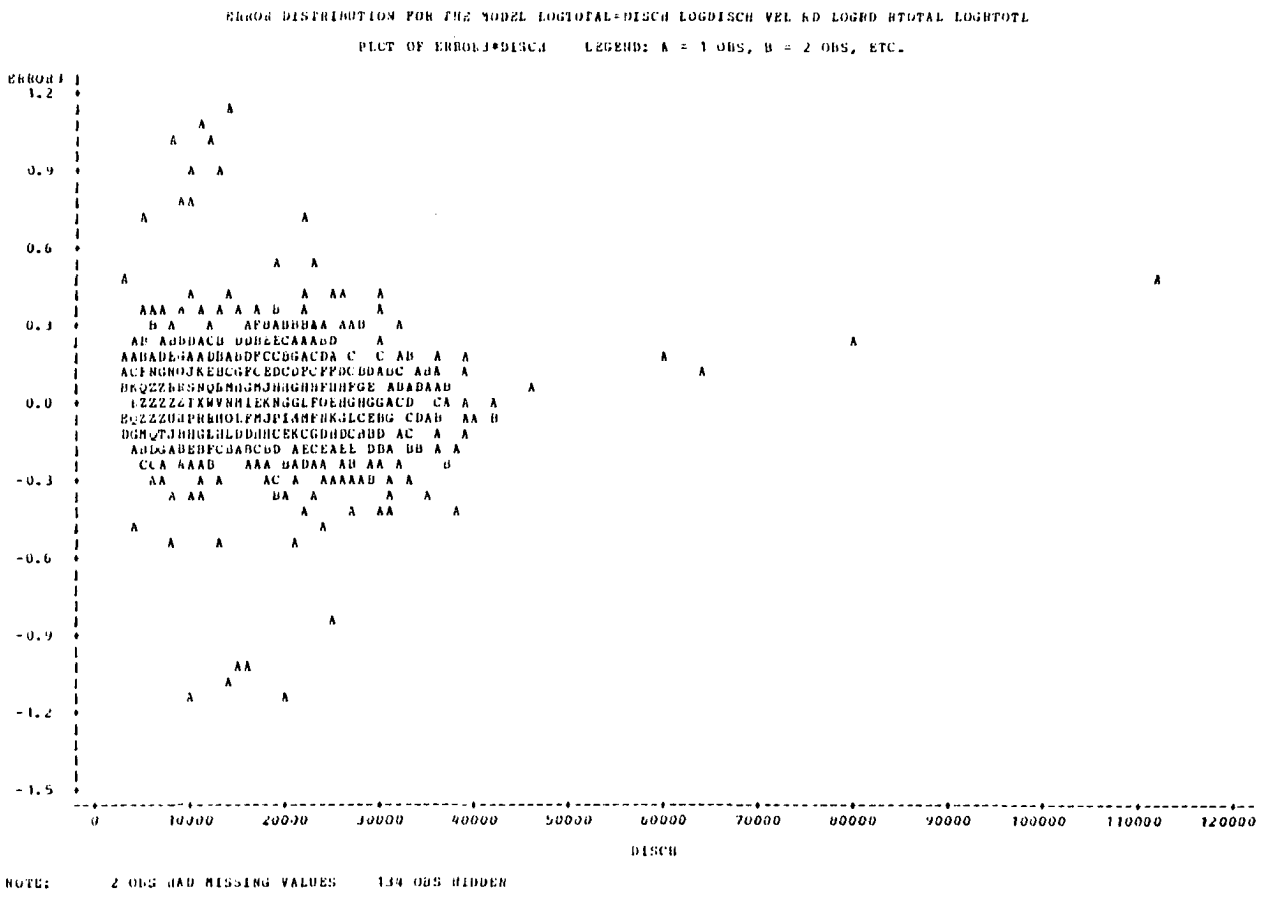

APPENDIX 3--Continued

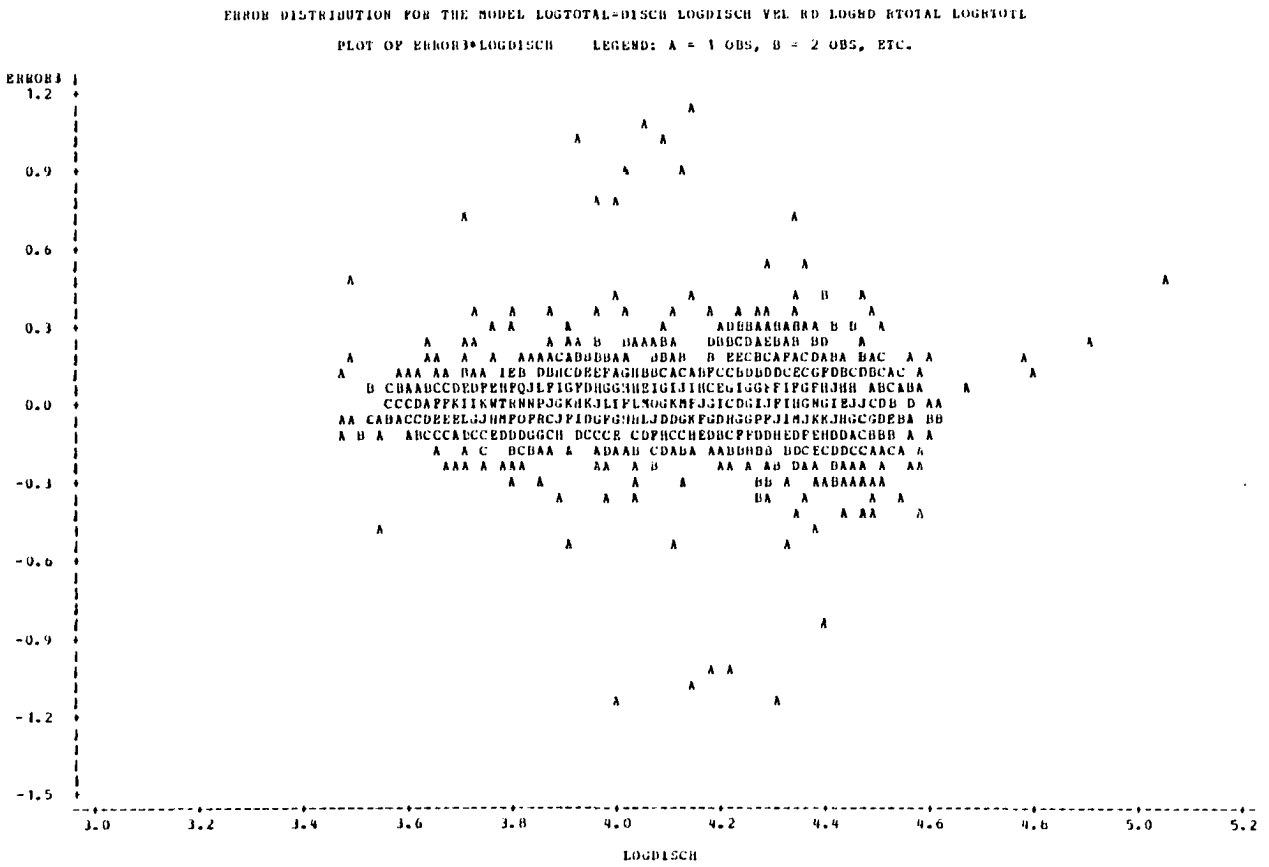

NOTE: 2 OBS HAD MISSING VALUES

APPENDIX 3--Continued

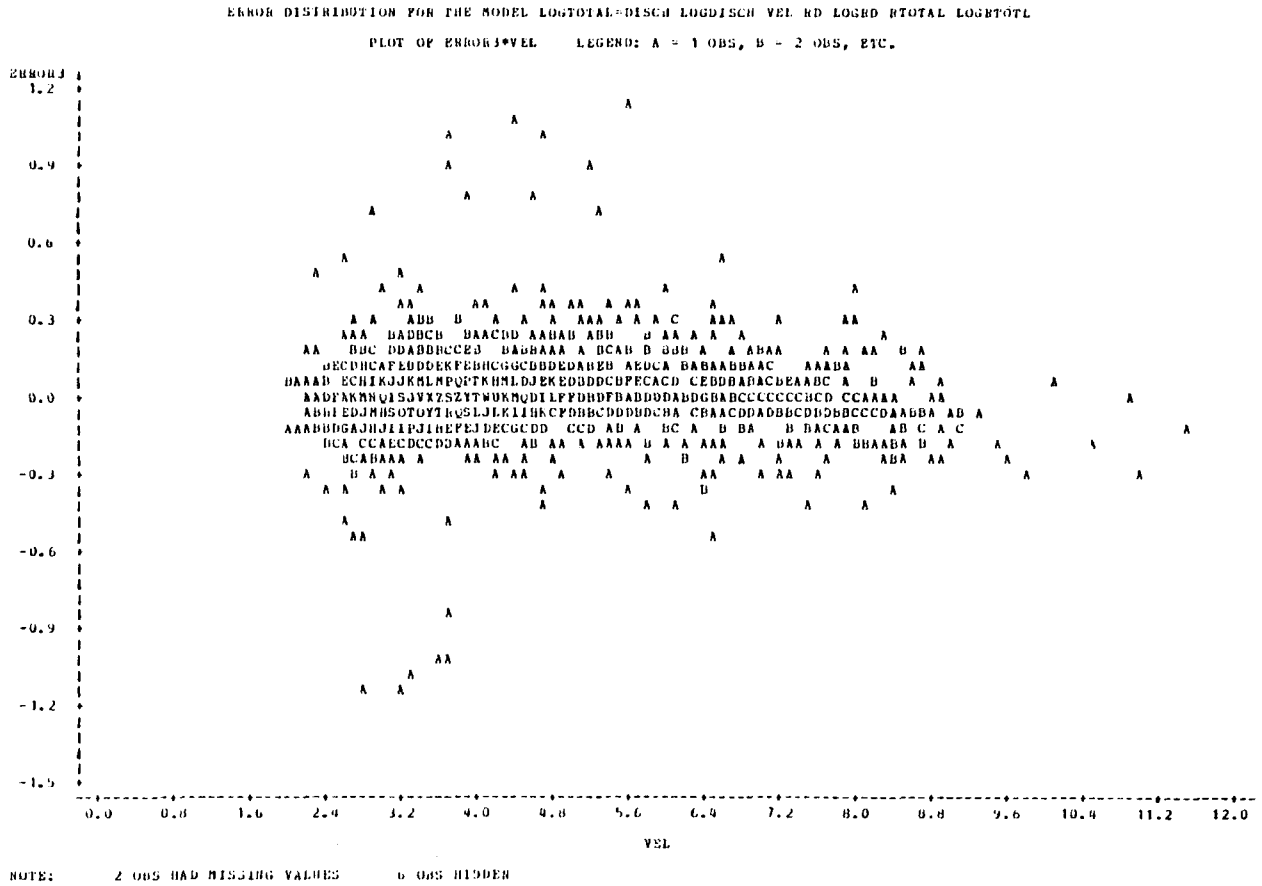

APPENDIX 3--Continued

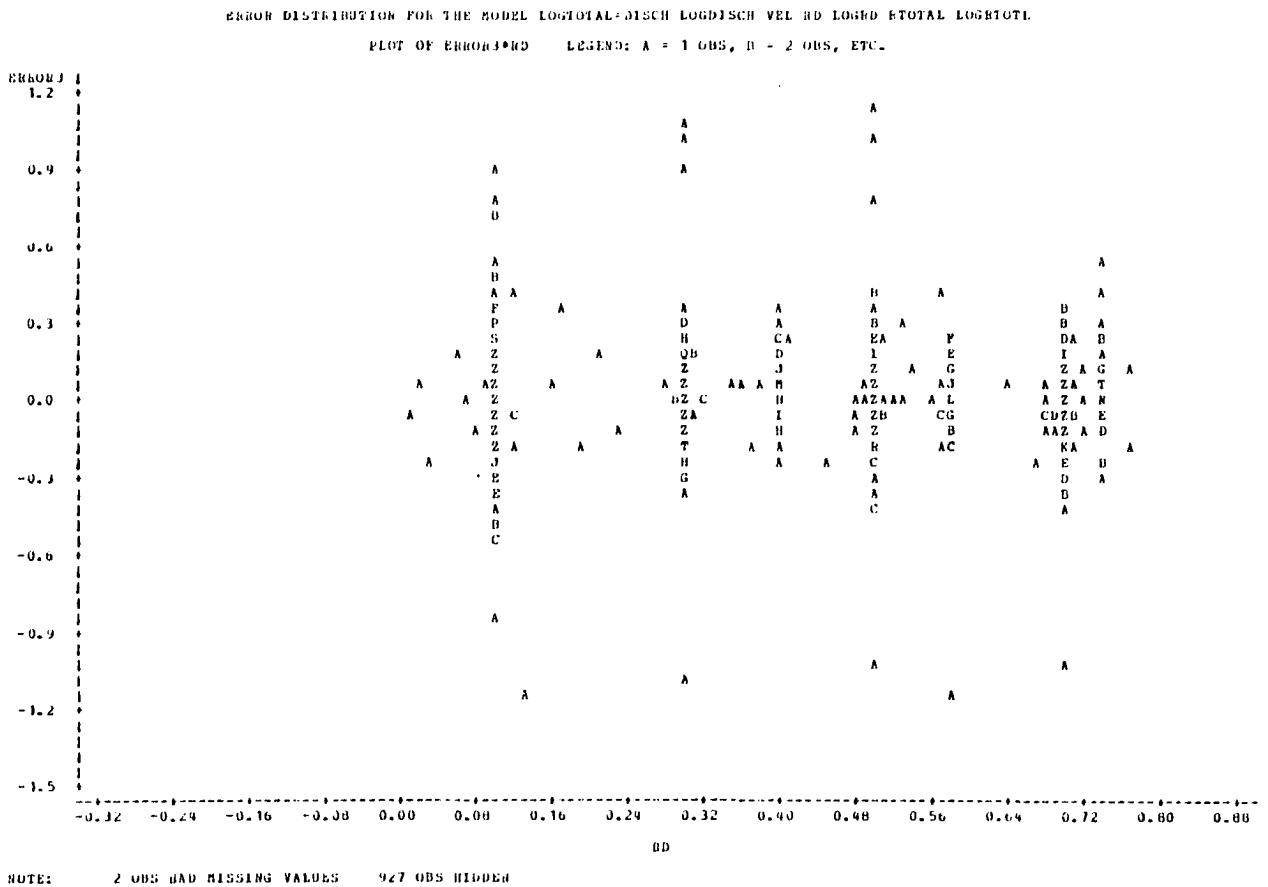

NOTE: 2 OBS HAD MISSING VALUES 927 OBS HIDDEN

APPENDIX 3--Continued

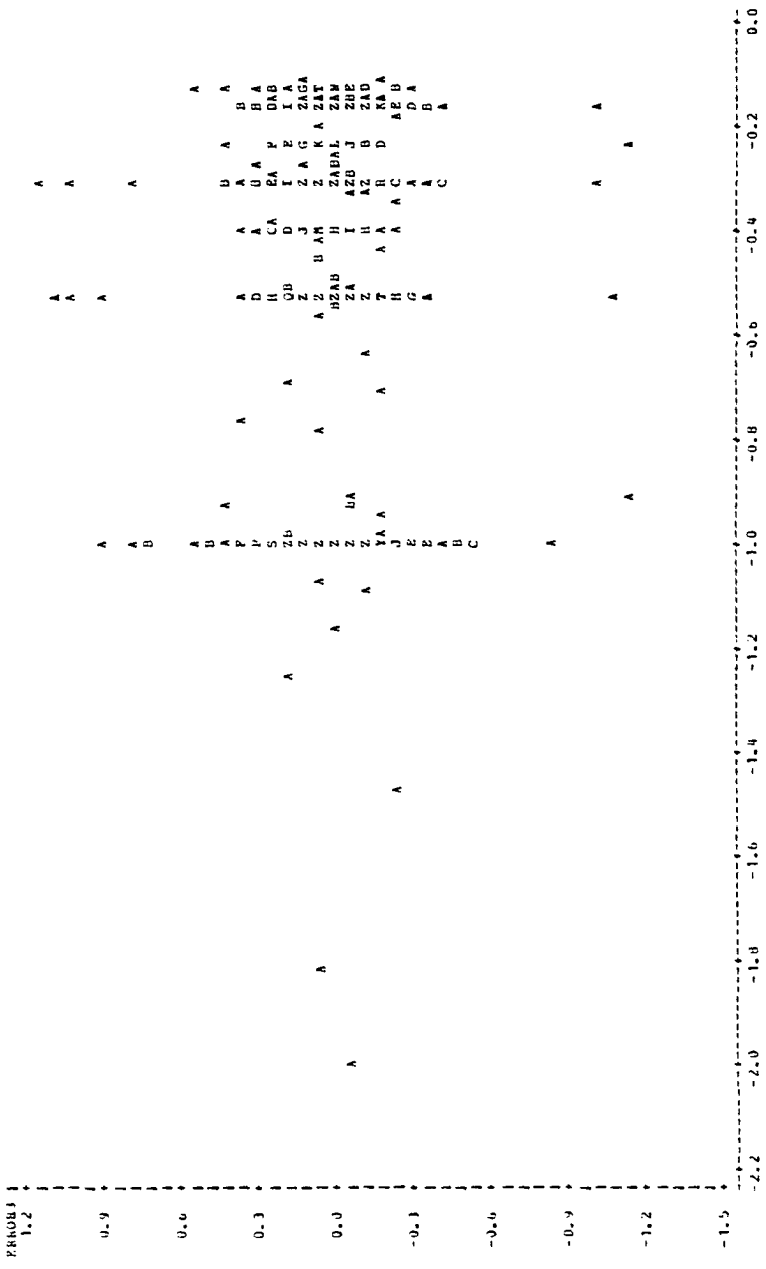

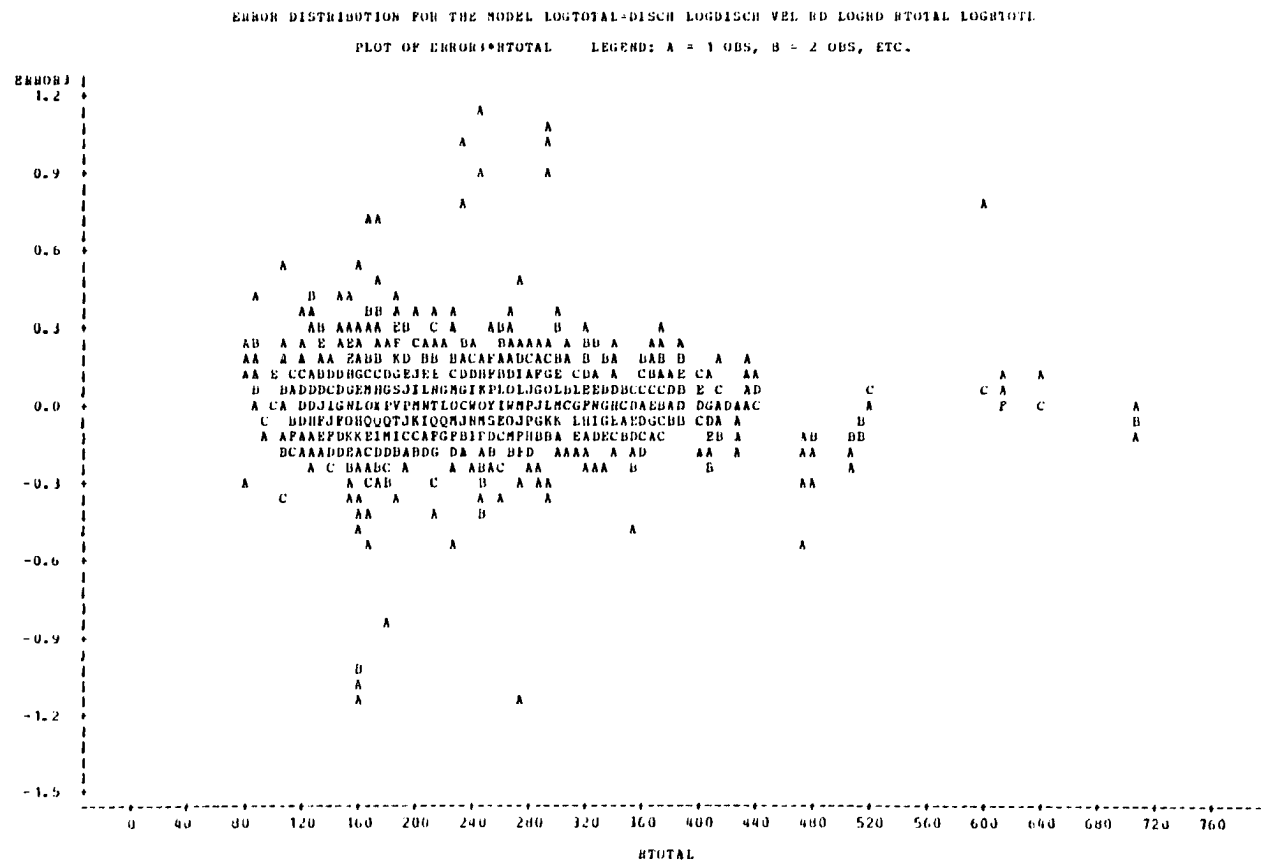

NOTE: 2 OBS HAD MISSING VALUES

APPENDIX 3--Continued

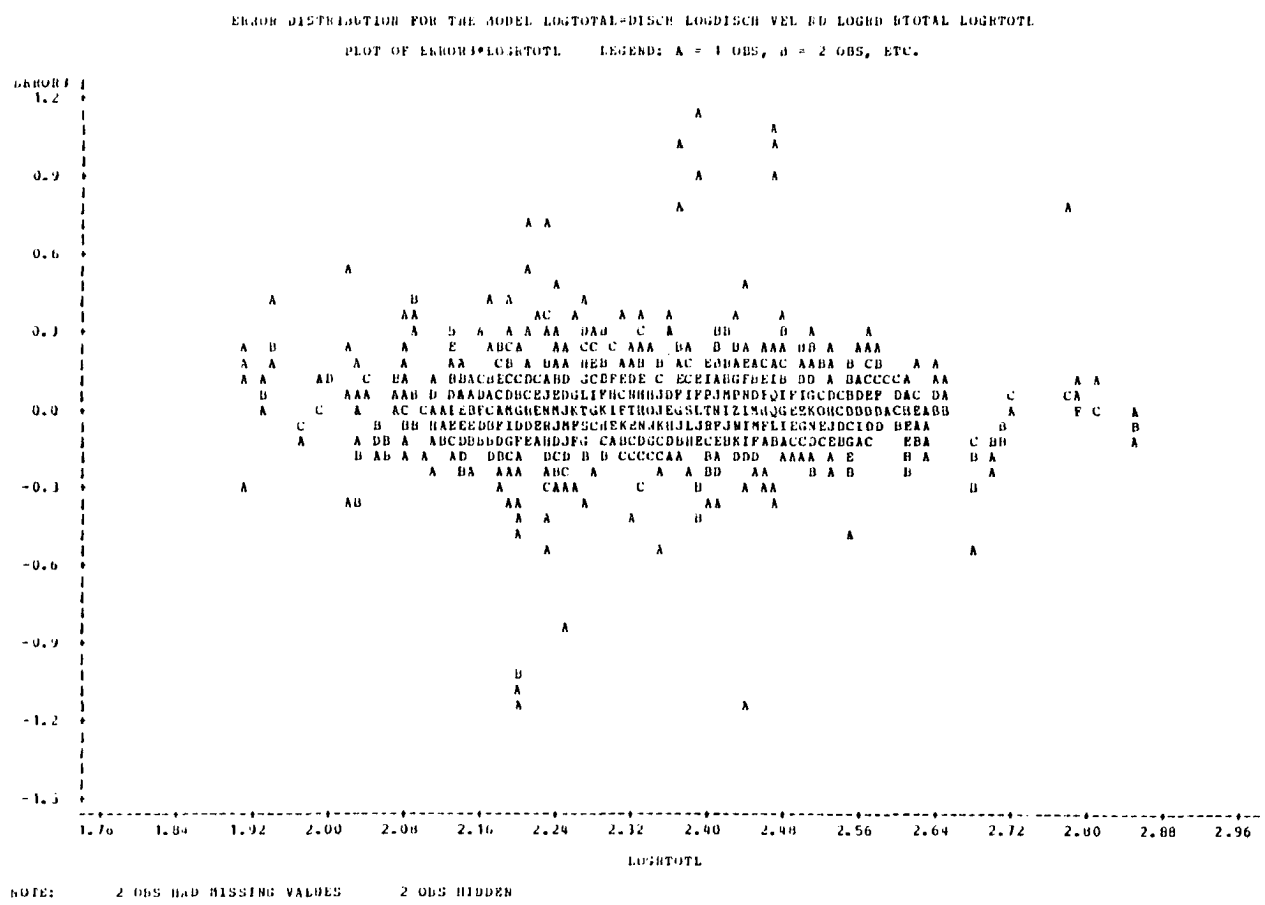

APPENDIX 4

THEORETICAL BACKGROUND OF THE FORBES-PEARSON DESTRIPPING METHOD

Let A_{ijk} be the radiance values recorded in CCT's for the ith channel (i = 1,....,4), the jth detector (or scan line, j = 1,....,6), and the kth element (k = 1,....,6). For each six-element by six-scan area, average values

$$m = \frac{1}{6} \sum_{j=1}^{6} \overline{A}_{ij}$$

are obtained for each channel, where $\overline{A}_{ij} = \frac{1}{6} \sum_{k=1}^{6} A_{ijk}$ and m = 0, 1,....,127 (corresponding to the dynamic range of the sensor). For the areas of a given m, then, adjusted values of $\overline{A}_{ij}$ are obtained as follows:

$$D_{mij} = \{6\,\overline{A}_{ij} + D_{mi}7 \times (D_{mij})_0\} \;/\; DD$$

thus, for each channel,

$$(D_{mi1})^1 = (6\,\overline{A}_{i1}) \;/\; 6$$

$$\vdots$$

$$(D_{mi6})^1 = (6\,\overline{A}_{i6}) \;/\; 6$$

$$(D_{mi1})^2 = \{6\,\overline{A}_{i1} + 6 \times (D_{mi1})^1\} \;/\; 12$$

$$\vdots$$

$$(D_{mi6})^{2} = \{6\ \bar{A}_{i6} + 6 \times (D_{mi6})^{1}\} / 12$$

$$(D_{mil})^{3} = \{6\ \bar{A}_{il} + 12 \times (D_{mil})^{2}\} / 18$$

$$\vdots$$

$$(D_{mi6})^{r} = \{6\ \bar{A}_{i6} + 6\ (r-1) \times (D_{mi6})^{r-1}\} / 6r$$

where the superscripts denote individual six-element by six-scan areas. Therefore, 6r equals total number of scan lines for a given m.

The adjusted mean values (D_{mi8}) of D_{mij} are obtained as follows: Let m_1 = min (m) and m_H = max (H) where $D_{mi7} \geq 300$. For $m_L \leq m \leq m_H$.

$$\bar{A}_i = \frac{1}{6} \sum_{j=1}^{6} D_{mij}$$

and let $d = \max | \bar{A}_i - D_{mij} |$. Suppose that d resulted where $j = j'$. Then,

$$\bar{A}_i' = (6\bar{A}_i - d) / 5$$

Further, let $d = \max \bar{A}_i - D_{mij}$ for $j \neq j'$. Then

$$\bar{A}_i'' = (5\bar{A}_i' - d') / 4 = D_{mi8}$$

Suppose that $D_{mi7} < 300$ and $m_L < m < m_H$. Then, D_{mij} are obtained using

$$D_{mij} = \frac{D_{mi7}}{300} \times (D_{mij})_0 + \left(1 - \frac{D_{mi7}}{300}\right) \left(\frac{D_{mi8} - D_{m_s i8}}{D_{m_T i8} - D_{m_s i8}} \right)$$

where m_s = max (m) with $D_{mi7} \geq 300$ and $m_s < m$ and m_T = min (m) with $D_{mi7} \geq 300$ and $m_T > m$.

Finally, let $m = q$ and $D_{mij} \leq h < D_{(m+1)ij}$. Then the final adjusted values LT_{hij} are obtained such that

$$LT_{hij} = (D_{(q+1)i8} - D_{qi8}) \left(\frac{h - D_{qij}}{D_{(q+1)ij} - D_{qij}} \right) + D_{qi8}$$

LT_{hij} so obtained are rounded to the nearest integer.

VITA

Soon Tae Kim was born on July 30, 1944, in Seoul, Korea. He received a Bachelor of Arts in geography from Seoul National University in 1971 and a Master of Science and a Master of Applied Statistics from Louisiana State University in 1974 and 1977, respectively. He is a candidate for the degree of Doctor of Philosophy in physical geography.

EXAMINATION AND THESIS REPORT

Candidate: Soon Tae Kim

Major Field: Geography

Title of Thesis: A QUANTITATIVE EVALUATION OF LANDSAT FOR MONITORING SUSPENDED SEDIMENTS IN A FLUVIAL CHANNEL

Approved: Anthony J. Lewis
Robert A. Muth

Major Professor and Chairman

James B. Traynham

Dean of the Graduate School

EXAMINING COMMITTEE:

M. O. Hunter, Jr.

Charles A. Hasler

Samuel Thomson

Prentiss E. Schilling

Date of Examination: November 26, 1979